GLASILO SLOVENSKIH TEKSTILCEV • SLOVENE JOURNAL FOR TEXTILE AND CLOTHING TECHNOLOGY, DESIGN AND MARKETING

tekstilec

1/2019 • vol. 62 • 1–73
ISSN 0351-3386 (tiskano/printed)
ISSN 2350 - 3696 (elektronsko/online)
UDK 677 + 687 (05)

http://www.tekstilec.si

tekstilec (ISSN: 0351-3386 tiskano, 2350-3696 elektronsko) je znanstvena revija, ki podaja temeljne in aplikativne znanstvene informacije v fizikalni, kemijski in tehnološki znanosti, vezani na tekstilno in oblačilno tehnologijo, oblikovanje in trženje tekstilij in oblačil. V prilogah so v slovenskem jeziku objavljeni strokovni članki in prispevki o novostih v tekstilni tehnologiji iz Slovenije in sveta, prispevki s področja oblikovanja tekstilij in oblačil, informacije o raziskovalnih projektih ipd.

tekstilec *(ISSN: 0351-3386 printed, 2350-3696 online) the scientific journal gives fundamental and applied scientific information in the physical, chemical and engineering sciences related to the textile and clothing industry, design and marketing. In the appendices written in Slovene language, are published technical and short articles about the textile-technology novelties from Slovenia and the world, articles on textile and clothing design, information about research projects etc.*

Dosegljivo na svetovnem spletu/*Available Online at*
www.tekstilec.si

Tekstilec je indeksiran v naslednjih bazah/*Tekstilec is indexed in*
Emerging Sources Citation Index – ESCI/Clarivate Analytics
SCOPUS/Elsevier
Ei Compendex
DOAJ
WTI Frankfurt/TEMA® Technology and Management/TOGA® Textile Database
World Textiles/EBSCO Information Services
Textile Technology Complete/EBSCO Information Services
Textile Technology Index/EBSCO Information Services
Chemical Abstracts/ACS
ULRICHWEB – global serials directory
LIBRARY OF THE TECHNICAL UNIVERSITY OF LODZ
dLIB
SICRIS: 1A3 (Z, A', A1/2)

tekstilec

Ustanovitelja / *Founded by*
• Zveza inženirjev in tehnikov tekstilcev Slovenije /
Association of Slovene Textile Engineers and Technicians
• Gospodarska zbornica Slovenije – Združenje za tekstilno,
oblačilno in usnjarsko predelovalno industrijo /
Chamber of Commerce and Industry of Slovenia – Textiles, Clothing and Leather Processing Association

Revijo sofinancirajo / *Journal is Financially Supported*
• Univerza v Ljubljani, Naravoslovnotehniška fakulteta / *University of Ljubljana, Faculty of Natural Sciences and Engineering*
• Univerza v Mariboru, Fakulteta za strojništvo /
University of Maribor, Faculty for Mechanical Engineering
• Industrijski razvojni center slovenske predilne industrije /
Slovene Spinning Industry Development Centre – IRSPIN
• Javna agencija za raziskovalno dejavnost Republike Slovenije /
Slovenian Research Agency

Izdajatelj / *Publisher*
Univerza v Ljubljani, Naravoslovnotehniška fakulteta /
University of Ljubljana, Faculty of Natural Sciences and Engineering

Naslov uredništva/*Editorial Office Address*
Uredništvo Tekstilec, Snežniška 5, SI–1000 Ljubljana
Tel./*Tel.*: + 386 1 200 32 00, +386 1 200 32 24
Faks/*Fax*: + 386 1 200 32 70
E–pošta/*E–mail*: tekstilec@ntf.uni–lj.si
Spletni naslov/*Internet page*: http://www.tekstilec.si

Lektor za slovenščino / *Slovenian Language Editor* Milojka Mansoor
Lektor za angleščino / *English Language Editor* Barbara Luštek Preskar, Tina Kočevar Donkov, Glen David Champaigne

Oblikovanje platnice / *Design of the Cover* Tanja Nuša Kočevar
Oblikovanje / *Design* Vilma Zupan
Oblikovanje spletnih strani / *Website Design* Jure Ahtik

Tisk / *Printed by* PRIMITUS, d. o. o.

Revija Tekstilec izhaja štirikrat letno / *Journal Tekstilec appears quarterly*
Revija je pri Ministrstvu za kulturo vpisana v razvid medijev pod številko 583.
Letna naročnina za člane Društev inženirjev in tehnikov tekstilcev je vključena v članarino.
Letna naročnina za posameznike 38 € za študente 22 €
za mala podjetja 90 € za velika podjetja 180 €
za tujino 110 €
Cena posamezne številke 10 €

Na podlagi Zakona o davku na dodano vrednost sodi revija Tekstilec med proizvode, od katerih se obračunava DDV po stopnji 9,5 %.

Transakcijski račun 01100–6030708186
Bank Account No. SI56 01100–6030708186
Nova Ljubljanska banka d.d.,
Trg Republike 2, SI–1000 Ljubljana,
Slovenija, SWIFT Code: LJBA SI 2X.

tekstilec VOLUME 62 • TEKSTILEC 1 • 2019 ISSN 0351-3386 (tiskano/printed)
UDK 677 + 687 (05)

SCIENTIFIC ARTICLES/ Znanstveni članki

Emilija Toshikj, Goran Demboski, Igor Jordanov, Biljana Mangovska
Sts. Cyril & Methodius University, Faculty of Technology and Metallurgy, Ruger Boskovic 16, 1000 Skopje, Macedonia

Functional Properties and Seam Puckering on Cotton Shirt Influenced by Laundering

Uporabne lastnosti in nabiranje šivov bombažne srajčevine pri pranju

Original Scientific Article/*Izvirni znanstveni članek*
Received/*Prispelo* 10-2018 • Accepted/*Sprejeto* 1-2019

Abstract

Plain cotton fabrics of various mass per unit area, commercially available for manufacturing men's shirts, were seamed by applying three types of seams. The seaming was conducted on an industrial sewing machine under the sewing parameters commercially adopted by apparel manufacturers. The selected samples were laundered three times with two different commercially available detergents under the same washing conditions. The seam puckering and fabric properties were analysed before and after the laundering. It was found out that the degree of seam puckering after the laundering was affected by the type of seam and used detergent. The samples treated with a powder detergent showed greater changes in the fabric structure compared to those washed with a liquid detergent.
Keywords: dress shirt, safety seam, French seam, English seam, seam thickness

Izvleček

Komercialne bombažne tkanine različnih ploščinskih mas v vezavi platno, ki so namenjene za izdelavo moških srajc, so bile šivane s tremi vrstami šivov na industrijskem šivalnem stroju pri pogojih, povzetih po proizvajalcih oblačil. Izbrani vzorci so bili trikrat prani pri enakih pogojih z dvema različnima komercialnima detergentoma. Nabiranje šivov in lastnosti tkanin so bile analizirane pred pranjem in po njem. Ugotovljeno je bilo, da sta na stopnjo nabiranja šivov po pranju vplivala vrsta uporabljenega šiva in vrsta detergenta. Vzorci, prani s praškastim detergentom, so izkazali večje spremembe v strukturi tkanin v primerjavi z vzorci, pranimi s tekočim detergentom.
Ključne besede: majica, varnostni šiv, francoski šiv, angleški šiv, debelina šiva

1 Introduction

Shirts represent a traditional piece of men's clothing. A great-looking shirt adds style to any outfit. Slim fit cuts and narrow fit cuts are currently in fashion, both in the business world and for casual wear.

Shirts can be made of different materials and with cuts emphasizing different styles. They are made of 100% cotton, cotton/polyester blends or linen, wool, silk or their blends, woven and dyed in various patterns and colours. Pure cotton is probably the most popular material [1]. The fabric weight varies from 70 to 200 g/m^2. Superimposed and lapped seams are the most frequently used seam classes in shirt manufacturing, ranging from plain, safety, French, to English and other types of seams. Since shirts are usually worn seven or more than seven hours a day, they should be frequently changed and properly cared for. Laundering is a part of the dress shirt care [2]. Shirts have to exhibit good heat and moisture transfer, durability, smoothness, and the ability to recover the shape when washed and ironed.

The overall shirt appearance depends on the characteristics of the shirt style, shirt pattern design,

Corresponding author/*Korespondenčna avtorica:*
Dr. Emilija Toshikj, Assistant Professor
E-mail: tosic_emilija@tmf.ukim.edu.mk

fabric, quality of seams, final assembly and finishes. Shirt manufacturing includes choosing a suitable fabric, seam type and sewing parameters.

Seam pucker is one of the major problems the garment industry has been facing with for many years [3, 4]. Seam pucker appears when the sewing parameters and material properties are not chosen properly, thus reducing the garment quality. Factors affecting seam pucker are sewing thread and fabric characteristics, stitch formation, sewing thread tension, fabric feeding and seam type [5]. Seam thread properties, sewing parameters and their compatibility during the sewing have been investigated in several papers [6–12]. The effect of sewing parameters on seam pucker was examined most frequently [13, 14]. Researchers have been investigating the relationship between fabric sewability, optimization of sewing and fabric features to predict seam pucker [15, 16].

People prefer cotton shirts due to their softness and natural feeling; however, the soft-to-touch quality brings along less resilience and durability. The textile hand, hydrophilicity, friction and other properties are affected by the laundering [17, 18]. The shrinkage of a fabric after the laundering may have a considerable influence on seam pucker. To the best of our knowledge, the influence of seam type on seam pucker has been scarcely investigated [9], while the effects of laundering and detergent type on seam puckering were evaluated in our previous paper where the effects of seam type and laundering after 3 washing cycles on seam puckering and functional properties of cotton/polyester shirt fabric were discussed [19]. It was concluded that the seam type and laundering affected seam puckering, irrespective of detergent type. The highest pucker grade (less puckering) after the laundering was noticed on the safety seam followed by the English and French seams.

The aim of this investigation was to estimate the influence of seam type, laundering and detergent type on seam puckering, on the structural and mechanical properties, and on the air permeability of cotton shirt fabrics.

2 Materials and methods

2.1 Materials

Plain woven fabrics made of 100% cotton or of a cotton/Lycra blend, of white or light colour and various weight, intended for men's shirts were seamed and analysed. The seam types applied were as follows: safety seam, double lap of French seam and English seam (Figure 1). Fabric characteristics are shown in Table 1. The test specimens were prepared in warp direction according to the AATCC Test Method 88B.

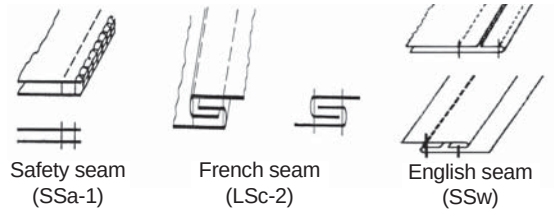

Figure 1: Investigated seam types

Table 1: Structural properties of reference fabrics

No.	Fabric composition	Colour	Fabric weight [g/m^2]	Fabric thickness [mm]	Fabric density [cm^{-1}]		Linear density [tex]	
					Warp	Weft	Warp	Weft
A	100% Cotton	White	72.6	0.22	53.3	33.7	7.4	10
B	100% Cotton	White	89.3	0.22	57.0	35.7	9	9
C	100% Cotton	White	97.2	0.24	57.3	31.3	14	10
D	100% Cotton	White	106.7	0.26	50.0	27.7	12.5	12.5
E	100% Cotton	Light colour	108.5	0.24	47.3	29.7	17	14
F	100% Cotton	Stripes	114.2	0.25	48.0	25.0	14	17
G	100% Cotton	Light colour	115.5	0.33	50.0	36.0	12.5	14
H	100% Cotton	Light colour	115.9	0.22	51.7	31.7	14	14
I	100% Cotton	Light colour	122.1	0.24	42.7	23.0	17	20
J	97% Cotton/3% Lycra	Light colour	123.2	0.35	53.3	27.0	14	20
K	97% Cotton/3% Lycra	White	125.8	0.29	57.3	27.0	12.5	17

The sewing was performed using sewing machines with industrial settings. The samples (with and without seams) were subjected to 3 washing cycles, using two detergents with different formulations. The evaluation of seam pucker was made after the washing and drying cycles on non-ironed shirts.

2.2 Laundering procedure

The laundering was carried out using a front loading domestic washing machine with a horizontal axis under the following conditions: total load weight of 1.8 kg at 60 °C for 106 min. The detergents selected for the laundering procedure had different formulations and were commercially available. The declared composition of the powder detergent (P) was anionic (5–15%) and nonionic (5%) surfactants, soap, phosphate, zeolites, enzymes, polycarbonates, bleaching agent, optical brighteners and fragrances. The liquid detergent (L) was composed of anionic surfactant (15–30%), benzyl benzoate, 2-(4-tetra-butylbenzyl) propyl aldehyde, hexyl-cinnamon aldehyde, coumarin, linalool, formaldehyde and fragrance. The quantity of liquid and powder detergents was 160 ml and 150 g per wash load, respectively. The samples were dried in vertical position at room temperature after the laundering. Three laundering cycles were applied.

2.3 Measurements

The structural and mechanical properties, and air permeability as well as the seam characteristics of cotton shirt fabrics were investigated. The structural properties of cotton shirt fabrics were analysed by assessing fabric weight, warp and weft densities, fabric thickness, yarn linear density and shrinkage after 3 washing cycles. The mechanical properties of cotton shirt fabrics were analysed by evaluating tensile strength and elongation at break. Moreover, the seam characteristics of samples, e.g. seam thickness and seam pucker, were analysed. The investigated properties and the standards applied are shown in Table 2.

2.4 ANOVA analysis of variance

The influence of seam type, laundering process and detergent type on seam pucker was then determined using the ANOVA analysis of variance. One- and two-factor designs were used to structure the experiment, wherein the independent (factor) variables were seam type (3 levels: safety, French and English seams), laundering process (2 levels: un-laundered and laundered) and detergent type (2 levels: powder detergent P and liquid detergent L). The response (dependent) variable was the grade of seam pucker determined by the AATCC Test Method 88B. P-values lower than 0.05 show a significant influence of independent (factor) variables on the investigated property.

3 Results and discussion

3.1 Functional properties of reference and laundered fabrics

The structural properties of tested fabrics are given in Table 3. The selected fabrics weighing between 72 and 126 g/m^2 had an unbalanced woven structure with higher thread density in warp direction (Table 3). The fabrics exhibited shrinkage after the laundering with both detergents, in warp and weft direction, ranging between 0.5–9% and 0.5–4%, respectively (Table 3). Higher shrinkage was noticed in warp direction, due to the stress applied to warp during the weaving. Cotton fibres swell by about

Table 2: Investigated properties and used standards

Property	Standard
Fabric weight	ISO 3801
Warp and weft densities	BS EN 1049-2
Fabric thickness	ISO 5084
Linear density	ISO 7211-5
Shrinkage	BS EN 25077
Tensile strength and elongation at break	BS EN ISO 13934-1
Air permeability	ISO 9237
Seam thickness	ISO 5084
Seam pucker	AATCC 88B

40% in volume when immersed in water [2]. This is mostly accounted by radial swelling, while the longitudinal swelling presents only an increase by about 1–2% in fibre length. In a woven structure, wet relaxation caused by fibre swelling leads to an increase in yarn crimp and thickening of the yarn cross-section. As a result, laundered fabrics have higher fabric weight, fabric warp and weft densities, fabric thickness (Table 3), elongation and tensile strength at break (Table 4). The fabric weight after the laundering increases slightly with the increase in warp and weft densities of a fabric resulting from the shrinkage. Fabric weight after the laundering with both detergents increased from 1.12 to 9.31% (Table 3). Fabric elongation at break and tensile strength increase slightly with the increase in fabric weight, resulting from fabric densities and interlacing yarns. The loss of tensile strength of a cotton shirt fabric after 25 washing cycles was evaluated in our previous paper, where the secondary effects of multiple laundering on cotton shirts were analysed through damage (loss of tensile strength), deposits of inorganic compounds and air permeability [20]. Slightly greater increases in fabric weight, fabric thickness and elongation at break were observed at fabrics laundered with a powder detergent, compared to those washed with a liquid detergent (Tables 3 and 4). As the temperature, time and mechanical action during the laundering were the same for both used detergents, the differences in analysed properties came from different washing product ingredients. The powder detergent contained phosphate and zeolites as chelating agents, polycarbonates as soil dispersing agent, bleaching agent for the removal of stains, and optical brighteners and some fragrances commonly used to mask the odour of other chemical ingredients. Calcium ion binding is pH dependent and deteriorates markedly below pH 9.5. Phosphates provide alkalinity for calcium ion binding and activation of the bleaching system. 10% powder detergent solution provides the pH between 10 and 11. The liquid detergent contained a higher amount of surfactant, benzyl benzoate, linalool, coumarin and formaldehyde as preservative and did not contain bleaching agents; hence, the 10% detergent provided pH from 8.1 to 8.6. The swelling of cotton is pH dependable and is thus higher during the washing in a powder detergent solution than in a liquid detergent solution. A higher degree of swelling led to an increase of yarn crimp (weave angle) thickening of yarn cross-section as well as the fabric [2]. Shrinkage by more than 3% can produce undesirable problems [6].

Air permeability is an important property of fabric since clothing ventilation determines its comfort. However, air permeability is significantly influenced by yarn and fabric properties, e.g. yarn crimp, yarn cross-section, shape of fabric pores [21]. In the

Table 3: Structural properties of reference fabrics (R), and fabrics laundered with powder (P) and liquid (L) detergents

No.	Fabric weight [g/m^2]			Density [cm^{-1}]						Fabric thickness [mm]			Shrinkage [%]			
				Warp			Weft						P		L	
	R	P	L	R	P	L	R	P	L	R	P	L	Warp	Weft	Warp	Weft
A	72.6	75.9	74.8	53.3	60.5	57.7	33.7	40.5	39.0	0.22	0.29	0.25	4	1.5	3	2
B	89.3	97.6	93.5	57.0	64.0	62.3	35.7	44.0	42.3	0.22	0.30	0.27	9	3.5	4	2.5
C	97.2	120.5	116.0	57.3	64.0	63.0	31.3	35.5	34.7	0.24	0.30	0.30	3	3	1	2.5
D	106.7	109.5	107.9	50.0	56.0	54.0	27.7	33.5	32.3	0.26	0.31	0.32	4	1.5	3	0.5
E	108.5	116.3	115.3	47.3	60.0	58.3	29.7	34.5	33.0	0.24	0.30	0.30	1	1	1	1
F	114.2	116.8	117.0	48.0	55.0	53.3	25.0	29.0	28.0	0.25	0.31	0.29	1	2	1	2.5
G	115.5	119.7	120.4	50.0	61.0	60.0	36.0	42.0	40.7	0.33	0.43	0.40	1.5	3	0.5	4
H	115.9	118.7	118.2	51.7	60.0	58.0	31.7	37.0	34.7	0.22	0.29	0.26	2	1.5	1.5	2.3
I	122.1	124.2	122.1	42.7	55.5	47.0	23.0	30.0	25.0	0.24	0.33	0.29	2	1	0	0.5
J	123.2	129.3	124.6	53.3	62.0	60.0	27.0	34.0	31.7	0.35	0.39	0.42	4	1	2.5	0
K	125.8	129.4	130.7	57.3	70.0	67.7	27.0	31.0	29.3	0.29	0.33	0.34	1.5	3	1	3

Table 4: Mechanical properties and comfort of reference (R) fabrics, and fabrics laundered with powder (P) and liquid (L) detergents

No.	Tensile strength $_{(warp)}$ [N]			Elongation at break $_{(warp)}$ [%]			Air permeability [l/(m²/s)]		
	R	P	L	R	P	L	R	P	L
A	463	469	469	7.3	9.9	9.3	466	283	353
B	680	568	632	12.3	18.5	16.3	543	167	280
C	743	789	745	12.8	14.3	13.2	125	81	127
D	504	441	524	12.8	15.6	14.7	273	142	200
E	435	466	435	5.8	6.6	6.2	488	372	472
F	592	634	601	8.3	9.2	8.7	357	285	334
G	683	679	667	7.7	8.0	7.7	474	299	318
H	636	596	641	10.0	10.1	9.9	196	167	200
I	535	529	562	5.8	6.9	6.6	465	409	506
J	600	577	602	16.8	10.1	18.8	75	49	61
K	990	893		13.4	14	14.3	94	61	61

present study, air permeability decreased with an increase in fabric weight. Lighter fabrics, i.e. fabrics A and B, had higher air permeability (Table 4). The increase in shrinkage, fabric weight, and warp and weft densities, and probably the thickening of yarn cross-section and formation of smaller pores after the laundering as well led to lower air permeability. A greater alteration in the structural properties of the fabrics laundered with a powder detergent suggests more intensive changes in the yarn cross-section and pore shape, which determined a decrease in air permeability, compared to the properties of the fabrics washed with a liquid detergent.

The changes in the structural characteristics discussed above may have an influence on seam puckering as well.

3.2 Seam puckering of reference and laundered samples

The results of subjectively evaluating the seam pucker for the analysed seam types at the initial stage of fabrics are shown in Table 5. Grade 5 represents the best

Table 5: Seam pucker and seam thickness of reference (R) samples, and samples laundered with powder (P) and liquid (L) detergents as function of seam type

No.	Seam pucker grade									Seam thickness [mm]								
	Safety			French			English			Safety			French			English		
	R	P	L	R	P	L	R	P	L	R	P	L	R	P	L	R	P	L
A	2	2	2.5	2.33	1	2	3.33	2	3	0.78	0.69	0.66	0.86	0.80	0.90	0.90	0.88	0.99
B	1.66	3	3	3	2.67	3	3.66	3	3	0.78	0.68	0.66	0.91	0.94	1.05	0.96	1.07	1.02
C	3.33	4	4	4	2.67	3.33	4	3	3.33	0.93	0.83	0.84	1.02	1.06	0.98	1.18	1.31	1.13
D	2.33	4	3.5	4	2.33	3.67	4	2.67	3.67	0.86	0.76	0.75	1.06	1.06	1.02	1.18	1.26	1.21
E	3.17	3.5	4	3.33	2	3	4	2.33	3	0.96	0.84	0.76	1.06	1.11	0.95	1.20	1.20	1.06
F	2.66	3	3	2.33	2	2	4	3	3	0.94	0.83	0.89	1.09	1.05	1.03	1.19	1.17	1.19
G	2.67	3	3	4	2.67	2.33	4.33	3	2.33	0.85	0.79	0.85	1.05	1.09	1.15	1.25	1.36	1.32
H	2.66	3	3	3.33	1.33	2	4	2	3	0.88	0.74	0.70	1.09	1.05	0.99	1.20	1.10	1.08
I	3.33	2	3	3	1	3	3.33	2	3	0.90	0.79	0.80	1.10	1.14	1.07	1.34	1.29	1.22
J	2.66	3	4	3.6	3.33	3	4.66	3	3	0.82	0.74	0.74	1.03	1.05	1.02	1.27	1.33	1.31
K	2.75	3	3	4	2.5	4	4	3	2.5	0.80	0.69	0.73	0.97	1.01	1.00	1.16	1.21	1.18

level of seam appearance, while grade 1 represents the poorest one. In general, fabrics react differently to sewing due to their nonlinear structure [22]. The increase in fabric weight and fabric thickness for the reference fabrics resulted in smaller seam puckering for all seam types. Yarns in light fabric weight are aligned in very thin layers that could easily compensate for the sewing thread as it is introduced into the seam. In the case of thin fabrics, there could be sufficient space to accommodate a sewing thread with displacement of yarns. Hence, stitching along a straight line will distort and push adjacent yarns in the fabric, which will cause seam pucker. It is known that thicker and more rigid fabrics crease less [6]. Some dependence was found between fabric weight and seam pucker for the reference samples, and a positive linear correlation between fabric thickness and seam pucker for the English seam (correlation coefficient 0.78). Dependence between fabric thickness and seam pucker was also found for the French seam; however, not for the safety seam.

The average values of seam pucker for the analysed seam types are presented in Figure 2. The results in Figure 2 show that the English seam determined the smallest seam puckering, followed by the French and safety seams. The significant influence of seam type on seam pucker was confirmed by the analysis of variance (ANOVA) (Table 6).

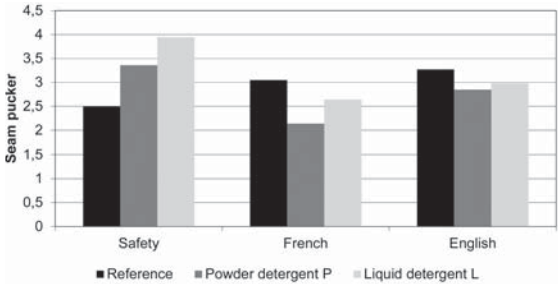

Figure 2: Average values of seam pucker of reference samples, and samples laundered with powder (P) and liquid (L) detergents as function of seam type

The thickness of analysed seam types is shown in Table 5, which reveals that the English seam has the highest seam thickness, followed by the French and safety seams. Furthermore, fabrics of higher weight show higher seam thickness. However, seam thickness also varies within the same type of seam due to the increased fabric weight. A positive linear correlation between the fabric weight and seam thickness was found for the English and French seams (correlation coefficients of 0.87 and 0.74, respectively).

Seam pucker may be acceptable after the sewing, but under the impact of laundering, as the fabric shrinks, puckering may worsen. The results of evaluating the seam pucker of laundered samples with powder and liquid detergents as a function of seam type are shown in Table 5. The influence of seam type on the seam pucker of the samples laundered with a powder detergent P is shown in Figure 2. It may be noted that the safety seam led to the least seam puckering, followed by the English and French seams. A single row of stitches in the safety seam, compared to the French seam, which contains two close rows of stitches and more fabric layers in the seam cross-section (Figure 1), [23] can lead to the least distortion of the material. Thus, it may be concluded that the French seam is more inclined to cause seam pucker. Despite the English seam also containing more rows of stitches (in the first stage two parallel rows and in the second stage an additional one), compared to the French seam, this seam shows less puckering due to the longer distance between the first two rows of stitches. The analysis of variance (ANOVA) confirmed that the seam type is an influencing factor for seam puckering (Table 6). A similar behaviour was found for cotton/polyester shirt fabrics – the safety seam exhibited a higher pucker grade (less puckering), followed by the English and French seams [19].

The influence of seam type on seam puckering for the samples laundered with a liquid detergent L is shown in Figure 2. The safety seam shows the least seam puckering, followed by the English and French seams. This trend could also be observed on the samples subjected to the laundering with a powder detergent P. However, ANOVA confirmed that the seam type did not have a significant influence on the seam pucker for the samples laundered with a liquid detergent L (Table 6). The changes in the structural properties of the laundered samples had a great influence

Table 6: Influence of seam type on seam pucker analysed by p-value (ANOVA analysis of variance)

ANOVA outputs	Dependent variables (responses) – seam pucker grade		
Independent variables (Factors)	Reference	Powder detergent P	Liquid detergent L
Seam type	0.000	0.008	0.185

on the seam thickness. A positive linear correlation between the fabric weight and seam thickness was found for the French (correlation coefficient 0.83) and English (correlation coefficient 0.83) seams subjected to the laundering with a powder detergent P.

The influence of the laundering process and seam type on seam pucker is shown in Figure 2. The seam pucker of the samples washed with a powder detergent P followed the same evolving trend as that for the samples laundered with a liquid detergent L. The safety seam showed the least seam puckering, followed by the English and French seams. The laundering with both detergents affected the seam pucker grades for the English and French seams, while the safety seam was not affected. ANOVA analysis confirmed that the laundering process with both detergents and seam types, as well as their combined effects has a significant influence on seam puckering (Table 7).

However, analysing the influence of the detergent and seam type on seam pucker (Figure 2), a significant difference in seam pucker can be observed. Higher seam puckering was observed when laundering with a powder detergent P, compared to the liquid one. The significant influence of detergent type and seam type on seam pucker was also confirmed by ANOVA analysis (Table 8). The differences in seam pucker on the samples laundered with the two detergent types could be explained by the fact that the samples undergo some quality changes during the laundering, which are also related to the detergent formulation.

4 Conclusion

The present study revealed that the structural and mechanical properties, and air permeability of cotton shirt woven fabrics were affected by laundering after 3 washing cycles because of shrinkage and by detergent type. The laundering with a powder detergent induced a greater increase in fabric weight, fabric thickness and elongation at break, and decreased its air permeability. These changes also influenced seam pucker and seam thickness. Seam type had a significant influence on seam pucker both before and after the laundering; however, generally, laundering increased seam pucker. The safety seam demonstrated the least seam puckering after the laundering, followed by the English and French seams. The reference samples exhibited the opposite trend.

In conclusion, determining the relation between seam pucker, seam type, laundering process and detergent type can help apparel manufacturers in the selection of fabrics.

References

1. RIANA, M. A., GLOY, S. T., GRIES, T. Weaving technologies for manufacturing denim. In *Denim manufacture, finishing and applications*. Edited by Paul Roshan. Aachen, Germany : Woodhead Publishing, 2015, pp 159–186, 10.1016/B978-0-85709-843-6.00006-8.

Table 7: Influence of laundering process and seam type on seam pucker analysed by p-value (ANOVA analysis of variance)

ANOVA outputs	Dependent variables (responses) – seam pucker grade	
Independent variables (Factors)	Powder detergent P	Liquid detergent L
Laundering process	0.000	0.035
Seam type	0.007	0.009
Laundering process*Seam type	0.000	0.000

Table 8: Influence of detergent and seam type on seam pucker analysed by p-value (ANOVA analysis of variance)

ANOVA outputs	Dependent variables (Responses)
Independent variables (Factors)	Seam pucker grade
Detergent type	0.004
Seam type	0.001
Detergent type*Seam type	0.369

2. BISHOP, D. P. Physical and chemical effects of domestic laundering processes. In *Chemistry of the textile industry*. Edited by C. M. Carr. Glasgow, UK : Springer, 1995, pp. 125–171.
3. DOBILAITE, Vaida, JUCEINE, Milda, Mackevičiene, Egle. The influence of technology parameters on quality of fabric assemble. *Materials Science (Medžiagotyra)*, 2013, **19**(4), 428–432, doi: 10.5755/j01.ms.19.4.2482.
4. KUNG, Jin Tae, KIM, Chang Soo, SUL, Hwan In, YOUN, Ryoun Jae, CHUNG, Kwansoo. Fabric surface roughness evaluation using wavelet-fractal method part I: wrinkle, smoothness and seam pucker. *Textile Research Journal*, 2005, **75**(11), 751–760, doi: 10.1177/0040517605058855.
5. DOBILAITĖ, Vaida, JUCIENĖ, Milda. Evaluation of seam pucker using shape parameters. *Materials Science (Medžiagotyra)*, 2010, **16**(2), 154–158.
6. DOBILAITĖ, Vaida, JUCIENĖ, Milda. The influence of mechanical properties of sewing threads on seam pucker. *International Journal of Clothing Science and Technology*, **18**(5), 2006, 335–345, doi: 10.1108/09556220610685276.
7. FAN, J., LEEUWNER, W. The performance of sewing threads with respect to seam appearance. *Journal of Textile Institute*, 1998, **89**(1), 142–154, doi: 10.1080/00405009808658605.
8. MORI, Mori, NIWA, Masako, KAWABATA, Sueo. Effect of thread tension on seam pucker. *Seni I Gakkaishi*, 1997, **3**(6), 217–225, doi: 10.2115/fibre.53.6_2017.
9. FATHY SAYED EBRAHIM, F. The impact of sewing threads properties on seam pucker. *Journal of Basic and Applied Scientific Research*, 2012, **2**(6), 5773–5780.
10. CHOUDHARY, A. K., GOEL, Amit. Effect of some fabric and sewing conditions on apparel seam characteristics. *Journal of Textiles*, **2013**, 2013, 1–7, doi: 10.1155/2013/157034.
11. RUDOLF, Andreja, GERŠAK, Jelka. The effect of drawing on PET filament sewing thread performance properties. *Textile Research Journal*, 2012, **82**(2), 148–160, doi: 10.1177/0040517511420761.
12. RUDOLF, Andreja, GERŠAK, Jelka, UJHELYIOVA, Anna, SFILIGOJ-SMOLE, Majda. Study of PES sewing thread properties. *Fibres and Polymers*, 2007, **8**(2), 212–217, doi: 10.1007/BF02875794.
13. DOBILAITE, Vaida, JUCIENE, Milda. Influence of sewing machine parameters on seam pucker. *Tekstil*, 2007, **56**(5), 286–292.
14. JUCIENĖ, Milda, DOBILAITĖ, Vaida. Seam pucker indicators and their dependence upon the parameters of a sewing machine. *International Journal of Clothing Science and Technology*, 2008, **20**(4), 231–239, doi: 10.1108/09556220810878856.
15. PARK, Kyu Chang, KANG, Jin Tae. Objective evaluation of seam pucker using artificial intelegence part III: Using the objective evaluation method to analyze the effects of sewing parameters on seam pucker. *Textile Research Journal*, 1999. **69**(12), 919–924, doi: 10.1177/004051759906901206.
16. STYLIOS, G., LOYD, D. W. Prediction of seam pucker in garments by measuring mechanical properties and geometrical relationship. *International Journal of Clothing Science and Technology*, 1990, **2**(1), 6–15, doi: 10.1108/eb002954.
17. JUODSNUKYTĖ, Daiva, GUTAUSKAS, Matas, KRAULEDAS, Sigitas. Influence of fabric softeners on performance stability of the textile materials. *Materials Science (Medžiagotyra)*, 2005, **11**(2), 179–182.
18. TRUNCYTĖ, Dainora, DAUKANTIENĖ, Virginija, GUTAUSKAS, Matas. The influence of washing on fabric wearing properties. *Tekstil*, 2007, **56**(8), 493–498.
19. TOSHIKJ, Emilija, JORDANOV, Igor, DEMBOSKI, Goran, MANGOVSKA, Biljana. Influence of seam type and laundering on seam puckering and functional properties of cotton/polyester shirt fabrics. *AATCC Review*, 2015, **15**(2), 41–49, doi: 10.14504/ar.15.2.2.
20. TOSHIKJ, Emilija, JORDANOV, Igor, DEMBOSKI, Goran, MANGOVSKA, Biljana. Influence of multiple laundering on cotton shirts properties. *Tekstil ve Kofeksiyon*, 2016, **26**(4), 393–399.
21. OGULATA, Tugrul. Air permeability of woven fabrics. *Journal of Textile and Apparel, Technology and Management*, 2006, **5**(2), 1–10.
22. PAVLINIC, Zavec Daniela, GERŠAK, Jelka. Investigation of the relation between fabric mechanical properties and behaviour. *International Journal of Clothing Science and Technology*, 2003, **15**(3/4), 231–240, doi: 10.1108/09556220310478332.
23. SEETHARM, G., NAGARAJAN, L. Evaluation of sewing performance of plain twill and satin fabrics based on seam slippage seam strength and seam efficiency. *Journal of Polymer and Textile Engineering*, 2014, **1**(3), 9–21, doi: 10.9790/019X-0130921.

Tanja Furlan, Ivan Nešković, Nina Špička, Barbara Golja, Mateja Kert, Brigita Tomšič, Marija Gorjanc, Barbara Simončič
University of Ljubljana, Faculty of Natural Sciences and Engineering, Aškerčeva 12, 1000 Ljubljana, Slovenia

Multifunctional Hydrophobic, Oleophobic and Flame-retardant Polyester Fabric

Večfunkcionalna vodo- in oljeodbojna ter ognjevarna poliestrska tkanina

Original Scientific Article/*Izvirni znanstveni članek*
Received/*Prispelo* 11-2018 • Accepted/*Sprejeto* 1-2019

Abstract

Technical textile materials with multifunctional protective properties represent one of the largest and fast growing segments of the textile industry. Multifunctional water- and oil-repellent and flame-retardant coating on polyester (PES) fabric was prepared in this research using fluoroalkyl-functional siloxane (FAS) as the water- and oil-repellent finishing agent and organophosphonate (OP) as the flame-retardant agent. A finishing solution containing FAS and OP of appropriate concentrations was applied to the untreated and oxygen plasma-treated PES fabric samples using the pad-dry-cure method. For comparison, single-component FAS and OP finishing solutions were applied to the fabric samples under the same conditions. The coated PES samples were washed under standard conditions. The morphological, chemical and functional properties of the coated PES samples were determined with scanning electron microscopy, Fourier transform infrared spectroscopy, wet pick up, liquid contact and sliding angles measurements as well as oil repellence and vertical burning tests. The results reveal that oxygen plasma treatment prior to finishing significantly increased the wettability of the PES fibres, which directly resulted in increased concentration of the absorbed finishing agents. This treatment enabled the creation of PES fabric with simultaneous superhydrophobic, oleophobic and flame-retardant properties. Although the superhydrophobic and oil-repellent characteristics of the coating were preserved after washing, the flame retardancy was hindered because of the removal of OP in the washing bath.

Keywords: polyester fibre, finishing, multifunctional properties, water and oil repellence, flame retardancy, washing fastness

Izvleček

Tehnični tekstilni materiali z večfunkcionalnimi zaščitnimi lastnostmi so eden največjih in najhitreje rastočih segmentov tekstilne industrije. V raziskavi so pripravljene večfunkcionalne vodo- in oljeodbojne ter ognjevarne apreture na poliestrski (PES) tkanini z uporabo fluoroalkil-funkcionalnega siloksana (FAS) kot vodo- in oljeodbojnega apreturnega sredstva in organofosfonata (OP) kot ognjevarnega apreturnega sredstva. Apreturna kopel, ki je vključevala FAS in OP ustrezne koncentracije, je bila nanesena na neobdelano in s plazmo kisika predhodno obdelano tkanino PES s postopkom, ki je vključeval impregniranje, sušenje in kondenziranje. Za primerjavo sta bili na tkanino PES pri enakih pogojih naneseni tudi enokomponentni apreturni kopeli s FAS oziroma z OP. Apretirani vzorci tkanine PES so bili oprani pri standardnih pogojih. Morfološke, kemijske in funkcionalne lastnosti apretiranih vzorcev so bile določene z vrstično elektronsko mikroskopijo, infrardečo spektroskopijo s Fourierjevo transformacijo, nanosom kopeli, stičnimi koti in koti zdrsa tekočin, oljeodbojnostjo in ognjevarnostjo. Iz rezultatov je razvidno, da je obdelava s plazmo kisika pred apretiranjem močno povečala omočljivost vlaken PES, kar je neposredno vplivalo na povečanje koncentracije adsorbiranih apreturnih sredstev. Takšna kombinacija obdelave je

Corresponding author/*Korespondenčna avtorica:*
Prof dr. Barbara Simončič
E-mail: barbara.simoncic@ntf.uni-lj.si

Tekstilec, 2019, 62(1), 12-22
DOI: 10.14502/Tekstilec2019.62.12-22

omogočila pripravo tkanine PES s hkratnimi superhidrofobnimi, oleofobnimi in ognjevarnimi lastnostmi. Medtem ko sta se superhidrofobnost in oleofobnost ohranili tudi po pranju, se je ognjevarnost poslabšala zaradi postopne odstranitve sredstva OP med pranjem.
Ključne besede: poliestrsko vlakno, apretura, večfunkcionalne lastnosti, vodo- in oljeodbojnost, ognjevarnost, pralna obstojnost

1 Introduction

Technical textile materials with multifunctional protective properties represent one of the largest and fast growing segments of the textile industry, and these materials have wide uses in different economic sectors. In technical applications, polyester fibres are the most frequently used synthetic material because of their low cost, durability, ease of care, good dimensional stability, low moisture absorbency and compatibility with cotton in blends [1]. These extraordinary properties enable polyester to be increasingly applied in the production of textile materials for protective clothing and in the sport and leisure, transportation, construction and agricultural industries.

However, in addition to the desired characteristics, polyester fibres suffer from certain important disadvantages related to their functionality, such as electrostatic charging and flammability, which decrease the value and usefulness of the end products. The susceptibility of polyester fibres to electrostatic problems is directly influenced by their hydrophobicity, leading to generation and accumulation of electrostatic charges [2–4]. The latter attract particulate soils from the air, resulting in fibre soiling. In contrast, due to the hydrophobic properties of polyester, wetting and swelling of fibres with detergent solution during laundering is hindered, which importantly decreases the effectiveness of removal of the adhered soil [5–7]. To overcome these problems, tailoring of a self-cleaning coating characterised by superhydrophobic, oleophobic and low-adhesive properties is crucial. According to the theory, self-cleaning biomimetic solid surfaces exhibit low-adhesion superhydrophobicity, which is simultaneously characterised by a static water contact angle greater than 150° and a water sliding angle less than 10° as a result of a low contact angle hysteresis [8]. These surfaces include micro- and nanoscale roughness topographies coated with water-repellent polymer films [9–12]. However, in addition to particulate soils, oily stains are important contaminants of textile fibres, and thus creation of a coating with oleophobicity is of great importance. A coating that is simultaneously oleophobic and self-cleaning could effectively repel different types of soils and prevent their adhesion as well as ensure removal of adherent soils via their collection by water droplets when rolling off the surface.

Inherent flammability with intensive burning melt/dripping and release of toxic smoke represents a serious hazardous drawback of polyester, which poses great risk and danger to human lives and material goods [13]. Because highly effective flame retardants including brominated diphenyl esters, brominated phosphates and tri-aryl-phosphates have been restricted and prohibited by the European Union's Registration, Evaluation and Authorisation of Chemicals (REACH) because of their toxicological problems and environmental unsustainability, different environmentally friendly phosphorous-containing compounds have been synthesised to produce flame-retardant polyester [14–16]. The flame-retardant mechanism of phosphorous-containing compounds is directly influenced by their chemical structure. In general, depending on the oxidation state of the phosphorous atom, flame-retardant substances are active in both the condensed phase and the gas phase [14, 17, 18]. In the condensed phase, phosphorous compounds promote char formation by influencing the fibre decomposition pathway, and in the gas phase, phosphorous compounds decompose to radical scavengers, which terminate oxidative radical chain reactions in the combustion cycle.

In this study, we first prepared multifunctional water- and oil-repellent and flame-retardant polyester fabric with the use of two chemical finishes, i.e., fluoroalkyl-functional siloxane as a water- and oil-repellent agent and organophosphonate as a flame-retardant agent. To enhance the hydrophilicity of polyester fibres and consequently increase their absorptivity to the finishing solution, fibre functionalisation with oxygen-rich groups was performed using an oxygen plasma pretreatment. It has been established that oxygen plasma treatment can cause an increase in the surface activity and also an increase in surface roughness [19–23], therefore an important goal of our research was to

investigate whether the coating exhibits self-cleaning properties. To determine the coating durability, the functional properties of polyester fabric were investigated before and after washing.

2 Experimental

2.1 Textile material and finishing agents

Plain-weave 100 % polyester (PES) woven fabric with a weight of 67 g/m^2 was used in the study. The fabric was washed with a solution of non-ionic surfactant at a concentration of 2.5 g/l. After washing, the fabric was rinsed in distilled water, squeezed and dried at room temperature. Two commercially available finishing agents were chosen, i.e., fluoroalkyl-functional water-born siloxane (FAS) as a water- and oil-repellent agent under the trade name Dynasylan F 8815 (Degussa, Germany) and organophosphonate (OP) as a flame-retardant agent under the trade name Apyrol CEP (Bezema, Switzerland). Both finishing agents can be mixed with water to any desired concentration.

2.2 Plasma treatment, finishing and washing

PES fabric samples with a size of 20 x 20 cm were treated with oxygen plasma (O_2 gas) for 30 seconds under 60 Pa pressure in a low-pressure inductively coupled radiofrequency plasma system.

Untreated and plasma-treated PES samples were finished with a mixture of 100 g/l FAS and 200 g/l OP using the pad-dry-cure process. Acetic acid was used in pH adjustment of the finishing bath to pH 4–5. The process included full immersion of samples for one minute at room temperature, squeezing between padded rollers at a constant pressure and roller velocity, followed by drying at 100 °C and curing at 150 °C for 5 minutes. For comparison, single-component FAS and OP finishing agents were also applied to the untreated and plasma treated PES samples under the same conditions. The PES samples codes and the procedures for the fabric surface modifications are listed in Table 1.

The finished PES samples were washed in a Gyrowash 815 (James Heal, UK) testing instrument according to the EN ISO 105C06 standard. Washing was performed in 150 ml of 4 g/l ECE phosphate reference detergent B solution at 40 °C for 45 min in the presence of ten steel balls that supply an accelerated washing treatment that corresponds to 5 domestic washes. After washing, the samples were rinsed in distilled water at 40 °C, rinsed in cold tap water, and dried at room temperature.

Table 1: PES fabric sample codes and procedures for fabric surface modifications

Sample code	Procedure of the fabric surface modification
PES-Un	No treatment
PES-P	Plasma treatment
PES/FAS	Finishing with 100 g/l FAS
PES-P/ FAS	Plasma treatment followed by finishing with 100 g/l FAS
PES/OP	Finishing with 200 g/l OP
PES-P/OP	Plasma treatment followed by finishing with 200 g/l OP
PES/ FAS+OP	Finishing with the mixture of 100 g/l FAS and 200 g/l OP
PES-P/ FAS+OP	Plasma treatment followed by finishing with the mixture of 100 g/l FAS and 200 g/l OP

2.3 Analytical methods

Wettability of PES fabric samples

The wettability of PES fabric samples was determined based on the amount of the finishing solution applied to the samples in the "wet on dry" process. To this end, the pressure and the velocity of the padded rollers were set to 300 kPa and 1.5 m/min, respectively, and held constant during the squeezing process. The amount of the applied finishing solution was referred to as the wet pickup (WPU), which was calculated by the following equation [2]:

$$WPU = \frac{mass\ of\ sollution\ applied}{mass\ of\ dry\ fabric\ sample} \times 100\ (\%) \qquad (1)$$

Five measurements were performed for each sample, and the corresponding WPU value was reported in terms of the mean value and the standard error.

Scanning electron microscopy (SEM)

SEM images of the untreated and treated PES fibres were obtained using a JSM 6060 LV scanning electron microscope (JEOL, Japan) operated with a primary electron beam accelerated at 10 kV. All samples were coated with a thin layer of gold prior to observation to supply conductivity and enhance the quality of the images.

Fourier transform infrared (FT-IR) spectroscopy
Fourier transform infrared (FT-IR) spectra were obtained on a Spectrum GX I spectrophotometer (Perkin Elmer, Great Britain) equipped with an attenuated total reflection (ATR) cell and a diamond crystal (n = 2.0). The spectra were recorded over a range of 4000 cm^{-1} to 600 cm^{-1} using 32 scans at a resolution of 4 cm^{-1}.

Contact angle measurements
The static contact angles θ of water and n-hexadecane on the PES samples were measured using a DSA 100 contact angle goniometer (Krüss, Germany). Liquid droplets of 5 μl were placed on different points of each fabric sample, and the values of θ were determined after 30 seconds of droplet deposition using the Young-Laplace fitting method. Ten measurements were collected for each fabric sample, and the corresponding θ value was reported as the mean value and the standard error.

Sliding angle measurements
The water-sliding (or roll-off) angles α were measured in the warp direction of the fabric samples and determined as the critical angle at which the droplet of 50 µl began to slide or roll off the gradually inclined fabric surface. Five measurements were collected for each fabric sample, and the corresponding α value was reported as the mean value of the standard error.

Oil-repellent properties
The oil repellence of the PES samples was determined under static conditions using AATCC test method 118-1978 with eight hydrocarbon liquids in a series of decreasing surface tension. Paraffin oil was denoted with the rating number 1 and n-heptane was given the rating number 8. Drops of the standard test liquids were placed on the fabric surface and observed for wetting. The repellence rating was the highest numbered test liquid that did not wet the fabric in 30 seconds.

Vertical test of flammability
The combustion behaviour was determined via the vertical test of flammability according to DIN 53906. A fabric sample of size 15 × 7.5 cm, arranged vertically, was exposed to a propane flame for 6 s at the bottom of the sample. After removal of the flame source, the after-flame time and after-glow time were determined. Seven measurements were collected for each sample in the warp direction, and the measured quantities were reported as the mean values and the standard deviations.

3 Results and discussion

3.1 Characterisation of PES fabric samples

The results of WPU are presented in Figure 1. It can be observed that the value of WPU is directly influenced by the sample pretreatment as well as the characteristics of the finishing solutions. Plasma treatment of fabric samples prior to the finishing process significantly increased the WPU of all finishing solutions regardless of their properties, which was attributed to the increased wettability of the plasma-treated PES fibres. This result confirms that the oxygen plasma treatment caused the formation of new polar functional groups on the surface of PES fibres, which significantly increases their hydrophilicity and thus their wettability. The enhanced fibre wettability directly resulted in an increased concentration of the absorbed finishing agents. Furthermore, in the case of the untreated fabric samples, the surface tension of the finishing solution importantly influenced the WPU. Accordingly, the WPU of the FAS solution with low surface tension was 2 times lower than the WPU of the high-surface-tension PO solution. Because this phenomenon was insignificant in the case of the plasma-treated samples, this difference represents an important advantage of oxygen plasma treatment of hydrophobic textile fibres.

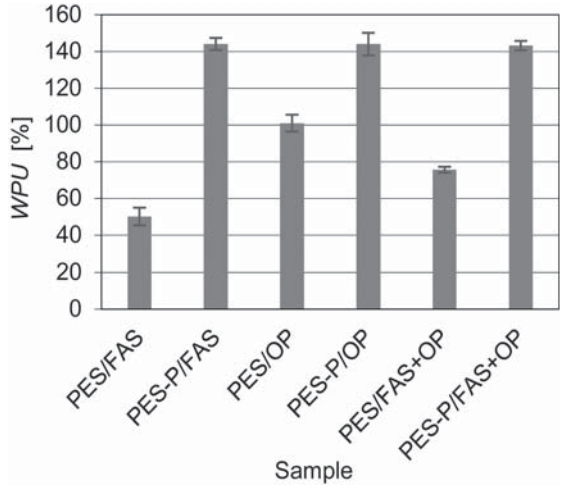

Figure 1: Wet pickup (WPU) of untreated and plasma-treated fabric samples

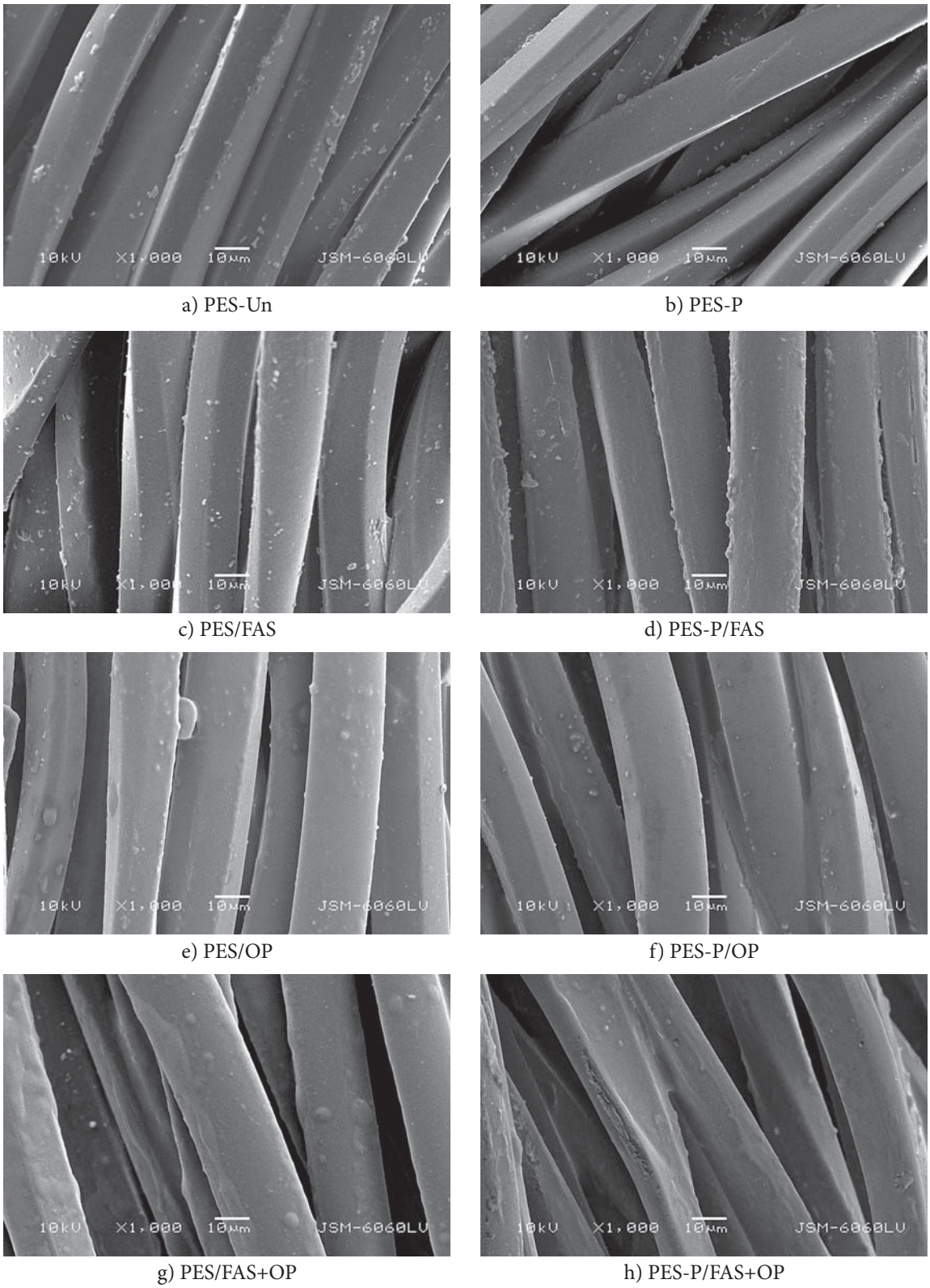

a) PES-Un

b) PES-P

c) PES/FAS

d) PES-P/FAS

e) PES/OP

f) PES-P/OP

g) PES/FAS+OP

h) PES-P/FAS+OP

Figure 2: SEM images of untreated and plasma-treated PES fibres and PES fibres finished with different finishing solutions

SEM images of the PES fibres before and after different procedures for the fabric surface modifications are presented in Figure 2. It can be observed from the images that the oxygen plasma treatment did not significantly change the surface morphology of the fibres, suggesting that the bulk properties of the fibres remained undamaged. It is also evident that the applied finishing agents coated the fibres, which caused light thickening and gluing of the fibres in certain places on the surface. The latter was the most pronounced when the mixture of FAS and OP was applied to the plasma-treated fabric sample. Figure 3 shows the ATR FT-IR spectra of representative plasma-treated and finished PES fabric samples as well as the untreated sample for comparison. In all spectra, the following bands that are characteristic for PES fibres can be observed: the absorption band of low intensity at 3340 cm^{-1} due to intermolecular O–H bonds; the absorption bands in the 3000–2850 cm^{-1} spectral region attributed to stretching of νCH_2, νCH_3 and C–H; the absorption band at 1710 cm^{-1} due to strong C=O stretching vibrations of the carbonyl group of the ester bond; the band at 1577 cm^{-1} due to asymmetric stretching of the C–O bond of the carboxylate anions; the absorption bands at 1372, 1338, 1240 and 1095 cm^{-1} caused by the δ(C–O) and ν_{as}(C–O–C) vibrations of the polyester fibres; and the absorption bands at 848, 793 and 721 cm^{-1} due to the C–H and C–C vibrations of the benzene ring [24, 25]. The oxygen plasma treatment did not change the spectrum of the PES fibres, which suggests that the concentration of new functional groups incorporated onto the fibre surface was too low to be detected by FT-IR spectroscopy. Furthermore, in the case of the PES-P/FAS sample, the bands belonging to the FAS finishing agent at 1238 cm^{-1} due to $\nu_a(CF_2)$ mixed with rocking (CF_2), at 1144 cm^{-1} due to $\nu_s(CF_2)$ modes, and at 1208 cm^{-1} due to $\nu_a(CF_2)$ and $\nu_a(CF_3)$ vibrations [24, 26, 27] were blurred by the polyester fingerprint. The same applies to the band at 1227 cm^{-1} in the spectrum of the PES-P/OP sample, which corresponds to the P=O bonds of phosphonate [24, 28] and is characteristic of the OP finishing agent. However, a detailed insight into the spectrum of the PES-P/OP sample reveals an appearance of a broad band of low intensity at 930 cm^{-1} due to P–O stretching vibrations of phosphonate [24].

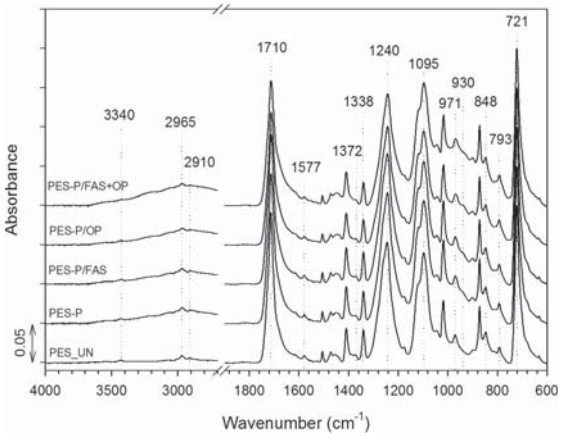

Figure 3: ATR spectra of representative PES fabric samples: PES-Un, PES-P, PES-P/FAS, PES-P/OP and PES-P/FAS+OP

3.2 Functional properties of PES fabric samples

The results of the water and n-hexadecane static contact angle measurements on the unwashed and washed samples containing FAS are presented in Figures 4 and 5. For the PES fabric samples that were not finished with FAS, i.e., PES-Un, PES-P, PES/OP and PES-P/OP, the liquid static contact angles were less than 90° and therefore could not be measured. The results in Figure 4 reveal that the presence of the FAS coating supplied excellent water repellence to the PES fibres, with contact angles in the range of 148° to 153°, which could be characterised as notably high superhydrophobic properties. A comparison of the PES/FAS and PES-P/FAS samples shows that pretreatment of PES fibres with oxygen

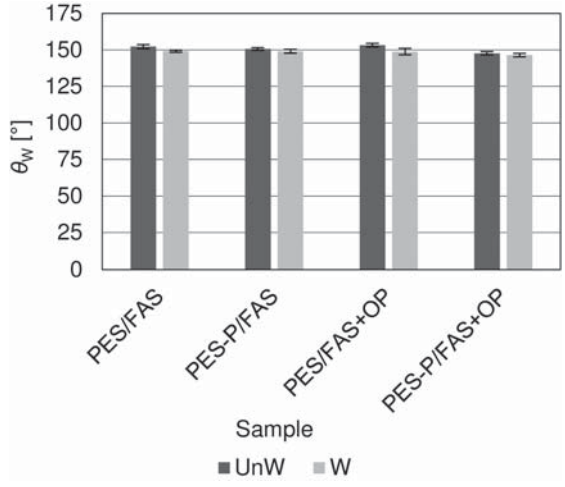

Figure 4: Static contact angles of water (θ_w) determined on unwashed (UnW) and washed (W) PES fabric samples finished with FAS

plasma did not improve their water repellence, despite the fact that the WPU and the concentration of the applied FAS were increased on the plasma-treated sample. This result suggests that the FAS coating can create a superhydrophobic fabric surface at notably low concentration. The higher WPU of the FAS and OP mixture for the PES-P/FAS+OP sample compared with the PES/FAS+OP sample resulted in a slight reduction in water repellence. The reason for this result was attributed to a higher uptake of the hydrophilic OP finishing agent in the mixture, which hindered the superhydrophobic performance of FAS but still resulted in notably high hydrophobicity with a water contact angle equal to 148°. The FAS coating exhibited excellent washing fastness with an insignificant decrease of the water contact angles in the case of all washed samples.

However, the concentration of FAS uptake by the untreated PES/FAS and PES/FAS+OP samples was too low to supply sufficient oleophobicity of the PES fibres. On these samples, n-hexadecane did not form stable drops of constant shapes on the fabric surface but slowly spread and penetrated into its porous structure, which resulted in a decrease of the contact angles and therefore prevented the static contact angle measurements. In contrast, the increase of the WPU of the oxygen plasma-treated PES fibres (PES-P/FAS and PES-P/FAS+OP samples) influenced the creation of the uniform oleophobic FAS coating with n-hexadecane contact angles in the range of 120 to 124°, which exceeded 119° even after sample washing. Accordingly, oxygen plasma treatment prior to the finishing process is crucial to supply simultaneous water repellence and oil repellence properties to PES fibres.

To determine whether the superhydrophobic PES fabric samples are self-cleaning, the sliding angles of water were determined and are presented in Figure 6. As shown in Figure 6, the lowest water sliding angles of 15° and 13° were obtained for the PES/FAS and PES-P/FAS samples, respectively, indicating the nearly full self-cleaning properties of these samples. However, to decrease the water sliding angle, the low surface free energy micro- to nanostructured roughness of the fibres surface should be created in the chemical modification process, which could allow air to become trapped in the fibre topography, thus creating a composite surface that minimises the solid/water interface and maximises the water/air surface area. However, according to the SEM images, the oxygen plasma treatment and the finishing process did not significantly affect the topography of the PES fibres, which remained nearly unchanged. The results also show that the presence of OP in the coating increased the water sliding angles of the PES/FAS+OP and PES-P/FAS+OP samples to a great extent due to the sticking of the water droplet to the fibre surfaces. This phenomenon indicates that the hydrophilic character of OP strongly increased the adhesion between water and the coating. It is clear that OP does not contribute to creation of the self-cleaning properties of the

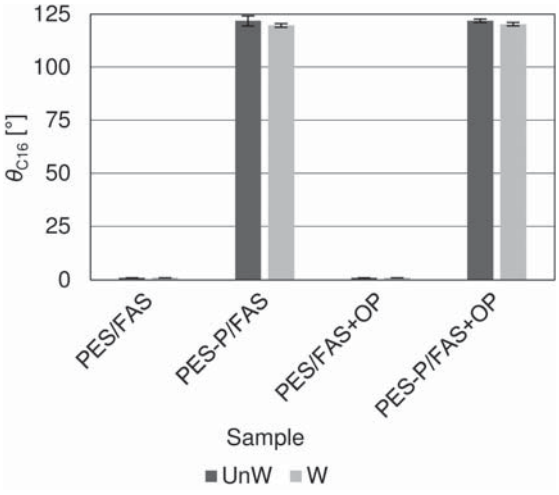

Figure 5: Static contact angles of n-hexadecane (θ_{C16}) determined on unwashed (UnW) and washed (W) PES fabric samples finished with FAS

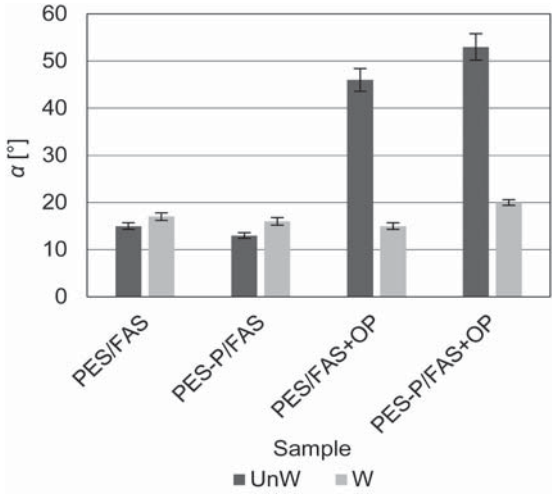

Figure 6: Sliding angles of water (α) determined on unwashed (UnW) and washed (W) PES fabric samples finished with FAS

coating. Although the water sliding angles for the PES/FAS and PES-P/FAS samples only slightly increased after washing, the water sliding angles dramatically decreased for the PES/FAS+OP and PES-P/FAS+OP samples. This result suggests that the coating structure was changed during washing and that the OP finishing agent released from the fibre surface.

The results of the oil repellence rating summarised in Table 2 gave additional information to the results presented in Figure 5. Although n-hexadecane penetrated into the PES fabric porous structure of the PES/FAS and PES/FAS+OP samples, the mixture of paraffin oil and n-hexadecane with a 1.6 mN/m higher surface tension than n-hexadecane did not wet these samples in 30 minutes. Because the same applies for paraffin oil, this result indicates that the PES/FAS and PES/FAS+OP samples were still repellent for different oils. The results in Table 2 also show the high oleophobicity of the PES-P/FAS and PES-P/FAS+OP samples, which repelled even n-decane with much a lower surface tension than n-hexadecane. The sample repellence only slightly deteriorated after washing.

The results of the burning behaviour of the PES fabric samples determined by the vertical test of flammability are summarised in Table 3. The results show that the samples differ from each other in the after-flame time and that none of the samples exhibited after-glow behaviour. The PES-Un and PES-P samples ignited easily and burned for between 20 and 30 seconds after the withdrawal of the igniting flame, and the time of burning significantly increased if the single-component FAS coating was present on the samples. This result suggests that the FAS polymer film stabilised the PES melt in the pyrolysis zone, causing prolongation of the burning time. In contrast, the presence of OP in the coating supplied excellent flame-retardant behaviour to the PES/OP and PES-P/OP samples, which did not burn after flame withdrawal and showed superior self-extinguishing behaviour. The application of FAS in combination with OP significantly impaired the flame retarding efficiency of OP, which was reflected by the increased after-flame time of the PES/FAS+OP sample, suggesting that the concentration of the adsorbed OP was too low to provide sufficient flame retardancy. Nevertheless, as stated before, plasma treatment influenced the increase of the FAS and OP adsorption, resulting in an excellent flame-retardant behaviour to the PES-P/FAS+OP sample which was comparable to that of the samples PES/OP and PES-P/OP. However, the results of burning behaviour of washed samples reveal that OP was neither covalently bonded to the PES fibre surface nor to the FAS polymer network but was only physically incorporated into the coating, which resulted in the movement of OP from the PES fibres during the washing process. Consequently, all washed PES fabric samples burned easily. These results also confirm our assumption based on the water sliding angle measurements that the reason for the sliding angle decrease on the PES/FAS+OP and PES-P/FAS+OP samples after washing was the absence of the OP finishing agent.

Table 2: Oil repellence rating of unwashed (UnW) and washed (W) PES fabric samples finished with FAS determined under static conditions using AATCC test method 118-1978.

Sample	Rating number[a)]		Test liquid[b)]		Surface tension[c)] [mN/m]	
	UnW	W	UnW	W	UnW	W
PES/FAS	2	1	PO:C16 (65:35)	PO	28.7	31.2
PES-P/FAS	6	5	C10	C12	23.5	25.1
PES/FAS+OP	2	2	PO:C16 (65:35)	PO:C16 (65:35)	28.7	28.7
PES-P/FAS+OP	6	5	C10	C12	23.5	25.1

a) Rating is the highest numbered test liquid which did not wet the fabric in 30 seconds.

b) Name of the highest numbered test liquid: PO – paraffin oil, C16 – n-hexadecane, C12 – n-dodecane, C10 – n-decane.

c) Surface tension of the highest numbered test liquid at 25 °C.

Table 3: After-flame time t_F and after-glow time t_G of unwashed (UnW) and washed (W) PES fabric samples determined via the vertical test of flammability according to DIN 53906

Sample	t_F [s]		t_G [s]	
	UnW	W	UnW	W
PES-Un	27 ± 3	25 ± 5	0	0
PES-P	24 ± 3	26 ± 3	0	0
PES/FAS	44 ± 5	32 ± 6	0	0
PES-P/FAS	43 ± 7	41 ± 5	0	0
PES/OP	0	25 ± 4	0	0
PES-P/OP	0	18 ± 4	0	0
PES/FAS+OP	14 ± 3	43 ± 5	0	0
PES-P/FAS+OP	0	45 ± 6	0	0

4 Conclusion

In this research, we successfully tailored the multifunctional superhydrophobic, oleophobic, and flame-retardant coating on PES fabric using a two-step chemical modification procedure consisting of oxygen plasma treatment followed by pad-dry-cure application of an FAS and OP mixture. A comparison of the functional properties of PES fabric treated by the FAS and OP mixture with those treated by single-component FAS or OP finishing solutions reveals the following:

- Application of the FAS finishing agent supplied washing-resistant superhydrophobic properties to the PES fibres, which was insignificantly affected by the presence of OP in the mixture;
- Oxygen plasma treatment of the surface of PES fibres dramatically increased the wet pick up of the fibres and therefore preserved the conditions for the creation of the uniform oleophobic coating with n-hexadecane contact angles in the range of 120 to 124°, which exceeded 119° even after sample washing;
- The presence of OP in the coating notably increased the water sliding angles because of the enhanced adhesion between water and the PES fibres surface, resulting in complete deterioration of the self-cleaning properties;
- Application of the OP finishing agent created excellent flame-retardant behaviour of the PES fibres, which did not burn after flame withdrawal and showed superior self-extinguishing behaviour;
- The flame retardancy of the PES fibres was not wash-resistant because OP was only physically incorporated into the coating and was removed during the washing process.

Acknowledgements

This work was carried out in the framework of the courses Advanced Finishing Processes and Chemical Functionalisation of Textiles in the Master Study Programme, Textile and Clothing Planning. The research was supported by the Slovenian Research Agency (Program P2-0213, Infrastructural Centre RIC UL-NTF). The authors would like to thank the employees at the Department of Surface Engineering and Optoelectronics at Jožef Stefan Institute who enabled us to work on plasma.

References

1. EAST, A. J. Polyester fibres. In Synthetic fibres: nylon, polyester, acrylic, polyolefin. Edited by J. E. McIntyre. Cambridge : Woodhead Publishing, 2005, pp. 95–166.
2. SCHINDLER, W. D. and HAUSER, P. J. Chemical finishing of textiles. Cambridge : Woodhead Publishing, 2004, pp. 121–128.
3. PERUMALRAJ, Rathinam. Characterization of electrostatic discharge properties of woven fabrics. Journal of Textile Science & Engineering, 2016, 6(1), 6, doi:10.4172/2165-8064.1000235.
4. SUH, M., SEYAM, A. M., OXENHAM W., THEYSON T. Static generation and dissipation

of polyester continuous filament yarn, The Journal of The Textile Institute, 2010, 101(3), 261–269, doi: 10.1080/00405000802377250.
5. DATYNER, Arved. Surfactants in textile processing. New York, Basel: Marcel Dekker, 1983, pp. 1–65.
6. ISLAM, Md. Mazedul, KHAN, Adnan Maroof. Functional properties improvement and value addition to apparel by soil release finishes – A general overview. Research Journal of Engineering Sciences, 2013, 2(6), 35–39.
7. KALAK, Tomasz, CIERPISZEWSKI, Ryszard. Correlation analysis between particulate soil removal and surface properties of laundry detergent solutions. Textile Research Journal, 2015, 85(18), 1884–1906, doi: 10.1177/0040517515578329.
8. ZHANG, Xi, SHI, Feng, NIU, Jia, JIANG, Yugui, WANG, Zhiqiang. Superhydrophobic surfaces: from structural control to functional application. Journal of Materials Chemistry, 2008, 18, 621–633, doi: 10.1039/b711226b.
9. BAE, Geun Yeol, JEONG, Young Gyu, MIN, Byung Gil. Superhydrophobic PET Fabrics achieved by silica nanoparticles and water-repellent agent. Fibers and Polymers, 2010, 11(7), 976–981, doi: 10.1007/s12221-010-0976-x.
10. ZHOU, Cailong, CHEN, Zhaodan, YANG, Hao, HOU, Kun, ZENG, Xinjuan, ZHENG, Yanfen, CHENG, Jiang. Nature-inspired strategy toward superhydrophobic fabrics for versatile oil/water separation. ACS Applied Materials and Interfaces, 2017, 9(10), 9184–9194, doi: 10.1021/acsami.7b00412.
11. OH, Ji-Hyun, PARK, Chung Hee. Robust fluorine-free superhydrophobic PET fabric using alkaline hydrolysis and thermal hydrophobic aging process. Macromolecular Materials and Engineering, 2018, 303(7), doi: 10.1002/mame.201700673.
12. ROSU, Cornelia, LIN, Haisheng, JIANG, Lu, BREEDVELD, Victor, HESS, Dennis W. Sustainable and long-time 'rejuvenation' of biomimetic water-repellent silica coating on polyester fabrics induced by rough mechanical abrasion. Journal of Colloid and Interface Science, 2018, 516, 202–214, doi.org/10.1016/j.jcis.2018.01.055.
13. ALONGI, Jenny, HORROCKS, Richard A., CAROSIO, Federico, MALUCELLI, Giulio. Update on flame retardant textiles: State of the art, environmental issues and innovative solutions. Shawbury : Smithers Rapra Technology, 2013, pp. 207–239.
14. WEIL, Edward D., LEVCHIK, Sergei V. Flame retardants for plastics and textiles : practical applications. Munich : Carel Hanser, 2016, pp. 141–160, doi: 10.3139/9783446430655.
15. ALONGI, Jenny, CIOBANU Mihaela, TATA, Jennifer, CAROSIO, Federico, MALUCELLI, Giulio. Thermal stability and flame retardancy of polyester, cotton, and relative blend textile fabrics subjected to sol–gel treatments. Journal of Applied Polymer Science, 2011, 119, 1961–1969, doi: 10.1002/app.32954.
16. JIANG, Zhenlin, WANG, Chaosheng, FANG, Shuying, JI, Peng, WANG, Huaping, JI, Chengchang. Durable flame-retardant and antidroplet finishing of polyester fabrics with flexible polysiloxane and phytic acid through layer-by-layer assembly and sol-gel process. Journal of Applied Polymer Science, 2018, 135(27), 46414, doi: 10.1002/app.46414.
17. Fire retardant materials. Edited by A. R. Horrocks, D. Price. Cambridge : Woodhead Publishing, 2001, pp. 31–181.
18. VELENCOSO, Maria M., BATTIG, Alexander, MARKWART, Jens C., SCHARTEL, Bernhard, WURM, Frederik R. Molecular firefighting – how modern phosphorus chemistry can help solve the flame retardancy task. Angewandte Chemie-International Edition, 2018, 57(33), 10450–10467, doi: https://doi.org/10.1002/anie.201711735.
19. VESEL, Alenka, JUNKAR, Ita, CVELBAR, Uroš, KOVAČ, Janez, MOZETIC, Miran. Surface modification of polyester by oxygen- and nitrogen-plasma treatment. Surface and Interface Analasis, 2008, 40(11), 1444–1453, doi 10.1002/sia.2923.
20. ZHANG, Chunming, ZHAO, Meihua, WANG, Libing, QU, Lijun, MEN, Yajing. Surface modification of polyester fabrics by atmospheric-pressure air/He plasma for color strength and adhesion enhancement. Applied Surface Science, 2017, 400, 304–311, doi: 10.1016/j.apsusc.2016.12.096.
21. NOVÁK, I., POPELKA, A., LUYT, A. S., CHEHIMI, M. M., ŠPÍRKOVÁ, M., JANIGOVÁ I., KLEINOVÁA, A., STOPKA, P., ŠLOUF, M. VANKO, V., CHODÁK, I., VALENTIN, M.

Adhesive properties of polyester treated by cold plasma in oxygen and nitrogen atmospheres. Surface and Coatings Technology, 2013, 235, 407–416, doi: 10.1016/j.surfcoat.2013.07.057.

22. ÖMEROĞULLARI, Zeynep, KUT, Dilek. Application of low-frequency oxygen plasma treatment to polyester fabric to reduce the amount of flame retardant agent. Textile Research Journal, 2012, 82(6), 613–621, doi: 10.1177/0040517511420758.
23. GOUVEIA, Isabel C., ANTUNES, Laura C., GOMES, Ana P. Low-pressure plasma treatment for hydrophilization of poly(ethylene terephthalate) fabrics. The Journal of The Textile Institute, 2011, 102(3), 203–213, doi: 10.1080/00405001003616777.
24. SOCRATES, George. Infrared and Raman characteristic group frequencies: Tables and charts. 3rd ed., Chichester, et al. : John Wiley & Sons, 2001.
25. PARVINZADEH, Mazeyar, MORADIAN, Siamak, RASHIDI, Abosaeed, YAZDANSHENAS, Mohamad-Esmail. Surface characterization of polyethylene terephthalate/silica nanocomposites. Applied Surface Science, 2010, 256(9), 2792–2802, doi: 10.1016/j.apsusc.2009.11.030.
26. LENK, T. J., HALLMARK, V. M., HOFFMANN, C. L., RABOLT, J. F., CASTNER, D. G., ERDELEN, C. & RINGSDORF, H. Structural investigation of molecular-organization in self-assembled monolayers of a semifluorinated amidethiol. Langmuir, 1994, 10, 4610–4617, doi: 10.1021/la00024a037.
27. RABOLT, John F., RUSSELL, T. P., TWIEG, R. J. Structural studies of semifluorinated n-alkanes. 1. Synthesis and characterization of $F(CF_2)_n(CH_2)_mH$ in the solid state. Macromolecules, 1984, 17(12), 2786–2794, doi: 10.1021/ma00184a045.
28. HEINZE Thomas, SARBOVA Velina, NAGEL Matilde Calado Viera. Simple synthesis of mixed cellulose acylate phosphonates applying n-propyl phosphonic acid anhydride. Cellulose, 2012, 19, 523–531, doi: 10.1007/s10570-011-9646-4.

Marija Nakić[1], Slavica Bogović[2]
[1]University of Mostar, Trg hrvatskih velikana 1, 88000 Mostar, Bosnia and Herzegovina
[2]University of Zagreb, Faculty of Textile Technology, Prilaz baruna Filipovića 28a, 10000 Zagreb, Croatia

Computational Design of Functional Clothing for Disabled People

Računalniško načrtovanje funkcionalne obleke za invalide

Scientific Review/*Pregledni znanstveni članek*
Received/*Prispelo* 1-2019 • Accepted/*Sprejeto* 1-2019

Abstract

The purpose of clothing is to express an individual's style, and to meet the wearer's protection, functionality and comfort needs. Each of these requirements must be met in order to satisfy human needs and achieve a garment's functionality. Another function of clothing is to hide physical disabilities, if possible. The sitting position is very common in daily life. All clothing should therefore be comfortable in this position, as well. This is particularly important for disabled people who are restricted to the sitting position for their entire life due to their disabilities. These are people who suffer from paraplegia, multiple sclerosis or some injuries, and who have limited mobility using wheelchairs. This paper presents research on improving clothing design, adjusted to the special needs and demands of an individual, through the application of new technologies. In that respect, taking measurements is very important, as is the virtual simulation of garment fitting as the result of cuts adapted to the sitting position.
Keywords: functional clothing, disabled people, 3D scanning, virtual garment simulation

Izvleček

Oblačila so namenjena izražanju človekovega osebnega stila, zaščiti pred zunanjimi vplivi, funkcionalnosti in zagotavljanju udobja. Vse naštete zahteve je treba izpolniti, če želimo zadovoljiti človekove potrebe in doseči uporabnost oblačil. Poleg omenjenih funkcij poskušamo z oblačili skriti tudi fizične okvare. Sedeči položaj je v vsakdanjem življenju zelo pogost, zato bi morala biti vsa oblačila v tem položaju enako udobna, kar je še zlasti pomembno za invalide, ki so vse življenje omejeni na sedeči položaj. To so osebe s paraplegijo, multiplo sklerozo ali drugimi poškodbami, ki imajo zaradi uporabe invalidskih vozičkov omejeno mobilnost. V članku so predstavljene raziskave o uporabi naprednih tehnologij in izboljšav pri oblikovanju oblačil s prilagoditvami posebnim potrebam in zahtevam posameznika. Pri tem je zelo pomembna faza jemanje mer, kot tudi virtualna simulacija oblačila s krojnimi deli, prilagojenimi sedečemu položaju.
Ključne besede: funkcionalna oblačila, invalidi, 3-D skeniranje, virtualna simulacija oblačil

1 Introduction

In addition to protection, functionality and comfort, clothing has an aesthetic function, the purpose of which is to express the wearer's personal style and hide physical disabilities. However, clothing cannot always hide the physical disabilities of people who suffer from more severe disabilities. In such cases, clothing must meet the needs of a disabled person, while achieving the pure aesthetics of garments, as design has a significant effect on the human social dimension [1, 2].

Disability is an umbrella term for the impairments, limited activities and participation restrictions of an individual while performing the activities of daily living. Wheelchair users (people suffering from

Corresponding author/*Korespondenčna avtorica:*
Marija Nakić
E-mail: marija.nakic@sum.ba

Tekstilec, 2019, ***62****(1), 23-33*
DOI: 10.14502/Tekstilec2019.62.23-33

paraplegia, multiple sclerosis, muscular dystrophy and other disorders of the locomotor system) are most affected [1].

The most frequently used disability classification, drawn up by the World Health Organisation (ICIDH), classifies disabilities as: behaviour disabilities, communication disabilities, personal care disabilities, locomotor disabilities, particular skill disabilities and situational disabilities. A disability (congenital or acquired) can be physical, cognitive, mental, sensory, emotional, developmental and even combinations of these [3–5].

The body characteristics of disabled people (shape, size and limb mobility) indicate the following [6, 7]:

- loss of balance due to spine injuries and changes in a body shape, which results in asymmetry and an irregular body shape;
- poor blood circulation, low body temperature, the physical inactivity of damaged body parts, impaired muscle functions and muscular atrophy; and
- the clear extension of the relevant muscle group of the upper extremities with wheelchair users.

2 Functional clothing requirements for disabled people

The functional requirements affecting garment design are the wearer's limited mobility and the need for a comfortable garment that does not cause additional health problems, such as skin irritation, blood flow obstruction, etc. [8, 9]. Clothing for disabled people must provide ergonomic comfort in the sitting position and improve the overall quality of life. It is designed for people from a physical and cognitive point of view, cultural and social aspects, and other aspects related to body dynamics [1, 10].

The problems faced by wheelchair users while dressing have been researched by Pruthi et al., and the following have been identified [11]:

- pain in the upper limbs while dressing and undressing;
- the removal of clothing from dormant legs;
- incontinence;
- bedsores caused by a lack of movement; and
- injuries caused by traction belts, etc. [12]

In order for the functionality of clothing for disabled people to be achieved, the following requirements must be met [1, 10, 13, 14]:

- moisture absorbency;
- the use of elastic fibres for comfort;
- the use of easy closure systems (zippers, hook-and-loop fasteners, buttons, etc.);
- easy to maintain clothing with a low level of electrostatic charging; and
- a minimum level of body odour retention (natural fibres with antibacterial finishing).

Clothing designed for disabled people must meet the following needs: sleeves should be adapted to the back and shoulders, facilitating more freedom of movement while pushing a wheelchair, comfort should be ensured, without fabric creases caused by sitting for long periods, trousers should not be too tight (blood flow obstruction due to strong pressure) or too loose (skin irritation on the back and hips due to fabric creases), and should be high-wasted on the back compared with standard clothing and should not tighten around the knees and create needless creases, and the pockets should not be sewed on the back of trousers and should be longer than standard cuts [13, 16]. Sleeves in the elbow area should also be shaped according to the principles of comfort, where it is possible to find constructional solutions, as shown in Figure 1.

Figure 1: Elbow part of an adaptive garment for wheelchair users [15]

Figure 2: Adaptive designs for sitting [20–22]

Research has shown that the comfort of trousers is affected by four main areas in which pressure occurs: waist (39.17%), knees (16.4%), crotch (13.96%) and the back of the thighs-calves (6.95%), while pressure on parts below the knees and the back of the thighs has no significant effect on wearing comfort. Wearing comfort is acceptable if pressure is below 20 kPa on the hips, waist and crotch, and below 10 kPa on the back of the thighs and knees [17, 18].
Research conducted in 2013 among 10 young women aged 18 to 38 with different types of disabilities suggested that design, form, function, self-expression and social identity were the essential factors that influence their clothing selection [19]. Standing posture measurements are not applicable to sitting posture measurements due to anatomical variations and different types of disabilities. For this reason, clothing designers and manufacturers should design this type of clothing according to the principles of universal design, i.e. inclusive design (Figure 2) [23–25].

3 3D virtual body scanning as a basis for designing personalised clothing for disabled people

Body measurement standards differ significantly between people with physical disabilities and non-disabled people. Thus, specific design requirements should be met when measuring disabled people [26–28].
When a person in the sitting position is being measured, it is important that seat surfaces be flat and horizontal, that the upper legs are positioned horizontally and the shins vertically, and that the feet

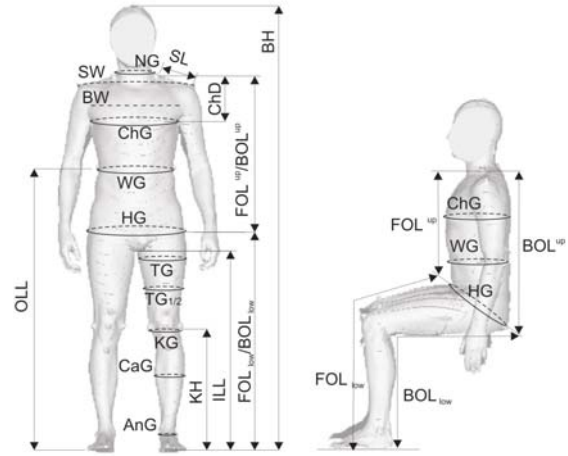

Figure 3: Definition of measurements on a 3D point cloud of the human body in the standing and sitting positions [29]

are positioned flat on a horizontal surface. The person must be barefoot and not wear any clothing except underwear [28, 30].
Body measurements can be taken manually or on a digitised human body. Depending on the applied measurement technique, differences in the volume of a body ranging from 0.72 cm to 1.71 cm and differences in body measurements in relation to the height and length of a body can arise [31, 32].
In order to take body measurements using a non-contact technique, digitisation with 3D body scanners is used, resulting in a point cloud of human body spatial coordinates. Scanning technologies can be classified into different categories: laser scanning, white light scanning, passive scanning, photogrammetry, visual body shape, silhouettes and the use of other active sensors [33–35].

The main advantage of a non-contact technique used for body measuring is the short scanning time required, which reduces the fatigue that occurs while maintaining specific and necessary postures during anthropometric measurements. It is possible to collect all relevant data from an anthropometric, biomechanical and ergonomic point of view, which is necessary for the development and design of clothing adapted to the different needs of specific segments of wearers. Given that anthropometry provides two body measurement systems static or structural referring to an individual's body variations, and dynamic or functional referring to biomechanical aspects related to different movements and daily tasks all of the afore-mentioned aspects can be comprised on the basis of 3D body scanning [10, 36].

Optoelectronic devices and scanners, which are based on recognising a silhouette from one or more images and can create a model with thousands of points using laser beams or structured light, are used to create a parametric model of the human body. However, a large number of points is redundant, noise is present and the surface for creating 3D models should be removed and filtered [37–39].

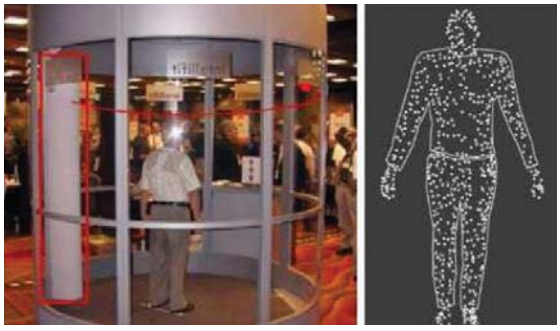

Figure 4: Intellifit radio scanner [39]

3D radio-wave scanners (Intellifit system) are based on radio-wave technology and use millimetre radio waves that pass through a subject's clothing and reflect off the body's surface. The reflected signal is subsequently detected by the receiver net, resulting in a 3D image of the subject (Figure 4) [37, 40–42].

The advancement of 3D scanning technology has enabled the creation of high-density point clouds. The process requires the use of certain algorithms that analyse the data of body topology in order to obtain the corresponding surface of the scanned object. At an early stage of data procession, discontinuities are discovered by the algorithms, so that the information can be kept during the complete process of surface interpolation.

The virtual prototyping of garments and simulation depend on numerous factors. The central focus of virtual image research is the development of the efficiency of mechanical and simulation models that can be reproduced. The second research aspect is aimed at 3D human body scanning and modelling in order to obtain a 3D human body model for the virtual prototyping of garments. Most research is based on the human body in the standing position with no or minor physical deformities. It is therefore aimed at the similar creation of virtual prototypes for wheelchair users [36, 40, 42–43].

Systems used for virtual garment fitting provide a standing parametric human body model of average height, with adapted shapes and dimensions. The aim of research is to design a generally acceptable 3D human body model adaptable to different poses and non-standard body shapes to enable the virtual prototyping of garments for people with limited body abilities; see Figure 5 [44–51].

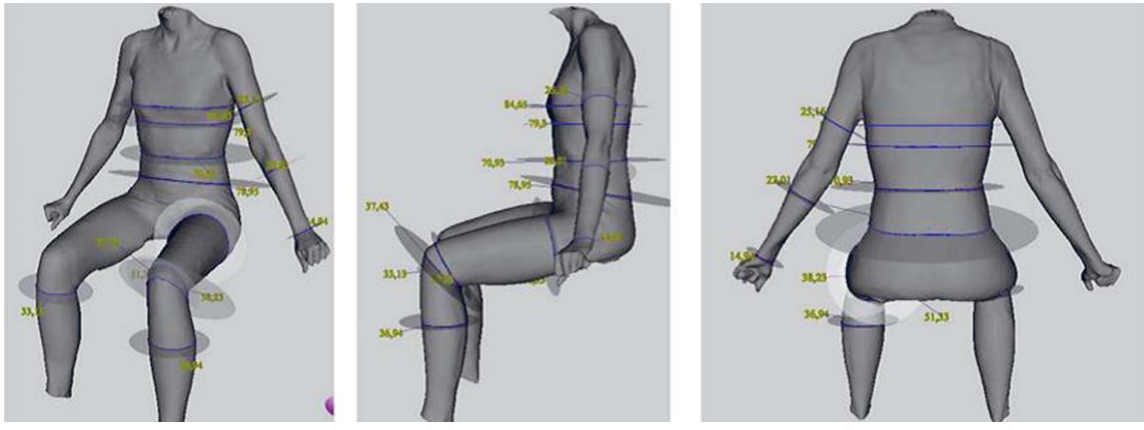

Figure 5: Parametric human body model in the sitting position [6]

The 3D point cloud has outliers in parallel with a lack of points on the digitised object. The point cloud is therefore reconstructed by removing outliers and closing the point cloud [39, 45]. The net must be completed by closing the point cloud in places where points are lacking. Taking into account the natural contours of the body, the points are added and the net is completed. The Poisson reconstruction algorithm is used for the surface reconstruction of a 3D body cloud.

Different methods for human body modelling have been developed. Their use has simplified the ways in which human body shapes and height are adapted. Linear regression is used for taking measurements [52–54].

4 Virtual garment design for people with disabilities

Adaptive clothing can be designed on the basis of a digitised human body. Characteristic body parts, such as the chest, shoulders, scapula, neck, back, hips and lateral parts, can be positioned depending on the actual body image, which is a prerequisite for virtual garment design. The research conducted and approaches applied have shown that the problem of adaptive design for people with disabilities, such as people with scoliosis, can be solved in this manner. The results of the research can thus be applied to mass production, facilitating rapid interaction between wearers and designers. In that regard, the parametric influence of textiles is crucial for adaptive clothing for wheelchair users [55–57].

An individual approach must be taken when designing garments for people with disabilities due to an individual's different physical deformities, which can be multiple with wheelchair users. For this purpose, a group of Slovenian researchers has developed the CASP method (C-curvature, A-acceleration, S-symmetry and P-proportionality) used to design clothing adapted to 3D virtual mannequins with physical deformities that have occurred as the result of disease. Curvature goes from minus (concavity) to plus (convexity), which can be calculated using the matrix expressions [58]:

$$\begin{bmatrix} a\,n-1,0 & \succ & a\,n-1,n-1 \\ \vdots & & \vdots \\ a\,0,0 & \succ & a\,0,n-1 \end{bmatrix} \quad (1).$$

The matrix enables the same points in the 3D space in the n × n matrix to be marked. Acceleration is a property referring to the basic surfaces in a longitudinal direction. Clothing symmetry is always preferable, and a value of zero means perfect symmetry. Proportionality indicates the size or width of the surface, and is calculated as a ratio of the length and width of the observed surface. The whole process is based on the use of the Grasshopper® (GH) graphical algorithm, which is an add-in used with the RH application through which the analysis of digitised surface geometries is based on the rules of the M. Müller & Son and the Optitex CAD/PDS construction system. The latter enables the XY clothing tightness on particular body parts to be recorded in order to design comfortable adaptive clothing for people with disabilities [58, 59].

With the use of a 3D-to-2D garment design method, clothing can be designed directly on a 3D virtual body model, resulting in 2D patterns obtained by flattening the existing parts. Adaptive clothing is designed using a CAD system for designing the virtual prototyping of garments. This enables garment fit testing and the adjustment of virtual body models to standard models [2, 6, 45, 49, 59].

Making a virtual body model using the 3ds MAX software is based on integrating female body scan data with a kinematic template**.** The template position

Figure 6: Adaptive clothing image created using a 3D-to-2D garment design method [49]

is adjusted to the scan data. The dimensions of bones and muscles are then adjusted to specific scan data.
In order for the animation to be realised, the interpolation weights must be transferred and calculated, enabling every joint to be marked and proportionally transferred between the skeleton and the network in order to obtain a uniform human body deformation. The process requires the use of different scripts developed for 3D kinematic model animation, the purpose of which is to create several lower body positions with different bending angles [60].
In research on the 3D construction and simulation of trousers designed using the Lectra DesignConcept, three distinctive positions with different degrees of bending at the knees and trunk have been described in detail. The contour of trousers has been defined and used for designing a mesh model from which 2D tailored pieces have been extracted. Research has shown that suitable tailored pieces cannot be extracted if a body has a high-degree bend. When the bend at the knees is 90° and 110° in the sitting position, it is automatically possible to design tailored pieces for well-fitting trousers. By changing the design and resizing the projected seam, a model that facilitates a bend of more than 130° at the knees and trunk is created, with no change in trouser fitting and the functionality of a garment for wheelchair users. The use of tailored pieces and the simulation generated positive

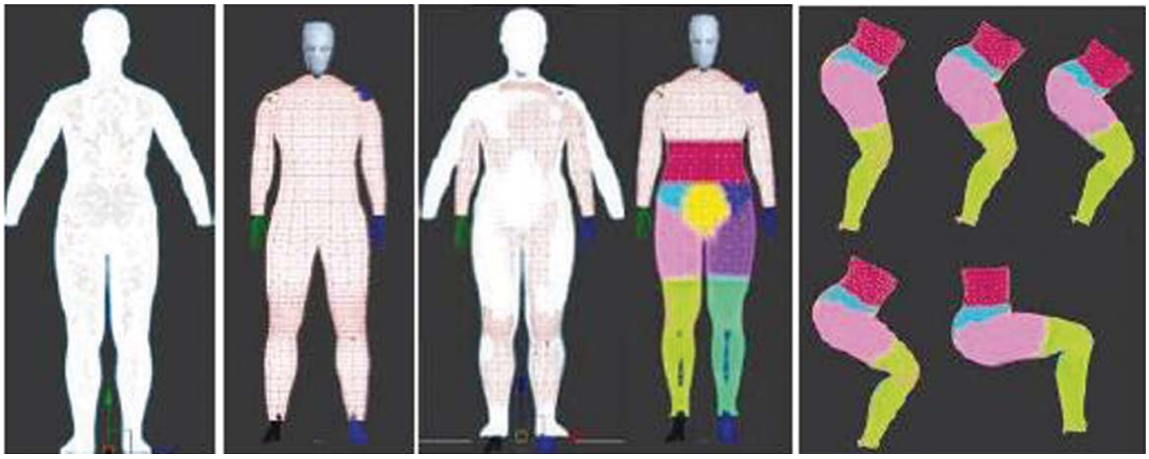

Figure 7: 3D human body animations in different positions [60]

Figure 8: Developing trouser patterns for people in the sitting position [65]

results, which is evident in prototyping. However, this method of design cannot be applied to all wheelchair users, as garment design depends on a person's individual needs and body morphology [61–63].

Research on improving the functionality of garments for wheelchair users has also been conducted. A robotic mannequin has been developed for the purpose of assessing clothing comfort based on the replication of body movements and data gathered through the senses while wearing clothing. A special application was developed for the purpose of this research. The application enables virtual garment fitting in the sitting position (wheelchair seating), provides a simulation of clothing adjustments according to changes to the standard model, performs 3D measurements on the basis of which a database is created, and verifies suitable results based on 3D visualisation. The purpose of the application was to provide a virtual service through adaptation, to enable wheelchair users to create a prototype wherever they wish and to gather data relating to apparel appearance [63–66].

5 Conclusion

After reviewing the relevant literature, it can be concluded that techniques for clothing simulation represent an important tool for textile and clothing designers. These techniques offer numerous advantages, such as fast and simple changes in clothing development. The primary advantage of virtual prototyping is the possibility of designing clothing and directly observing the adjustment of a silhouette to a person who is not physically present. Computer prototyping has great potential for producing clothing in a contemporary manner, as it facilitates a 3D prototype of a garment to be produced rapidly [67].

3D body scanning plays a key role in producing adaptive clothing for wheelchair users, as it allows body measurements to be taken while determining the posture and position of a body in the sitting position. Point clouds produced through the process of 3D scanning are used to create a virtual body, which is standard practice in the virtual prototyping of garments.

The standard software packages used for the virtual prototyping of garments can also be used for the virtual prototyping of garments for people with physical deformities. A systematic approach is necessary when designing clothing for people in wheelchairs. 3D scanning must be adapted to a person in the sitting position, particularly if the person is unable to sit without a seat back. When creating virtual bodies, an individual approach is required, as the point clouds of a body scan must be processed with the use of 3D image processing algorithms. The algorithms used for the standard standing position are not reliable enough for an automatic reconstruction of a 3D human body in the sitting position due to the differing body shapes of people with disabilities.

Software packages for apparel design are used to design a garment directly on a digitised 3D human body model. It is possible to either design and adjust a cut to a 3D body scan based on a simulation, or to create a garment directly on a 3D body by extracting the tailored pieces after 3D modelling.

Regardless of the selected method for garment design, obtaining satisfactory results is limited by a person's different body shape and physical limitations. It can thus be concluded that research on the computational design of clothing for people with disabilities has great potential. People with disabilities wish to emphasise their individuality, as aesthetically pleasing clothing decorates their physical appearance and enables them to enjoy a psychologically healthy environment [62].

Clothing for wheelchair users must be above all functional, must enable quick and independent dressing, must provide a psychical and psychological sense of comfort and stability, and be easy to maintain and trendy. The use of computer technologies is thus very important, as disadvantages to design can be foreseen and eliminated when developing and designing garments. The use of new technologies facilitates the design of functional garments for wheelchair users.

References

1. CURTEZA, Antonela, CRETU, Viorica, MACOVEI, Laura, POBORONIUC, Marian. Designing functional clothes for persons with locomotor disabilities. *AUTEX Research Journal*, 2014, *14*(4), 281–289, doi: 10.2478/aut-2014-0028.
2. HONG, Yan, ZENG, Xianyi, BRUNIAUX, Pascal, LIU, Kaixuan, CHEN, Yan, ZHANG, Xujing. Collaborative 3D-to-2D tight-fitting garment pattern design process for scoliotic people.

Fibres and Textiles in Eastern Europe, 2017, **25**, 113–117, doi: 10.5604/01.3001.0010.4637.

3. World Health Organization. International classification of impairment. *Activity and Participation (ICIDH-2)*, Geneva, Switzerland, WHO, 1980.
4. ROSENBAUM, Peter, STEWAR, Debra. The world health organization international classification of functioning, disability, and health: a model to guide clinical thinking, practice and research in the field of cerebral palsy. S*eminars in Pediatric Neurology,* 2004, **11**(1), 5–10, doi: 10.1016/j.spen.2004.01.002.
5. BICKENBACH, Jerome E., CHATTERJI, Somnath, BADLEY, E. M., USTUN, T. B. Models of disablement, universalism and the international classification of impairments, disabilities and handicaps, *Social Science and Medicine,* 1999, **48**(9), 1173–1187, doi: 10.1016/S0277-9536(98)00441-9.
6. RUDOLF, Andreja, CUPAR, Andrej, KOZAR, Tatjana, STJEPANOVIĆ, Zoran. Study regarding the virtual prototyping of garments for paraplegics. *Fibers and Polymers,* 2015, **16**(5), 1177–1192, doi: 10.1007/s12221-015-1177-4.
7. CHANG, Wei-Min, ZHAO, Yu-Xiao, GUO, Rui-Ping, WANG, Qi, GU, Xiao-Dan. Design and study of clothing structure for people with limb disabilities. *Journal of Fiber Bioengineering and Informatics,* 2009, **2**(1), 62–67, doi: 10.3993/jfbi06200910.
8. FORBES, Angus, WHILE, Alison, MATHES, Lucia, GRIFFITHS, Peter. Health problems and health-related quality of life in people with multiple sclerosis. *Clinical Rehabilitation*, 2006, **20**(1), 67–78, doi: 10.1191/0269215506cr880oa.
9. Das NEVES, Érica P., BRIGATTO, Aline C., PASCHOARELLI, Luis C. Fashion and ergonomic design: Aspects that influence the perception of clothing usability. *Procedia Manufacturing*, 2015, **3**, 6133–6139, doi: 10.1016/j.promfg.2015.07.769.
10. WANG, Yunyi, WU, Daiwei, ZHAO, Mengmeng, LI, Jun. Evaluation on an ergonomic design of functional clothing for wheelchair users. *Applied Ergonomics*, 2014, **45**(3), 550–555, doi: 10.1016/j.apergo.2013.07.010.
11. PRUTHI, Neelam, SEETHARAMAN, Chanchal, SEETHARAMAN, P. Protective clothing for paraplegic women. *Journal of Human Ecology*, 2006, **19**(4), 267–271, doi: 10.1080/09709274.2006.11905889.
12. BLOOMQUIST, Lorraine E. Injuries to athletes with physical disabilities: prevention implications. *The Physician and Sportsmedicine*, 2016, **14**(9), 96–105, doi: 10.1080/00913847.1986.11709170.
13. MEINANDER, Harriet, VARHEENMAA, Minna. Clothing and textiles for disabled and elderly people. Espoo 2002. *VTT Tiedotteita – Research Notes 2143*, 57 p. + app. 4 p.
14. BROGIN, Bruna, CAMPIGOTTO WEISS, Dalila, MARCHI, Sandra, RIBEIRO OKIMOTO, Maria Lucia, de OLIVEIRA, Sabrina Talita. Clothing custom design: Qualitative and anthropometric data collection of a person with multiple sclerosis. *Advances in Intelligent Systems and Computing,* 2016, **485**, 359–369, doi: 10.1007/978-3-319-41983-1_32.
15. Adaptive garment for wheelchair users [accessed 11. 6. 2018]. Available on World Wide Web: <https://i-d.vice.com/de/article/qv8wad/diese-junge-modedesignerin-entwirft-innovative-mode-fuer-rollstuhlfahrer-269>.
16. KUNŠTEK, Ana, BOGOVIĆ, Slavica. Customization of garment for invalid persons. *Book of proceedings of the 3rd International textile, clothing and design conference; Magic World of Textiles*. Edited by Zvonko Dragčević. Zagreb : Faculty of Textile Technology, 2006, p. 448–452.
17. LIU, Kaixuan, WANG, Jianping, HONG, Yan. Wearing comfort analysis from aspect of numerical garment pressure using 3D virtual-reality and data mining technology. *International Journal of Clothing Science and Technology*, 2017, **29**(2), 166–179, doi: 10.1108/IJCST-03-2016-0017.
18. THORNTON, Nellie. *Fashion for disable people*. London : Batsford, 1990, 128 p.
19. CHANG, Hyo Jung (Julie), HODGES, Nancy, YURCHISIN, Jennifer. Consumers with disabilities: Qualitative exploration of clothing selection and use among female college students. *Clothing and Textiles Research Journal,* 2014, 32(1), 34–48, doi: 10.1177/0887302X13513325.
20. Adaptive designs for sitting [accessed 10. 11. 2018]. Available on World Wide Web: <https://kottke.org/16/02/clothes-designed-especially-for-wheelchair-users>.
21. Adaptive designs for sitting [accessed 10. 11. 2018]. Available on World Wide Web: <https://i.pinimg.com/originals/f9/15/ac/f915ac67a779e5f216f98b666cb4d9aa.jpg>.

22. Adaptive designs for sitting [accessed 10. 11. 2018]. Available on World Wide Web: <https://i.pinimg.com/originals/5a/32/31/5a3231562088842d99456fad93929746.jpg>.
23. IMRAN, Aqsa, DREAN, Emilie, SCHACHER, Laurence, ADOLPHE, Dominique. Adaptive bra designs for the individuals with special needs. *IOP Conference Series: Materials Science and Engineering,* 2017, **254**, 072012, doi: 10.1088/1757-899X/254/7/072012.
24. SYBILSKA, Wiolleta, NAPIERALSKA, Lidia, MIELICKA, Elizbieta. Analysis of body measurements using a 3D contactless scanning method. *Autex Research Journal*, 2010, **10**(3), 77–79.
25. Inclusive design [accessed 24. 6. 2018]. Available on World Wide Web: https://shinyideas.wordpress.com/2015/07/25/wheelchair-users-benefit-from-this-revolutionary-fashion-design/.
26. PAQUET, Victor, FEATHERS, David. An anthropometric study of manual and powered wheelchair users. *International Journal of Industrial Ergonomics,* 2004, **33**(3), 191–204, doi: 10.1016/j.ergon.2003.10.003.
27. TALAB, Amir Hossein Davoudian, NEZHAD, Ahmad Badee, DARVISH, Nasrin Asadi, MOLAEIFAR, Hossein. Comparison of anthropometric dimensions in healthy and disabled individuals. *Jundishapur Journal of Health Sciences,* 2017, **9**(3), e59009, doi: 10.5812/jjhs.59009.
28. HAN, Hyunsook, NAM, Yunja, CHOI, Kyungmi. Comparative analysis of 3D body scan measurements and manual measurements of size Korea adult females. *International Journal of Industrial Ergonomics,* 2010, **40**(5), 530–540, doi: 10.1016/j.ergon.2010.06.002.
29. BOGOVIĆ, Slavica, STJEPANOVIČ, Zoran, CUPAR, Andrej, JEVŠNIK, Simona, ROGINA-CAR, Beti, RUDOLF, Andreja. The use of new technologies for the development of protective clothing: Comparative analysis of body dimensions of static and dynamic postures and its application *AUTEX Research Journal,* 2018, doi: 10.1515/aut-2018-0059.
30. UJEVIĆ, Darko, SZIROVICZA, Lajos, KARA–BEGOVIĆ, Isak. Anthropometry and the comparison of garment size systems in some European countries. *Collegium antropologicum,* 2005, **29**(1), 71–78.
31. KOZAR, Tatjana, RUDOLF, Andreja, JEVŠ–NIK, Simona, CUPAR, Andrej, PRINIOTAKIS, Georgios, STJEPANOVIČ, Zoran. Accuracy evaluation of a sitting 3d body model for adaptive garment prototyping. *14th AUTEX World Textile Conference,* Bursa, Turkey, 2014. Available on World Wide Web: <https://www.researchgate.net/publication/270477468_ACCURACY_EVALUATION_OF_A_SITTING_3D_BODY_MODEL_FOR_ADAPTIVE_GARMENT_PROTOTYPING>.
32. SIMMONS, Karla P., ISTOOK, Cynthia L. Body measurement techniques: Comparing 3D body-scanning and anthropometric methods for apparel applications *Journal of Fashion Marketing and Management: An International Journal*, 2003, **7**(3), 306–332, doi: 10.1108/13612020310484852.
33. Fotogrametrija [accessed 24. 9. 2018]. Available on World Wide Web: <https://hr.wikipedia.org/wiki/Fotogrametrija>.
34. D'APUZZO, Nicola. Recent advances in 3d full body scanning with applications to fashion and apparel. In: *Optical 3-D measurement techniques IX*. Edited by A. Gruen and H. Kahmen. Vienna, 2009, 10 p.
35. PETKOVIĆ, Tomislav, PRIBANIĆ, Tomislav, ĐONLIĆ, Matea, D'APUZZO, Nicola. Software synchronization of projector and camera for structured light 3D body scanning. In: *Proceeding of 7th International Conference on 3D Body Scanning Technologies.* Lugano, 2016, pp. 286–295, doi: 10.15221/16.286.
36. BARROS, Helda Oliveira, SOARES, Marcelo Márcio. Using digital photogrammetry to conduct an anthropometric analysis of wheelchair users. *Work*, 2012, **41**, 4053–4060.
37. SIMS, Ruth E., MARSHALL, Russell, GYI, Diane E., SUMMERSKILL, Steve, CASE, Keith. Collection of anthropometry from older and physically impaired persons: Traditional methods versus TC2 3-D body scanner. *International Journal of Industrial Ergonomics,* 2012, **42**(1), 65–72, doi: 10.1016/j.ergon.2011.10.002.
38. REMONDINO, Fabio. 3D reconstruction of static human body with a digital camera. *Videometrics VII*, 2003, **5013**, 38–45, doi: 10.1117/12.473090.
39. BÜTTGEN, Bernhad, OGGIER, Thierry, LEHMANN, Michael, KAUFMANN, Rolf, NEUKOM, Simon, RICHTER, Michael, SCHWEIZER, Matthias, BEYELER, David, COOK, Roger, GIMKIEWICZ, Christiane, URBAN, Claus, METZLER, Peter, SEITZ, Peter, LUSTENBERGER. Felix.

High-speed and high-sensitive demodulation pixel for 3D imaging. In: *Proceedings of the SPIE: Three-Dimensional Image Capture and Applications VII*. Edited by Brian D. Corner, Peng Li and Matthew Tocheri. 2006, **6056**, 22–33. doi. org/10.1117/12.642305.

40. BRAGANÇA, Sara, AREZES, Pedro, CARVALHO, Miguel, ASHDOWN, Susan P. Current state of the art and enduring issues in anthropometric data collection. *DYNA*, 2016, **83**(197), 22–30, doi: 10.15446/dyna.v83n197.57586.
41. TSOLI, Aggeliki, LOPER, Matthew, BLACK, Michael J. Model-based anthropometry: Predicting measurements from 3D human scans in multiple poses. *IEEE Winter Conference on Applications of Computer Vision,* 2014, pp. 83–90, doi: 10.1109/WACV.2014.6836115.
42. DAANEN, H. A. M., TER HAAR, F. B. 3D whole body scanners revisited. *Displays*, 2013, **34**(4), 270–275, doi: 10.1016/j.displa.2013. 8.011.
43. ALLEN, Brett, CURLESS, Brian, POPOVIĆ, Zoran. The space of human body shapes: Reconstruction and parameterization from range scans. *ACM Transactions on Graphics*, 2003, **22**(3), 587−594, doi:10.1145/882262.882311.
44. MAGNENAT-THALMANN, Nadia, THALMANN, Daniel. *Handbook of virtual humans. 1st ed.* Edited by N. Magnenat-Thalmann and D. Thalmann. Chichester et al. : John Wiley and Sons, 2004, pp.75−98.
45. LIU, Yong-Jin., ZHANG, Dong-Liang, YUEN, Matthew Ming-Fai. A survey on CAD methods in 3D garment design. *Computers in Industry,* 2010, **61**(6), 576–593, doi: 10.1016/j.compind. 2010.03.007.
46. MAGNENAT-THALMANN, Nadia. *Modelling and simulating bodies and garments. 1st ed.* London : Springer-Verlag, 2010, pp. 1−29, doi: 10. 1007/978-1-84996-263-6.
47. BOGOVIĆ, Slavica, ROGALE, Dubravko, TOMŠIĆ, Maja. 3D scanning and measuring of human body of disabled person. *Proceedings of the 7th International scientific conference on production engineering RIM 2009, Development and modernization of production*. Edited by: Isak Karabegović, Milan Jurković and Vlatko Doleček, Bihać : Tehnički fakultet Univerziteta u Bihaću, 2009, pp. 163−168.
48. KOZAR, Tatjana, RUDOLF, Andreja, CUPAR, Andrej, JEVŠNIK, Simona, STJEPANOVIC, Zoran. Designing an adaptive 3D body model suitable for people with limited body abilities. *Textile Science and Engineering,* 2014, **4**(5), 13 p., doi: 10.4172/2165-8064.1000165.
49. HONG, Yan, BRUNIAUX, Pascal, ZHANG, Junjie, LIU, Kaixuan, DONG, Min, CHEN, Yan. Application of 3D-TO-2D garment design for atypical morphology: A design case for physically disabled people with scoliosis. *Industria textilă,* 2018, **69**(1), 59−64.
50. BRUNIAUX, Pascal, CICHOCKA, Agnieszka, FRYDRYCH, Iwona. 3D digital methods of clothing creation for disabled people. *Fibres and Textiles in Eastern Europe,* 2016, **5**(119), 125−131, doi: 10.5604/12303666.1215537.
51. ALLEN, Brett, CURLESS, Brian, POPOVIĆ, Zoran. The space of human body shapes: Reconstruction and parameterization from range scans. *ACM Transactions on Graphics (TOG),* 2003, **22**(3), 587−594, doi: 10.1145/882262.882311.
52. HAMAD, Balkiss, HAMAD, Moez, THOMASSEY, Sébastien, BRUNIAUX, Pascal. 3D adaptive morphotype mannequin for target population. *Journal of Ergonomics,* 2018, **8**(2), 9 p., doi: 10.4172/2165-7556.1000229.
53. SAVONNET, Léo, WANG, Xuguang, DUPREY, Sonia. A parametric model of the thigh-buttock complex for developing FE model to estimate seat pressure. In: *5th International Digital Human Modeling Symposium, Jun 2017, Bonn, Germany.* 2017, <hal-01769922>.
54. MOCCOZET, Laurent, DELLAS, Fabien, MAGNENAT-THALMANN, Nadia, BIASOTTI, Silvia, MORTARA, Michela, FALCIDIENO, Bianca, MIN, Patrick, VELTKAMP, Remco. Animatable human body model reconstruction from 3D scan data using templates. In: *Proceedings of workshop on motion capture techniques for virtual environments,* 2004, 7 p.
55. D'APUZZO, Nicola. Intellifit revolutionary full body scanner. Millimeter waves based technology allows 3D scanning without undressing. *Human Body Measurement Newsletter*, 2005, **1**(1), 1–2.
56. DOUROS, Ioannis, DEKKER, Laura, BUXTON, Bernard F. An improved algorithm for reconstruction of the surface of the human body from 3D scanner data using local B-spline patches. In*: Proceedings IEEE international workshop on modelling people. MPeople'99,* 1999, doi: 10.1109/PEOPLE.1999.798343.

57. WEISS, Alexander, HIRSHBERG, David, BLACK, Michael J. Home 3D body scans from noisy image and range data. In: *International Conference on Computer Vision.* Barcelona : IEEE, 2011, doi: 10.1109/ICCV.2011.6126465.
58. STJEPANOVIČ, Zoran, CUPAR, Andrej, JEVŠNIK, Simona, KOCJAN STJEPANOVIĆ, Tanja, RUDOLF, Andreja. Construction of adapted garments for people with scoliosis using virtual prototyping and CASP method. *Industria textilă.* 2016, **67**(2), 141–148.
59. RUDOLF, Andreja, CUPAR, Andrej, KOZAR, Tatjana, STJEPANOVIĆ, Zoran. Study regarding the virtual prototyping of garments for paraplegics. *Fibres and Polymers*, 2015, **16**(5), 1177–1192, doi: 10.1007/s12221-015-1177-4.
60. ALUCULESEI, Bianca; KRZYWINSKI, Sybille, CURTEZA, Antonela. Three-dimensional construction and simulation of trousers for wheelchair users. *9th international textile, clothing and design conference – Magic World of Textiles. Zagreb :* University of Zagreb, Faculty of Textile Technology, 2018.
61. ICHIKARI, Ryosuke, ONISHI, Masaki, KURATA, Takeshi. Fitting simulation based on mobile body scanning for wheelchair users. *The Journal on Technology and Persons with Disabilities,* 2018, 15 p.
62. CALDAS, Artemisia, CARVALHO, Miguel, PIAUILINO, Thayna, MEDEIROS, Maria, CALDAS, Monique. Basic pattern design for care dependent elderly. In: *The 90th Textile Institute World Conference. Textiles: Inseparable from the human environment.* Poznan, Poland, 2016, 7 p.
63. HONG, Yan, BRUNIAUX, Pascal, ZENG, Xianyi, LIU, Kaixuan, CURTEZA, Antonela, CHEN, Yan. Visual-simulation-based personalized garment block design method for physically disabled people with scoliosis (PDPS). *AUTEX Research Journal,* 2018, **18**(1), 35–45, doi: 10.1515/aut-2017-0001.
64. RUDOLF, Andreja, BOGOVIĆ, Slavica, ROGINA CAR, Beti, CUPAR, Andrej, STJEPANOVIĆ, Zoran, JEVŠNIK, Simona. Textile forms' computer simulation techniques. In: *Computer simulation*, (Computer and Information Science, Computer Science and Engineering). Edited by Dragan CVETKOVIĆ. Rijeka : InTech. 2017, pp. 67–93, doi: 10.5772/67738.
65. BROOKS, Anthony L., PETERSSON BROOK, Eva. Towards an inclusive virtual dressing room for wheelchair-bound customers. In: *Proceedings of the 2014 International Conference on Collaboration Technologies and Systems.* Edited by W. W. Smari, G. C. Fox, and M. Nygård. 2014, pp. 582–589, doi: 10.1109/CTS.2014.6867629.
66. JEVŠNIK, Simona, STJEPANOVIČ, Zoran, RUDOLF, Andreja. 3D virtual prototyping of garments: Approaches, developments and challenges. *Journal of Fibre Bioengineering and Informatics,* 2017, **10**(1), 51–63, doi: 10.3993/jfbim00253.
67. PILAR, Tanja, STJEPANOVIČ, Zoran, JEVŠNIK, Simona. Evaluation of fitting virtual 3D skirt prototypes to body. *Tekstilec,* 2013, **56**(1), 47–62, doi: 10.14502/Tekstilec2013.56.47-62.

Andrea Ehrmann
Bielefeld University of Applied Sciences, Faculty of Engineering and Mathematics, ITES, Interaktion 1, 33619 Bielefeld, Germany

On the Possible Use of Textile Fabrics for Vertical Farming

O možnostih za uporabo tekstilnih materialov za vertikalno kmetovanje

Scientific Review/*Pregledni znanstveni članek*
Received/*Prispelo* 01-2019 • Accepted/*Sprejeto* 01-2019

Abstract

Vertical farming is one of several ideas that are being developed further by diverse research groups, companies and private citizens. Due to the growing problems of urbanisation and a growing population, vertical farming has presented itself as one possibility to feed people, particularly in large and densely crowded cities, in an efficient and eco-friendly way. Interestingly, while agrotextiles are often used in agriculture and textile fabrics can be bought, for example, as frames for small vertical farming solutions for private balconies, only a few researchers have studied the possibilities of using textile fabrics as substrates for vertical faming to date. This study provides an overview of possible future applications of textile fabrics in vertical farming solutions.
Keywords*:* vertical farming, vertical gardening, textile fabrics, agrotextiles, plants, algae, hydroponics, aeroponics, aquaponics

Izvleček

Vertikalno kmetovanje spada med ideje, ki jih razvijajo različne raziskovalne skupine, podjetja in zasebniki. Zaradi naraščajočih problemov urbanizacije in rasti svetovne populacije je vertikalno kmetovanje lahko ena od možnosti učinkovitega in okolju prijaznega načina zagotavljanja hrane, zlasti v velikih in gosto naseljenih mestih. Zanimivo pa je, da se kljub temu, da se agrotekstilije pogosto uporabljajo v kmetijstvu in da so na trgu na voljo tekstilni materiali za okvirne rešitve vertikalnega kmetovanja za zasebne balkone ipd., le manjše število raziskovalcev ukvarja z možnostjo uporabe tekstilij kot substrata za vertikalno kmetovanje. Članek predstavlja pregled možnosti za uporabo tekstilnih materialov za vertikalno kmetovanje v prihodnosti.
Ključne besede: vertikalno kmetovanje, vertikalno vrtnarjenje, tekstilne tkanine, agrotekstilije, rastline, alge, hidroponika, aeroponika, akvaponika

1 Introduction

According to the latest World Population Prospects, the world's population will grow continuously over the next decades [1]. Fighting hunger and malnutrition will become even more difficult than it is today, particularly in the poorest countries where population growth is expected to be highest [2]. Even in wealthier countries, however, total agricultural land area is frequently insufficient to cover the demands of the population for food. For example, a recent statistical report indicates a demand of $18.3 \cdot 10^6$ ha for food production in Germany for 2016, while only $14.0 \cdot 10^6$ ha of the total available agricultural land area of $16.7 \cdot 10^6$ ha were used for food production. The missing food, corresponding to the difference of $4.3 \cdot 10^6$ ha, was bought abroad [3].
This is one of the reasons why vertical farming is of major interest in research and development. The main idea of vertical farming is to grow vegetables

Corresponding author/*Korespondenčna avtorica:*
Prof. Dr. Dr. Andrea Ehrmann
E-mail: andrea.ehrmann@fh-bielefeld.de

or other plants vertically, typically inside of high buildings. One possibility is to have several floors (or thinking on a smaller scale, several levels in a large shelf-like structure) that are used for farming. Water is often transported from the highest levels down to the next levels until it reaches the lowest level and is pumped back to the highest level, ideally achieving a closed water recycling system. On the largest scale, entire skyscrapers can be used for vertical farming, possibly including a restaurant or a supermarket where vegetables are sold. On a smaller scale, vegetables are harvested from the paths between the shelfs on which they grow. In this way, as Pinstrup-Andersen recently pointed out, indoor vertical farming may support improved nutrition, reduce water consumption and decrease the risks associated with outdoor farming due to increasing climate change and extreme weather conditions [4]. Particularly in highly urbanised areas, vertical farming may offer a certain amount of independence [5]. Interestingly, vertical farming can even compete economically with fresh food grown in greenhouses, despite the high cost of artificial lighting [6, 7]. From a technical point of view, relatively new technologies such as hydroponics, aeroponics and aquaponics facilitate efficient farming in the city [8–10]. Hydroponics is a hydroculture technology used to grow plants without soil, i.e. in water with additional nutrients, possibly using perlite or a similar structure, to support the roots of plants. Aeroponics goes one step further and grows plants in humid air or mist, but without inserting the roots in water. Finally, aquaponics uses another approach by creating a symbiosis between plants and aquatic animals, where water and animals' by-products are used as a source of nutrients for plants. It should be noted that the location and design of these technologies must be tailored carefully to achieve a sustainable food supply [11].

Another technology based on the same idea of growing plants vertically to save space is demonstrated by the BIQ Algenhaus in Hamburg, Germany. The façade of this building is used as a bioreactor in which microalgae are grown. During growth, the microalgae absorb the radiation on the façade, converting it partly into biomass, while the residual radiation is used for heating the building. Nutrients are provided by the waste water from the building, again achieving a high recycling rate that is seen in common vertical farming technologies [12].

Despite these advantages and even the possible necessity of vertical farming that could be only be mentioned briefly here, there is surprisingly little literature available about new technologies specifically for vertical farming. Even textile fabrics that are well-known as agrotextiles used to protect diverse plants from wind, low temperatures or insects cannot be found in literature about vertical farming. An overview will be given here of the possible use of different textile fabrics for vertical farming applications, subdivided into the farming of plants and algae.

2 Textile fabrics for algae immobilisation and harvesting

Algae are eukaryotes that are, depending on the cited study, regarded as simple plants or as plant-like species [13, 14]. A broad spectrum of algae exists, from the smallest micro-algae such as *Chlamydomonas reinhardtii*, a well-known model organism for photosynthesis or starch metabolism, to large seaweed formed by red, brown or green macro-algae. Several algae are studied comprehensively, as they can produce chlorophyll, carotenoids, fucoidans and other healthy ingredients. Other algae can be eaten, are used in cosmetics, can serve as a base for bio-ethanol, can be used to clean waste water, etc. Algae are thus of great interest in recent research, but are already farmed on a large scale, particularly in Asian countries such as China, Japan or Korea. Despite recent approaches to growing algae in a vertical arrangement, such as the BIQ Algenhaus [12], scientific literature mostly reports on common growth methods using bioreactors or round tanks.

Combinations with textile fabrics can only rarely be found in literature. Kerrison *et al.* describe textiles substrates for the macro-alga *Saccharina latissimi*, which was seeded on fabrics in different development stages. Using a binder solution, the seaweed-forming macro-alga was affixed to a polyester rope and a non-woven fabric. Facilitating the outplanting of algae in this way at a seaweed farm at an earlier stage not only increased the amount of biomass produced, but also helped decrease the necessary volume of hatchery tanks [15].

The seaweed *Gayralia sp.* was studied by Pellizzari *et al.* [16]. They found polypropylene nets placed close to a mangrove fringe in the bay in southern Brazil

where they performed their experiment enabled cultivation using a simple technology and resulting in a reliable algae growth rate, and provided the local inhabitants a secure income.

An integrated photobioelectrochemical system, combining a microbial fuel cell with algae growth for domestic wastewater treatment, was suggested by Luo *et al.* [17]. In such a combination, electrogenic bacteria produce electricity through oxygen reduction, while at the same time degrading organic compounds. The algae produce oxygen by photosynthesis, thus eliminating the need for external aeration while also serving as biomass. Luo *et al.* studied six different mesh membranes from polyester or nylon with varying pore sizes, ranging from 0.11 mm to 5.31 mm for algal attachment to support algae harvesting, and found polyester slightly superior to nylon, while the smaller pore sizes of 0.11 mm and 0.53 mm resulted in significantly higher biomass productivity than the largest pore size.

Nylon meshes were also used by Lee *et al.* to increase the biomass productivity of diverse microalgae [18]. In addition, the harvesting and de-watering of the algal biomass were found to be easier and less expensive, as the meshes with adhered algae could simply be taken out of the culture.

Focusing on microalgae, electrospun nanofiber mats from polyamide and polyacrylonitrile were studied and compared with a non-woven polypropylene microfiber fabric (Figure 1) [19]. Cell adhesion, however, was poor, contrary to a previous study of *Chlamydomonas reinhardtii* on polysulfon nanofiber mats [20].

Gross *et al.* studied the effect of materials and structures on algal cell attachment. Working with a non-sterile *Chlorella vulgaris* culture including other diverse green algae and cyanobacteria, they investigated various metals, polymers and rubber. In addition to smooth surfaces, meshes with different pore sizes were studied. In general, polypropylene and nylon meshes with openings of 0.5–1.25 mm were found to be ideal for initial cell attachment and long-term adherent growth [21].

Different technologies were suggested for harvesting microalgae. Amongst them, filtration is a technology in which textile meshes or membranes are used. One possibility is the use of so-called microstrainers, rotating filters with fine meshes (pores measuring between 35 μm and 62 μm), combined with continuous backwash. Wilde *et al.* suggested a double-stage microstrainer to increase performance and cost-efficiency [22].

The exact mesh pore size for such filtration methods is determined by the size of the algae. *Chlorella sp.* (5–6 μm) and *Chlorella vulgaris* (0.1 μm) can be harvested through microfiltration [23, 24], while a microfiber disc filter was used for *Nannochloropsis salina* [25]. For *Chlorella pyrenoidosa*, Chu *et al.* studied a stainless steel mesh with a pore size of 75 μm, on which a diatomite cake layer was formed as the dynamic membrane module [26, 27]. For the dewatering of *Chlorella vulgaris*, Munshi *et al.* studied a forward osmosis polyethersulfone membrane, supported by a polypropylene permeable mesh to prevent membrane rupture, in combination with different draw solutions, such as NaCl or NH_4Cl,

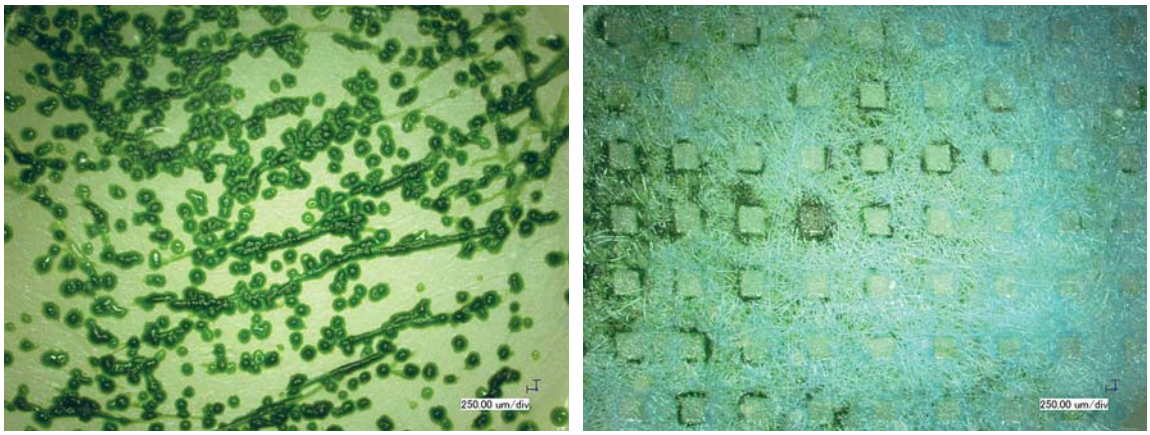

a) b)

Figure 1: Growth of Chlamydomonas reinhardtii on a polyamide nanofiber mat (a) and on a polypropylene non-woven fabric (b). For a detailed description of the experiments, cf. Ref. 19.

and found this membrane combination generally suitable [28].

It should be mentioned that the opposite objective has been reported in several publications: textile fabrics can also be prepared to protect buildings from algae (particularly in consortia with bacteria) growing on them or to serve other biocidal functions [29].

While the possible uses of nets, membranes and several other textile structures for algae growth and harvesting described above exist, no research can be found in literature regarding woven, warp or weft knitted structures as substrates for algae growth.

Nevertheless, algae, particularly microalgae, belong to a species that can be of great interest for vertical farming, e.g. for vertical agriculture in space [30], while the outdoor cultivation of temperature-tolerant algae such as *Chlorella sorokiniana* in column photobioreactors may also be a research objective aimed at sustainable food production [31]. This suggests that there is a broad area of research of possible new findings and developments related to the growth of adherent algae on diverse textile fabrics with potential vertical farming applications.

3 Plants

Agrotextiles are typically used as covers, not as substrates for growing plants. Although they can be degraded by UV irradiation and the effects of weather, and then destroyed by mechanical impacts [32], their advantages seem to outweigh these problems.

In an unheated greenhouse during the winter, lettuce was found to grow best if covered by a combination of mulch and an agrotextile [33]. Outdoor studies showed that an agrotextile or polyethylene foil resulted in an increased lettuce yield in the early growth phase [34]. In another study, a cloth cover resulted in the strongest lettuce plants, while straw mulch resulted in the weakest plants [35]. Agrotextiles were found more suitable than black plastic and sawdust for strawberries with a high ascorbic acid content [36]. Traditional straw mulch, however, resulted in the best fruit size and yield [37]. For an early potato harvest, a covering made from agrotextiles resulted in larger potatoes than a covering made from a perforated plastic film or no covering at all [38]. On the other hand, litchi fruit harvesting periods could be delayed successfully by shading the trees with an agronet of 30% or 50% light transmission, thus preventing the ripening of all litchis within a few days [39].

Several research groups are working on different approaches to further develop these simple agrotextiles. Dan *et al.* developed a new textile composite material that was UV resistant and clearly increased the growth of spinach and two lettuce varieties [40]. A knitted alternative to typical non-woven fabrics was suggested by Scarlat *et al.*, who prepared warp knitted nets from polyester and polyamide, and found good mechanical properties compared with typical agrotextiles [41].

It should be mentioned that agrotextiles such as row covers are used to protect plants, not only from the wind and sun, but also from virus vectors and other undesirable pests. Honeydew melons could be protected from the sweet potato whitefly and vegetable leaf miner using different row covers with varying success [42]. For tomatoes, whiteflies are also a major pest that sometimes results in complete crop loss. In combination with planting aromatic basil between tomato rows, an agronet cover could reduce whitefly infestation by more than two thirds [43]. The same effect was found when French bean plants were protected from the silverleaf whitefly and black bean aphids. In addition, the covered plants developed faster and yielded a higher quality [44]. While the latter study showed no clear correlation between the protective effect and the impregnation of the net with an alphacypermethrin-based insecticide, another study found that the mortality rate of whiteflies exposed to alphacypermethrin-treated agronets doubled [45]. To prevent crops from bacterial contaminations, antibacterial nanosilver coatings were deposited on high-density polyethylene nets and studied with respect to their antibacterial properties on gram-positive and gram-negative bacteria [46].

To summarise these findings, textile fabrics can be used for a broad variety of agricultural applications, in particular protecting plants from excessively cold or warm weather, insects, bacterial contaminations, etc. It should be mentioned, however, that there are also some negative aspects that are usually not reported in literature, but must not be overlooked, such as birds and other animals becoming entangled in nets meant to protect fruit against them, or the exposure of the environment to non-biodegradable polymer parts if agrotextiles are destroyed by

a) b)

Figure 2: Growth of cress (a) and grass (b) in different textile substrates

heavy wind, etc. These aspects, however, are not relevant for indoor vertical farming, and can be addressed through intelligent textile constructions for outdoor vertical farming ideas.

Because the step from covering plants with agrotextiles to letting plants grow on agrotextiles in hydroponic applications is not actually large, it is surprising that no reports regarding other textile applications in agriculture can be found in scientific literature. Textile fabrics are commercially available as base materials for outdoor vertical farming systems for individuals, and contain bags in which plant pots can be fixed. However, the direct combination of textile and plant, i.e. using a fabric as a substrate to which the plant roots adhere, is only scarcely found. This is particularly hard to understand, as the shape and chemistry of textile fabrics can be tailored according to the requirements of the roots of each plant (Figure 2).

4 Conclusion and outlook

Textile fabrics are used for several applications in agriculture and algae farming. Surprisingly, no reports can be found in scientific literature about the obvious implications of studying the ability of diverse textile fabrics for their possible use in hydroponics and other vertical farming applications.

Due to the increasing need for vertical farming solutions in the coming decades, vertical farming can be developed further based on the well-known advantages of textile fabrics: the wide variety of structures and chemical compositions of fibres, the possibilities of creating one-, two- and, to a certain extent, even three-dimensional fabrics, and relatively inexpensive and long-established textile production technologies.

In the author's personal opinion, vertical farming is a technologically available method to address the severe problem of supplying sufficient food for a growing population in cities with increasingly less space, without destroying even more forests and other natural wildlife habitats. Numerous examples of the use of textile fabrics for diverse agricultural applications suggest that recent progress in innovative agrotextiles and algae harvesting nets should be transferred into textile-based solutions for vertical farming. This transfer could pave the way to new technologies for ecologically and economically reasonable food production.

Acknowledgment

This study was partly funded by the Federal Ministry for Economic Affairs and Energy in the scope of the ZIM project ZF4036107.

References

1. United Nations, Department of Economic and Social Affairs, Population Division. World Population Prospects: The 2017 Revision, Key Findings and Advance Tables. Working Paper No. ESA/P/WP/248, 2007.
2. Global Hunger Index [online]. Results – Global, Regional, and National Trends [accessed 31. 12. 2018]. Available on World Wide Web: http://www.globalhungerindex.org/results/.
3. MAYER, Helmut, SCHUH, Marc, FLACHMANN, Christine. Umweltökonomische Gesamtrechnungen. Flächenbelegung von Ernährungsgütern

2008–2016. Statistisches Bundesamt (Destatis), 2018, no. 5385101-16900-4.
4. PINSTRUP-ANDERSON, Per. Is it time to take vertical indoor farming seriously? *Global Food Security*, 2018, **17**, 233–235, doi: 10.1016/j.gfs.2017.09.002.
5. JANUSZKIEWICZ, Krystyna, JARMUSZ, Malgorzata. Envisioning urban farming for food security during the climate change era. Vertical farm within highly urbanized areas. *IOP Conference Series – Materials Science and Engineering*, 2017, **245**, 052094, doi: 10.1088/1757-899X/245/5/052094.
6. EAVES, James, EAVES, Stephan. Comparing the profitability of a greenhouse to a vertical farm in Quebec. *Canadian Journal of Agricultural Economics*, 2018, **66**(2), 43–54, doi: 10.1111/cjag.12161.
7. YUSOF, Sharifah Syafinaz Syed, THAMRIN, Norashikin M., NORDIN, Mohd Khairi, YUSOFF, Aiza Syuhada Mohd, SIDIK, Norrizah Jaafar. Effect of artificial lighting on typhonium flagelliforme for indoor vertical farming. In *IEEE International Conference on Automatic Control and Intelligent Systems : book of proceedings*. Malaisya : Institute of Electrical and Electronics Engineers Inc., 2016, pp. 7–10.
8. AL-KODMANY, Kheir. The vertical farm: A review of developments and implications for the vertical city. *Buildings*, 2018, **8**(2), 24, doi: 10.3390/buildings8020024.
9. TOULIATOS, Dionysios, DODD, Ian, C., McAINSH, Martin. Vertical farming increases lettuce yield per unit area compared to conventional horizontal hydroponics. *Food and Energy Security*, 2016, **5**(3), 184–191, doi: 10.1002/fes3.83.
10. DESPOMMIER, Dickson. Farming up the city: the rise of urban vertical farms. *Trends in Biotechnology*, 2013, **31**(7), 388–389.
11. AL-CHALABI, Malek. Vertical farming: Skyscraper sustainability? *Sustainable Cities and Society*, 2015, **18**, 74–77, doi: 10.1016/j.scs.2015.06.003.
12. KERNER, Martin. Anaerobic domestic waste water treatment coupled to a bioreactor facade for the production of biogas, heat and biomass. In *Powerskin Conference : proceedings*. Munich, Germany, 2017.
13. STILLER, John W., RILEY, Jennifer, HALL, Benjamin D. Are red algae plants? A critical evaluation of three key molecular data sets. *Journal of Molecular Evolution*, 2001, **52**, 527–539, doi: 10.1007/s002390010183.
14. LI, Hua-Bin, CHENG, Ka-Wing, WONG, Chi-Chun, FAN, King-Wai, CHEN, Feng, JIANG, Yue. Evaluation of antioxidant capacity and total phenolic content of different fractions of selected microalgae. *Food Chemistry*, 2007, **102**(3), 771–776, doi: 10.1016/j.foodchem.2006.06.022.
15. KERRISON, Philip D., STANLEY, Michele S., HUGHES, Adam D. Textile substrate seeding of *Saccharina latissimi* sporophytes using a binder: An effective method for the aquaculture of kelp. *Algal Research*, 2018, **33**, 352–357, doi: 10.1016/j.algal.2018.06.005.
16. PELLIZZARI, Franciane Maria, ABSHER, Theresinha, YOKOYA, Nair S., OLIVEIRA, Eurico C. Cultivation of the edible green seaweed *Gayralia* (Chlorophyta) in southern Brazil. *Journal of Applied Phycology*, 2007, **19**, 63–69, doi: 10.1007/s10811-006-9111-1.
17. LUO, Shuai, SAMPARA, Pranav Sai Shankar, HE, Zhen. Effective algal harvesting by using mesh membrane for enhanced energy recovery in an innovative integrated photobioelectrochemical system. *Bioresource Technology*, 2018, **253**, 33–40, doi: 10.1016/j.biortech.2018.01.001.
18. LEE, Seung-Hoon, OH, Hee-Mock, JO, Beom-Ho, LEE, Sang-A, SHIN, Sang-Yoon, KIM, Hee-Sik, LEE, Sang-Hyup, AHN, Chi-Yong. Higher biomass productivity of microalgae in an attached growth system, using wastewater. *Journal of Microbiology and Biotechnology*, 2014, **24**(11), 1566–1573, doi: 10.4014/jmb.1406.06057.
19. GROßERHODE, Christina, WEHLAGE, Daria, GROTHE, Timo, GRIMMELSMANN, Nils, FUCHS, Sandra, HARTMANN, Jessica, MAZUR, Patrycja, RESCHKE, Vanessa, SIEMENS, Helena, RATTENHOLL, Anke, HOMBURG, Sarah Vanessa, EHRMANN, Andrea. Investigation of microalgae growth on electrospun nanofiber mats. *AIMS Bioengineering*, 2017, **4**(3), 376–685, doi: 10.3934/bioeng.2017.3.376.
20. KESKIN, Nalan Oya San, CELEBIOGLU, Asli, UYAR, Tamer, TEKINAY, Turgay. Microalgae immobilized by nanofibrous web for removal or reactive dyes from wastewater. *Industrial and Engineering Chemistry Research*, 2015, **54**(21), 5802–5809, doi: 10.3934/bioeng.2017.3.376.

21. GROSS, Martin, ZHAO, Xuefei, MASCARENHAS, Vernon, WEN, Zhiyou. Effects of the surface physico-chemical properties and the surface textures on the initial colonization and the attached growth in algal biofilm. *Biotechnology for Biofuels*, 2016, **9**, 38, doi: 10.1186/s13068-016-0451-z.
22. WILDE, Edward W., BENEMANN, John R., WEISSMAN, Joseph C., TILLETT, David M. Cultivation of algae and nutrient removal in a waste heat utilization process. *Journal of Applied Phycology*, 1991, **3**(2), 159–167, doi: 10.1007/BF00003698.
23. SHEKHAR, Mayank, SHRIWASTAV, Amritanshu, BOSE, Purnendu, HAMEED, Shemeera. Microfiltration of algae: impact of algal species, backwashing mode and duration of filtration cycle. *Algal Research*, 2017, **23**, 104–112, doi: 10.1016/j.algal.2017.01.013.
24. MILLEDGE, John J., HEAVEN, Sonia. A review of the harvesting of micro-algae for biofuel production. *Reviews in Environmental Science and Bio/Technology*, 2013, **12**(2), 165–178, doi: 10.1007/s11157-012-9301-z.
25. RASHID, Naim, UR REHMAN, Muhammad Saif, SADIQ, Madeha, MAHMOOD, Tariq, HAN, Jong-In. Current status, issues and developments in microalgae derived biodiesel production. *Renewable and Sustainable Energy Reviews*, 2014, **40**, 760–778, doi: 10.1016/j.rser.2014.07.104.
26. CHU, Huaqiang, ZHAO, Yangying, ZHANG, Yalei, YANG, Libin. Dewatering of *Chlorella pyrenoidosa* using a diatomite dynamic membrane: Characteristics of a long-term operation. *Journal of Membrane Science*, 2015, **492**, 340–347, doi: 10.1016/j.memsci.2015.05.069.
27. ZHANG, Yalei, ZHAO, Yangying, CHU, Huaqiang, ZHOU, Xuefei, DONG, Bingzhi. Dewatering of *Chlorella pyrenoidosa* using diatomite dynamic membrane: Filtration performance, membrane fouling and cake behavior. *Colloids and Surfaces B: Biointerfaces*, 2014, **113**, 458–466, doi: 10.1016/j.colsurfb.2013.09.046.
28. MUNSHI, Faris M., CHURCH, Jared, MCLEAN, Rebecca, MAIER, Nicholas, SADMANI, A. H. M. Anwar, DURANCEAU, Steven J., LEE, Woo Hyoung. Dewatering algae using an aquaporin-based polyethersulfone forward osmosis membrane. *Separation and Purification Technology*, 2018, **204**, 154–161, doi: 10.1016/j.seppur.2018.04.077.
29. RYPAROVÁ, Pavla, RÁCOVÁ, Zuzana. Biocidal efficiency on consortium algae and bacteria of nanofiber textiles doped by biocide substance. In *Nanocon 2015: 7th International Conference on Nanomaterials – Research & Application : proceedings*. Brno, Czech Republic, 2015, pp. 276–281.
30. WHEELER, Raymond M. Agriculture for space: people and places paving the way. *Open Agriculture*, 2017, **2**(1), 14–32, doi: 10.1515/opag-2017-0002.
31. BECHET, Quentin, MUNOZ, Raul, SHILTON, Andy, GUIEYSSE, Benoit. Outdoor cultivation of temperature-tolerant Chlorella sorokiniana in a column photobioreactor under low power-input. *Biotechnology and Bioengineering*, 2013, **110**(1), 118–126, doi: 10.1002/bit.24603.
32. DEMSAR, Andrej, ZNIDARCIC, Dragan, SVETEC, Diana Gregor. Impact of UV radiation on the physical properties of polypropylene floating row covers. *African Journal of Biotechnology*, 2011, **10**(41), 7998–8006, doi: 10.5897/AJB10.2538.
33. GOVEDARICA-LUCIC, Aleksandra, MOJEVIC, Mirjana, PERKOVIC, Goran, GOVEDARICA, Branka. Yield and nutritional quality of greenhouse lettuce (*Lactuca sativa* L.) as affected by genotype and production methods. *Genetika*, 2014, **46**(3), 1027–1036, doi: 10.9755/ejfa.v25i12.16738.
34. PONJICAN, O., BAJKIN, A., DIMITRIJEVIC, A., MILEUSNIC, Z., MIODRAGOVIC, R. The influence of soil mulching and greenhouse covering material on the temperature distribution in lettuce production. In *39th International Symposium on Agricultural Engineering, Actual Tasks on Agricultural Engineering : book of proceedings*. Zagreb : Zavod za mehanizaciju poljprivrede, Agronomski fakultet Sveučilišta u Zagrebu, 2011, **39**, pp. 393–401.
35. NIKOLICH, Ljiljana, DZIGURSKI, Dejana, LJEVNAICH-MASICH, Branka, CABILOVSKI, Ranko, MANOJLOVICH, Maja. Weeds of Lettuce (*Lactuca sativa* L. subsp. *Secalina*) in organic agriculture. *Bulgarian Journal of Agricultural Science*, 2011, **17**(6), 736–743.
36. SENER, Sevinc, TUREMIS, Nurgul Fetiye. Effects of various mulch materials on fruit quality characteristics on organically grown strawberries.

Fresenius Environmental Bulletin, 2017, **26**(7), 4616–4622.

37. LAMARRE, Michel, PAYETTE, Suzanne, LAREAU, Michel J. Influence des couvertures hivernales sur la productivité du fraisier au Québec. *Canadian Journal of Plant Science*, 1992, **72**(1), 299–305, doi: 10.4141/cjps92-035.
38. REBARZ, Katarzyna, BORÓWCZAK, Franciszek, GAJ, Renata, FRIESKE, Tomasz. Effects of cover type and harvest date on yield, quality and cost-effectiveness of early potato cultivation. *American Journal of Potato Research*, 2015, **92**(3), 359–366, doi: 10.1007/s12230-015-9441-0.
39. MITRA, S. K., SARKAR, A., MANDAL, D., PATHAK, P. K. Delaying the ripening of "Bombai" litchi. *Acta Horticulturae*, 2013, **975**, 299–302, doi: 10.17660/ActaHortic.2013.975.35.
40. DAN, Maria, VISILEANU, Emilia, DUMITRESCU, Iuliana, MOCIOIU, Ana-Maria, RADULESCU, Hortensia Clara, RADULESCU, Radu, LAGUNOVSCHI, Viorica Luchian. Manufactures textile cover meant for plant protection in the cold season. In *3rd International Conference on Advanced Materials and Systems : proceedings*. Bucharest, Romania : CERTEX, 2010, 33–38.
41. SCARLAT, Razvan, RUSU, Leonard, PRICOP, Floarea. Knitted agrotextiles for a sustainable agriculture. *Industria Textila*, 2017, **68**(5), 332–336.
42. NATWICK, Eric T., LAEMMLEN, Franklin F. Protection from phytophagous insects and virus vectors in honeydew melons using row covers. *Florida entomologist*, 1993, **76**(1), 120–126, doi: 10.2307/3496020.
43. MUTISYA, Stella, SAIDI, Mwanarusi, OPIYO, Arnold, NGOUAJIO, Mathieu, MARTIN, Thibaud. Synergistic effects of agronet covers and companion cropping on reducing whitefly infestation and improving yield of open field-grown tomatoes. *Agronomy*, 2016, **6**(3), 42, doi: 10.3390/agronomy6030042.
44. GOGO, Elisha Otieno, SAIDI, Mwanarusi, OCHIENG, Jacob Mugwa, MARTIN, Tihbaud, BAIRD, Vance, NGOUAJIO, Mathieu. Microclimate modification and insect pest exclusion using agronet improve pod yield and quality of French bean. *HortScience*, 2014, **49**(10), 1298–3104.
45. MARTIN, T., KAMAL, A., GOGO, E., SAIDI, M., DELÉTRÉ, E., BONAFOS, R., SIMON, S., NGOUAJIO, M. Repellent effect of alphacypermethrin-treated netting against *Bemisia tabaci* (Hemiptera: Aleyrodidae). *Horticultural Entomology*, 2014, **107**(2), 684–690, doi: 10.1603/EC12490.
46. DE SIMONE, Serena, LOMBARDI, Fiorella Anna, PALADINI, Federica, STARACE, Giuseppe, SANNINO, Alessandro, POLLINI, Mauro. Development of antibacterial silver treatments on HDPE nets for agriculture. *Journal of Applied Polymer Science*, 2015, **132**(11), 41623, doi: 10.1002/app.41623.

Zenun Skenderi[1], Dragana Kopitar[1], Sanja Ercegović Ražić[1], Goran Iveković[2]
[1]University of Zagreb Faculty of Textile Technology, Prilaz baruna Filipovića 28a, 10000 Zagreb, Croatia
[2]Predionica Klanjec d. o. o., Klanjec (Spinning Mill), Novodvorska 7, 49290 Klanjec, Croatia

Study on Physical-mechanical Parameters of Ring-, Rotor- and Air-jet-spun Modal and Micro Modal Yarns

Študij fizikalno-mehanskih lastnosti modalnih in mikromodalnih prej, izdelanih po prstanskem in rotorskem postopku ter po postopku z zračnim curkom

Original Scientific Article/*Izvirni znanstveni članek*
Received/*Prispelo* 12-2018 • Accepted/*Sprejeto* 1-2019

Abstract

The main physical-mechanical parameters of modal yarns (unevenness, faults, hairiness and spectrograms) were compared with the parameters of micro modal yarns of the same fineness and end-use. The difference in tenacity and elongation at break of different types of modal and micro modal-spun yarns is determined by yarn structure. The highest tenacity was achieved in the oriented structure of ring-spun yarn, followed by air-jet-spun and rotor-spun yarn, in the case of both modal and micro modal fibres. All types of modal yarns differ in overall unevenness and in terms of micro modal fibres. The values of the overall unevenness of ring-, rotor- and air-jet-spun modal yarns are greater than or equal to the same values of micro modal yarns. The spinning technique, and thus the yarn structure, determine the level of overall yarn evenness. The number of faults at different levels of sensitivity measurement to detect the highest number of thin and thick places and neps (–30%, +35% and +140%) is greater in rotor- and air-jet-spun yarn than in ring-spun yarn for both levels of fibre fineness. Periodic faults of short wavelengths with significant amplitude increase the number of yarn faults to a certain extent. Rotor-spun micro modal yarn shows the highest deviation from ideal unevenness, while ring-spun modal yarn shows the lowest deviation. Yarn hairiness depends on the spinning technique. Finer fibres cause lower hairiness in all yarn types.
Keywords: modal fibre, micro modal fibre, man-made cellulosic fibre, properties

Izvleček

Glavne fizikalno-mehanske lastnosti modalnih prej (neenakomernost, napake, dlakavost in spektrogrami) so bile primerjane z lastnostmi mikromodalnih prej enake finoče in končnega namena uporabe. Razlike v trdnosti in pretržnem raztezku različnih vrst modalnih in mikromodalnih prej določa njihova struktura. Najvišjo trdnost je dosegla prstanska preja z orientirano strukturo, tej sta sledili obe preji iz modalnih in mikromodalnih vlaken, izdelani po postopku z zračnim curkom (t. i. postopku air-jet) in rotorskem postopku. Modalne preje se med seboj razlikujejo v enakomernosti preje, prav tako tudi mikromodalne preje. Vrednosti enakomernosti prstanske, rotorske in z zračnim curkom (t. i. air-jet) spredene modalne preje so večje ali enake vrednostim mikromodalnih prej. Tehnika predenja in s tem struktura preje vplivata na njeno enakomernost. Število napak, merjeno pri različnih stopnjah občutljivosti, da bi zaznali najvišjo raven tankih in debelih mest ter nopkov (–30 %, +35 % in +140 %), je večje pri rotorski preji in preji z zračnim curkom (t. i. preji air-jet) kot pri prstanski preji pri obeh finočah vlaken. Na kratkih dolžinah ugotovljene periodične napake z veliko amplitudo povečajo število napak preje v določenem obsegu. Rotorska mikromodalna preja ima največje, prstanska modalna preja pa najmanjše odstopanje od idealne enakomernosti. Kosmatost preje je odvisna od postopka predenja. Finejša vlakna povzročajo manjšo kosmatost prej kot bolj groba vlakna.
Ključne besede: kemična celulozna vlakna, predivna preja, mikrovlakna, periodične napake

Corresponding author/*Korespondenčni avtor:*
Prof dr. sc. Zenun Skenderi
E-mail: zenun.skenderi@ttf.hr

Tekstilec, 2019, ***62****(1), 42-53*
DOI: 10.14502/Tekstilec2019.62.42-53

1 Introduction

Today, there is a broad range of applications for modal fibres in the clothing industry for making lighter-weight knitted garments and articles worn next to the skin. Knitted fabric characteristics are largely dependent on the raw material composition of yarn and the yarn type from which a knitted fabric is made. Parameters of mass irregularity, which include overall unevenness, yarn faults defined as thin places, thick places, neps and hairiness, affect the appearance and other characteristics of a fabric. In general, specific samples must be made to reduce the number of input parameters, in order to find a more precise relationship between the effect of fibre type, fibre properties and the spinning process (including the type of spinning machine) on the basic physical-mechanical properties of yarn (and thus on the appearance and properties of a knitted fabric).

A number of researchers have dealt with the properties of ring-spun yarn [1], the dynamic properties of air-jet-spun yarn and rotor-spun yarn [2], the geometric analysis of spun yarns with the aim of assessing the tensile properties of air-jet-spun yarn [3], the assessment of the tensile properties of air-jet-spun yarn [4], and the tensile properties of rotor-spun yarn [5]. Yarn unevenness and hairiness has also been studied by a number of researches [6–9]. The effect of periodic faults on overall unevenness and/or on the number of faults in yarn has only been studied to a small extent [10, 11]. However, it is not evident from literature that a more significant study of the effect of fibre fineness on the basic physical and mechanical properties of different yarn types has been undertaken.

In order to reduce the number of different input parameters and to find a clearer connection between parameters, yarn with one type of different fibre parameters should be spun using the same technological process, the same twist coefficient and the same fineness. Thus, the effect of the spinning technique (rotor and ring) used for micro modal fibres on unevenness [12] and the unevenness of air-jet-spun yarn relative to rotor- and ring-spun micro modal yarn has already been studied [13]. The latter studies still continue, so that modal yarns are also included. Thus, the aim of this paper is to present a comparison of the basic physical-mechanical properties of ring-, rotor- and air-jet spun yarn made from modal fibres, and to extend that comparison to the same types of micro modal yarns.

2 Experimental part

For the purposes of this study, ring-, rotor- and air-jet-spun yarns were spun with a nominal count of 20 tex (Nm 50) from 1.3 dtex fibres with a length of 38 mm. The basic properties of these yarns were compared with the properties of yarns having the same end-use (knitting) from 1 dtex micro modal fibres with a length of 39 mm. Modal yarns were spun under the same technological conditions as micro modal yarns [12, 13]:

a) Ring-spun modal yarn was produced using the carding manufacturing process, comprising fibre preparation phases (opening, blending and carding), spinning preparation (drawing, pre-spinning and ring spinning), winding and cleaning. A Zinser 351 ring spinning machine connected to an Autoconer X5 winding machine was used for the ring spinning process.
b) Rotor-spun modal yarn was produced using the carding manufacturing process, comprising fibre preparation phases (opening, blending and carding), spinning preparation (drawing) and rotor spinning. A Schlafhorst A8 rotor spinning machine was used for spinning.
c) Air-jet modal yarn was produced using the carding manufacturing process, comprising fibre preparation phases (opening, blending and carding), spinning preparation (three drawing passages) and air-jet spinning. A Rieter J 20 machine was used for spinning.
d) Yarn unevenness was determined in accordance with standard ASTM D1425/D1425M-14 Standard Test Method for Evenness of Textile Strands Using Capacitance Testing Equipment [16]. Unevenness, the number of yarn faults and hairiness were determined on an Uster Tester 4-S with a yarn throughput speed of 400 m/minute through the measuring field with a test time of 2.5 minutes. One measurement of each cross-wound package of each yarn type was performed.
e) The tensile properties of yarn were determined in accordance with standard ISO 2062:2009 Textiles – Yarns from packages – Determination of single-end breaking force and elongation at break using constant rate of extension (CRE) tester [17]. Measurements were performed on an Uster Tensorapid 4 instrument. A total of 100 measurements per package of each yarn type were performed.

The number of fibres in the cross-section (n_f) was determined from the ratio between yarn fineness (T_{ty}) and fibre fineness (T_{tf}) using the following equation:

$$n_f = \frac{T_{ty}}{Tt_f} \quad (1)$$

The limiting irregularity CV_{lim} was calculated for man-made fibres and cotton using the following equation [18]:

$$CV_{lim} = \frac{100}{\sqrt{n_f}} \quad (2)$$

The index of irregularity I was determined from the ratio between the coefficient of variation of unevenness (obtained by measuring CV_m) and limiting irregularity (CV_{lim}) using the following equation:

$$I = \frac{CV_m}{CV_{lim}} \quad (3)$$

The index of irregularity is a measure of the unevenness deviation of a certain fibre type that will be spun in an ideal situation where $I = 1$. It also shows how well the machines used in certain technological phases run and whether any deviations in their operation occur. Fibre distribution in yarn is not completely controlled. In practice, the orientation of fibres in yarn is regarded as a random occurrence. The goal to be achieved in production is to maintain a constant number of fibres in any yarn cross section.
Non-periodic faults can be thin places, thick places and neps. The level of measurement sensitivity is typically as follows: –30%, –40%, –50% and –60% for thin places; +35%, +50%, +70%, +100% for thick places; and +140%, +200%, +280% and +400% for neps. Periodic faults or system faults occur due to the periodic irregular motions of individual machine elements and/or due to damage to those elements (e.g. rollers, gears, belts, vibrations, etc.). Periodic faults are shown using a spectrogram. If unevenness reaches the ideal value ($I = 1$), the spectrogram has an ideal curve. The spectrogram function takes the following mathematical form [18]:

$$S = f(\lambda) = \frac{1}{\sqrt{\pi nf}} \frac{\sin \frac{l_o}{\lambda}}{\sqrt{\frac{\pi l_o}{\lambda}}} \quad (4)$$

where: S = spectrogram, n_f = number of fibres in the yarn cross-section, l_o = fibre length and λ = wavelength. The real spectrogram curve deviates from the ideal curve.

3 Results and discussion

The fineness of all modal yarn types is very consistent and ranges from 20.13 to 20.22 tex, and from 20.04 to 20.15 tex in the case of micro modal yarns. The coefficient of variation of fineness among cross-wound packages is very low, generally below 1% (Table 1). This indicates the very high consistency of high-quality production. The number of fibres in the yarn cross section is calculated using equation 1, from which it is apparent that fibre fineness determines the number of fibres in the yarn cross-section of the same yarn fineness. The number of modal fibres in the yarn cross-section ranges from 155 to 156, while the number of micro modal fibres in the yarn cross-section ranges from 200 to 202. The number of twists in all yarn types is uniform and is determined according to the end-use of yarn (knitting). The twist coefficient ranged from 3,280 to 3,350 m^{-1} tex $^{0.5}$.

3.1 Tensile properties

The values of basic physical-mechanical parameters and the breaking elongation properties of yarns with a nominal count of 20 tex used to make knit garments are given in Table 1 and shown in Figure 1. Ring-spun modal yarn has the highest tenacity (23.81 cN/tex), followed by aerodynamic (20.77 cN/tex) and rotors with the lowest tenacity (15.39 cN/tex). Yarn elongation at break follows yarn tenacity. The highest elongation at break among modal yarns was found in ring-spun yarn (10.83%), followed by air-jet-spun yarn (9.25%), while the lowest elongation at break was found in rotor-spun yarn (8.17%). The difference in tenacity and elongation at break of different types of spun modal yarns (as well as micro modal yarns) is caused by yarn structure, as the result of the spinning technique. In principle, a greater number of fibres increases the contact surface among fibres, and thus causes a greater overall friction force for a particular yarn type. With the same number of twists, ring and or spun modal yarn has a lower tenacity (23.81 and 15.38 cN/tex respectively) than ring- and rotor-spun micro modal yarn (24.09 cN/tex and 15.86 cN/tex respectively). However, yarns

from finer micro modal fibres did not impart significantly greater tenacity than yarns from coarser modal fibres in all yarn types. The highest performed work of rupture of modal yarn is observed in ring-spun yarn due to its oriented structure (14.84 N cm), followed by air-jet-spun yarn (11.22 N cm), while the lowest value of the performed work of yarn rupture is observed in rotor-spun yarn (7.66 N cm). The same sequence is also observed in micro modal yarns. By comparing modal and micro modal yarns, ring- and air-jet-spun yarn from finer micro modal fibres perform less work of yarn rupture (14.26 N cm, 10.78 N cm) than the same types of modal yarns (14.84 N cm, 11.22 N cm). In rotor-spun yarn, the higher fineness of micro modal fibres had practically no effect on the work of yarn rupture (7.70 N cm, 7.66 N cm).

3.2 Unevenness

The values of the unevenness parameters of all types of modal and micro modal yarns are given in Table 2 and shown in Figures 2–8. All types of modal yarns differ in overall unevenness and in micro modal fibres. Rotor-spun yarn has the greatest overall unevenness in the case of modal fibres (13.95 %), while ring-spun yarn has the lowest unevenness

Table 1: Main yarn parameters and tensile properties of ring-, rotor- and air-jet-spun modal and micro modal yarn

Type of material	Linear density		N[a)]	Twist		Tenacity		Elongation		Work
	$\bar{x}$ [tex]	CV_b [%]	$\bar{x}$	$\bar{x}$ [m^{-1}]	CV_b [%]	$\bar{x}$ [cN/tex]	CV_b [%]	$\bar{x}$ [%]	CV [%]	[N cm]
Ring modal	20.13	0.82	154.8	745.3	2.91	23.81	6.89	10.83	5.46	14.84
Ring micro modal	20.04	1.02	200.4	734	2.3	24.09	6.43	10.3	5.27	14.26
Rotor modal	20.22	0.78	155.5	750	–	15.39	9.29	8.17	8.81	7.66
Rotor micro modal	20.12	0.84	201.2	750	–	15.86	8.55	8	7.92	7.7
Air-jet modal	20.14	0.28	154.9	b)	c)	20.77	8.36	9.25	7.35	11.22
Air-jet micro modal	20.15	0.46	201.5	b)	c)	20.55	7.37	9.01	7.02	10.78

a) Number of fibres in cross section, b) Air pressure, c) 0.6 MPa

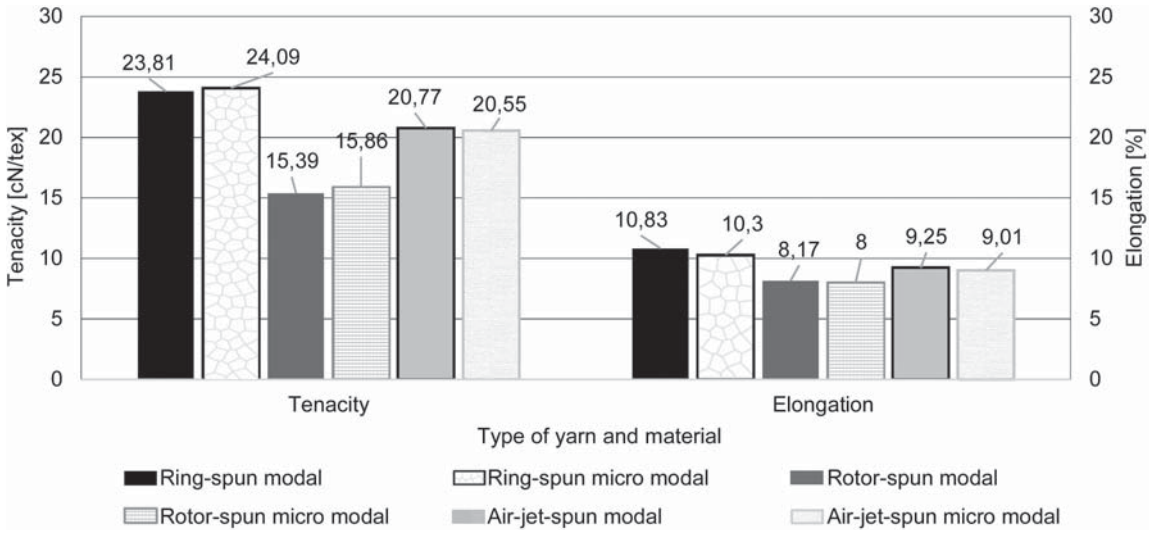

Figure 1: Tenacity and elongation of modal and micro modal ring-, rotor- and air-jet spun yarn

(10.21%). Furthermore, the values of the overall unevenness of ring-, rotor- and air-jet-spun modal yarn (10.21%, 10.95% and 12.33%) are higher than the same values of the micro modal yarns (9.67%, 12.69% and 12.12%). Thus, the spinning technique and consequently the yarn structure determine the level of overall yarn evenness. The coefficient of variation of the overall unevenness obtained as the mean value of 10 packages CV_b is highest in air-jet-spun modal yarn (2.44%) and air-jet-spun micro modal yarn (4.69%). The cause of the latter is the appearance of periodic faults with significant amplitudes in three packages of air-jet-spun modal yarn (1, 2 and 3) and in two packages of air-jet-spun micro modal yarn (3 and 4) at different wavelengths (Figures 7 and 8). Most yarns do not contain periodic faults with significant amplitudes. This is the reason CV_b values are low (Figures 3–6).

Overall yarn unevenness CV_m represents the effective (actual) value of yarn mass irregularity obtained through measurement. The limit value irregularity of yarn CV_{lim} is determined using equation 2, while the unevenness index of irregularity (I) is determined using equation 3. The value I of all modal yarn types ranges from 1.27 to 1.74. Because I is the value of the deviation of the achieved unevenness in production of one yarn type and one number of yarn twists in relation to ideal unevenness, the nearest value to the ideal value is obtained in ring-spun yarn (1.27), while the lowest value is obtained in the rotor-spun yarn

Table 2: Unevenness of ring-, rotor- and air-jet yarn spun from modal and micro modal fibres at different cut lengths

Type of material	Cut length															
	8 mm				1 m				3 m				10 m			
	CV_m [%]	CV_b [%]	CV_{lim} [%]	I	CV_m [%]	CV_b [%]	CV_{lim} [%]	I	CV_m [%]	CV_b [%]	CV_{lim} [%]	I	CV_m [%]	CV_b [%]	CV_{lim} [%]	I
Ring modal	10.21	0.98	8.04	1.27	3.49	4.51	–	–	2.74	7.4	–	–	2.25	10.98	–	–
Ring micro modal	9.67	1.96	7.06	1.37	3.25	3.89	–	–	2.28	5.66	–	–	1.61	8.72	–	–
Rotor modal	13.95	0.87	8.02	1.74	4.63	5.87	–	–	3.67	7.3	–	–	2.44	6.58	–	–
Rotor micro modal	12.69	0.67	7.05	1.80	4.41	4.51	–	–	3.56	5.41	–	–	2.56	4.59	–	–
Air-jet modal	12.33	2.44	8.03	1.54	3.74	6.68	–	–	2.32	7.07	–	–	1.23	8.37	–	–
Air-jet micro modal	12.12	4.69	7.04	1.72	2.91	3.47	–	–	2.11	5.59	–	–	1.21	8.52	–	–

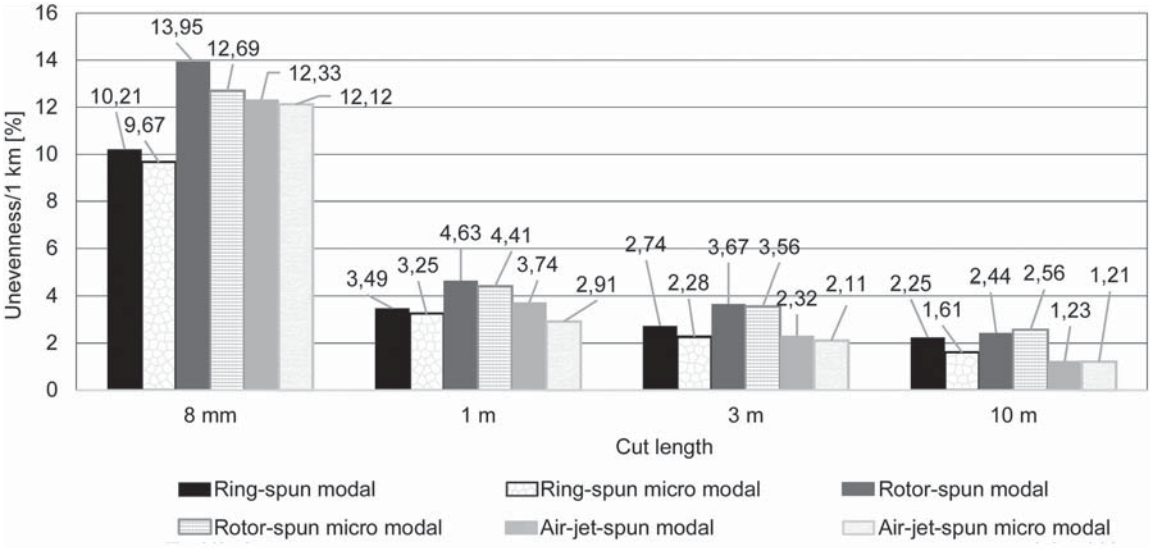

Figure 2: Unevenness of ring-, rotor- and air-jet-spun modal and micro modal yarns at different cut lengths

(1.74) in modal yarns. In micro modal yarns, *I* values range from 1.37 to 1.80. It can be concluded that the spinning technique also affects the irregularity index. In other words, coarser modal fibres cause a smaller deviation of yarn unevenness from ideal irregularity in the same fineness and end-use in all yarn types.

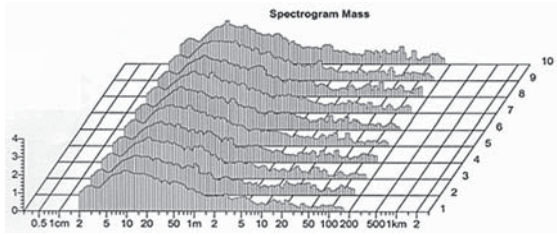

Figure 3: Mass spectrogram of modal ring-spun yarn

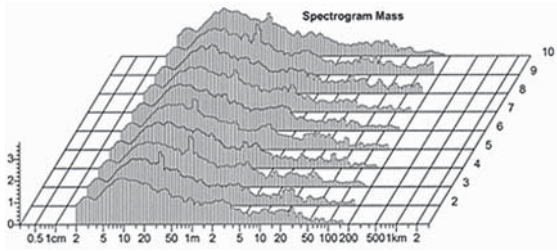

Figure 4: Mass spectrogram of micro modal ring-spun yarn

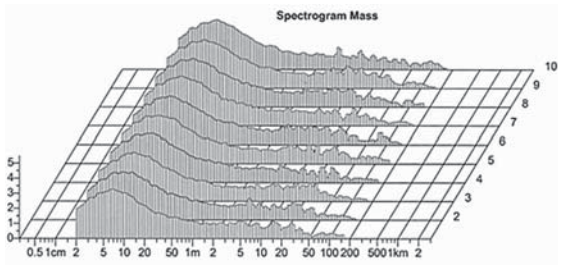

Figure 5: Mass spectrogram of modal rotor-spun yarn

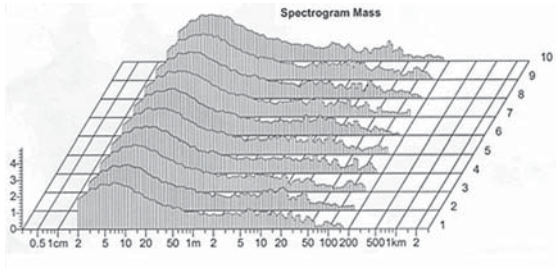

Figure 6: Mass spectrogram of micro modal rotor-spun yarn

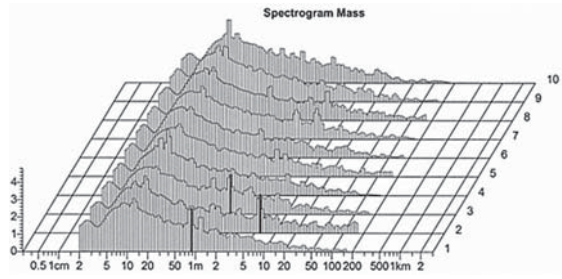

Figure 7: Mass spectrogram of modal air-jet spun yarn

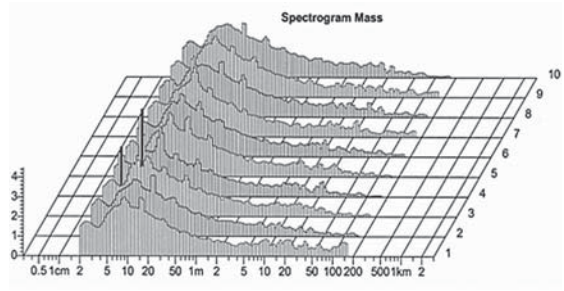

Figure 8: Mass spectrogram of micro modal air-jet spun yarn

3.3 Thin places

The number of thin places at different levels of sensitivity for all types of modal and micro modal yarns are given in Table 3 and shown in Figure 10. Rotor- (2316.8) and air-jet-spun yarn (1187.2) have a significantly higher number of thin places in modal yarn at a level of measurement sensitivity of –30% than ring-spun yarn (198.8). Comparing the same types of yarns spun from different fibres, it is evident that ring- and rotor-spun modal yarn have a greater number of thin places (198.8, 2316.8) than micro modal yarn (130.2, 1250.4). However, air-jet-spun modal yarn has a slightly smaller number of thin places (1187.29) than micro modal yarn (1197.4). The difference is 0.8% and can be ignored. At first glance, these results indicate that the greater fineness of micro modal fibres has no effect on the appearance of thin places in air-jet-spun yarn. However, because two periodic faults occurred with short wavelengths and significant amplitude in two out of 10 packages (Figure 8), the same faults increased the number of thin places. Accordingly, coarse modal fibres in ring and rotor spinning, particularly the spinning techniques (ring and rotor), create a greater number of thin places at a level of measurement sensitivity of –30% (greater weight reduction than the reference/

average weight of 100%) than finer micro modal fibres. To determine the effect of periodic faults on the number of thin places, more in-depth studies are necessary, with the specific preparation of yarn samples.
At the usual sensitivity level of –50%, which is typically used in spinning mills, rotor-spun yarn has a markedly greater number of thin places (8.1) than air-jet-spun (2) and ring-spun yarn (0.9) in the case of modal yarns. By comparing all types of modal yarns with micro modal yarns, yarns made from coarser modal fibres have a greater or a nearly equal number of thin places. Periodic faults of short wavelengths affect the number of thin places, as well as the coefficient of variation of unevenness of 10 packages CV_b. Figure 8 shows the systemic periodic fault of short wavelengths in air-jet-spun yarn, which increases the number of thin places and the value of CV_b.

3.4 Thick places

The number of thick places and the coefficient of variation of thick places of 10 packages are given in Table 4 and shown in Figure 11.
The number of thick places in all types of modal yarns at a level of measurement sensitivity of +35% is greatest in rotor-spun yarn (446), followed by air-jet-spun yarn (101.1), while the lowest number is seen in ring-spun yarn (29.7). In other words, the number of thick places in rotor-spun modal yarn is 15 times

Table 3: Thin places of ring-, rotor- and air-jet spun yarn from modal and micro modal fibres at different levels of sensitivity

Type of material	Level of sensitivity							
	–30%		–40%		–50%		–60%	
	Thin [km^{-1}]	CV_b [%]	Thin [km^{-1}]	CV_b [%]	Thin [km^{-1}]	CV_b [%]	Thin [km^{-1}]	CV_b [%]
Ring modal	198.8	13.78	5.2	28.46	0.1	316	0	0
Ring micro modal	130.2	26.8	1.4	90	0	0	0	0
Rotor modal	2316.8	3.72	235.8	9.62	8.1	44.07	0.1	316
Rotor micro modal	1250.4	2.96	61.1	9.31	0.9	122.2	0	0
Air-jet modal	1187.2	14.63	82	29.55	2	85	0	0
Air-jet micro modal	1197.4	32.7	79.7	60	1.8	190.5	0	0

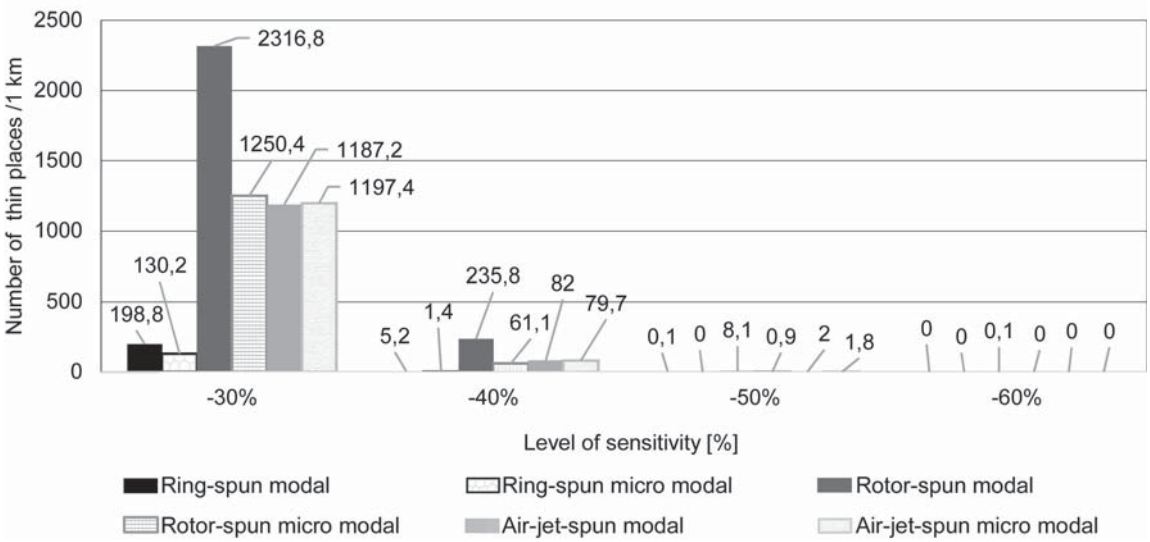

Figure 9: Number of thin places of modal and micro modal ring-, rotor- and air-jet-spun yarns for different levels of sensitivity

greater than in the ring-spun modal yarn, while the number of thick places in air-jet-spun modal yarn is 3.4 times greater than in ring-spun modal yarn.

At levels of measurement sensitivity of +50%, +70% and +100%, the sequence of thick places in modal yarns was the same as it was at a sensitivity level of +35%. The latter is analogous to micro modal yarns. By comparing the number of thick places at a level of measurement sensitivity of +35%, ring-spun yarns made from coarser modal and finer micro modal fibres have nearly the same number of thick places (29.7 and 30.4). Thus, the effect of fibre fineness on the number of thick places in ring-spun yarn at a sensitivity level of +35% is minimal. However, at a level of measurement sensitivity of +35%, a higher scattering of the number of thick places CV_b in ring-spun micro modal yarn (26.38%) is visible in relation to modal yarn (17.54%). The effect of the fineness of modal fibres on the number of thick places at a level of measurement sensitivity of +35% is significant in rotor-spun yarn. Thus, rotor-spun yarn from coarser modal fibres has a greater number of thick places at all levels of measurement sensitivity (446, 32.4 and 0.70) than rotor-spun yarn from finer micro modal fibres (245.8, 12.9, 0.1 and 0).

In air-jet-spun micro modal yarn, the number of thick places at a level of measurement sensitivity of + 35% does not decrease, but increases relative to or

Table 4: Thick places of ring-, rotor- and air-jet spun yarn from modal and micro modal fibres at different levels of sensitivity

Type of material	Level of sensitivity							
	+35%		+50%		+70%		+100%	
	Thick [km^{-1}]	CV_b [%]	Thick [km^{-1}]	CV_b [%]	Thick [km^{-1}]	CV_b [%]	Thick [km^{-1}]	CV_b [%]
Ring modal	29.7	17.54	1.8	57.22	0.3	225	0.1	316
Ring micro modal	30.4	26.38	5.8	76.21	2	115.5	0.3	160
Rotor modal	446	7.31	32.4	18.52	0.7	95.71	0	0
Rotor micro modal	245.8	7.19	12.9	28.91	0.1	320	0	0
Air-jet modal	101.1	16.09	3.4	60.76	0.4	174.7	0.1	316
Air-jet micro modal	132	46.25	5.4	56.7	0.4	130	0	0

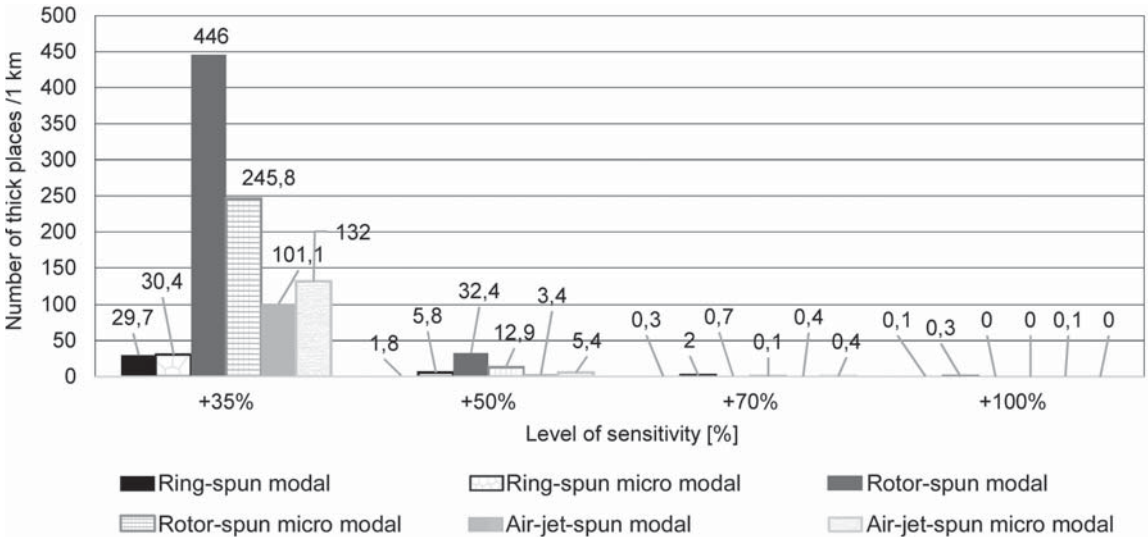

Figure 10: Number of thick places of modal and micro modal ring-, rotor- and air-jet yarns for different levels of sensitivity

is equal to (132, 5.4, 0.4 and 0) air-jet-spun modal yarn (101.1, 3.4, 0.4 and 0), which is analogous to the number of thin places in the same yarn. Here, too, the effect of the structure of air-jet-spun yarn and periodic faults in two out of 10 packages resulted in an increase in the number of thick places.

In spinning mills, the number of thick places is usually considered at a level of measurement sensitivity of +50%. The effect of finer micro modal fibres on the number of thick places is different and depends on the spinning technique. The use of micro modal fibres resulted in a 222.2% increase in the number of thick places at a level of measurement sensitivity of +50% in ring-spun yarn and a 28.8% increase in air-jet-spun yarn (including the effect of periodic faults), while a 60.2% reduction in the number of thick places was seen in rotor-spun yarn.

3.5 Neps

Since neps are actually thick places shorter than 4 mm, the number of neps in modal fibres follows the number of thick places (Table 5, Figure 12). Thus, the greatest number of neps in modal yarns at a sensitivity level of +140% is the smallest in the ring-spun yarn (72.7) followed by the air-jet-spun yarn (80.5) and the greatest in the rotor-spun yarn (1273.5). By comparing modal and micro modal yarns, it is evident that the ring- and air-jet-spun micro modal yarn has a greater number of neps (98.9, 280.6) than the modal yarn of the same type (72.7, 80.5). Only in

Table 5: Neps of ring-, rotor- and air-jet spun yarn from modal and micro modal fibres at different level of sensitivity

Type of material	Level of sensitivity							
	+140%		+200%		+280%		+400%	
	Neps [km^{-1}]	CV_b [%]	Neps [km^{-1}]	CV_b [%]	Neps [km^{-1}]	CV_b [%]	Neps [km^{-1}]	CV_b [%]
Ring modal	72.7	15.26	11	24.24	2.5	33.99	0.8	52.75
Ring micro modal	98.9	19.2	28.5	32.1	7.8	61	1.9	109.5
Rotor modal	1273.5	9.63	68.5	13.8	1.4	69.29	0.2	210
Rotor micro modal	778.8	5.96	31.2	20.1	1.3	81.5	0.1	100
Air-jet modal	80.5	33.42	5.3	35.66	0.6	86.67	0.1	316
Air-jet micro modal	280.6	63.4	14.1	65	1.6	89.4	0.2	210

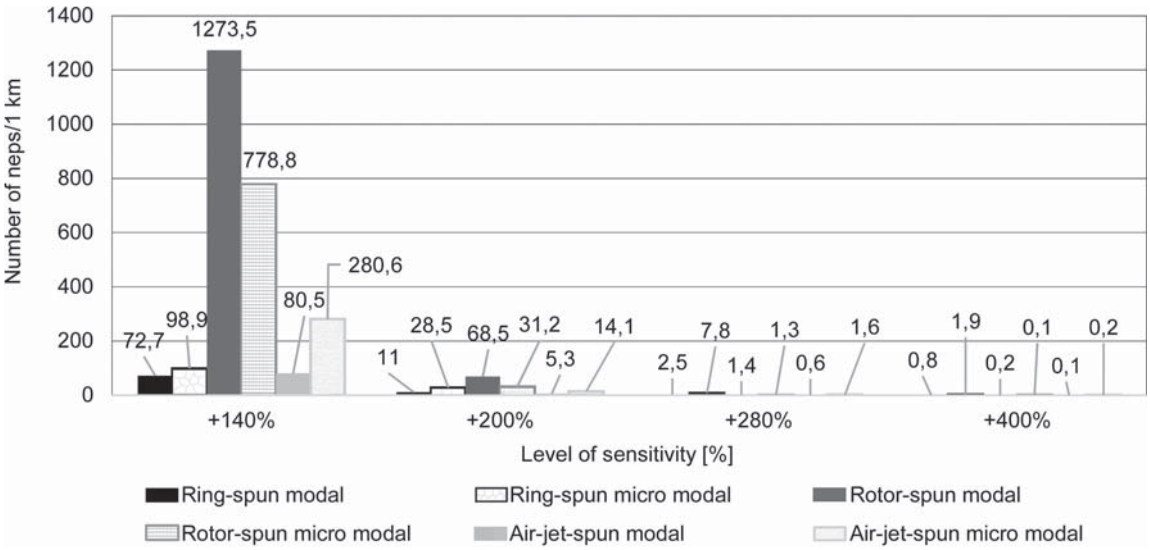

Figure 11: Number of neps of modal and micro modal ring-, rotor- and air-jet-spun yarns for different levels of sensitivity

the rotor-spun yarn from finer micro fibres the number of neps is smaller (778.8) in relation to the rotor-spun yarn from coarser modal fibres (1273.5). In other words, at a level of measurement sensitivity of +140% finer micro modal fibres increase the number of neps in the ring- and air-jet spinning, while their number decreases in the rotor spinning. In the air-jet-spun yarn the influence of periodic faults of short wavelengths with significant amplitude is, as with thin and thick places, probably significant. At a level of measurement sensitivity of +200% the sequence of the number of neps is different. In modal yarns the smallest number of neps is found in the air-jet-spun yarn (5.3), followed by the ring-spun yarn (11) and finally the rotor-spun yarn (68.5). By comparing modal and micro modal yarns, it is apparent that the sequence of the number of neps is retained as well as at a level of measurement sensitivity of + 280% and +400%. Thus, finer micro modal fibres increase the number of neps in the ring- and air-jet-spun yarn at a level of measurement sensitivity of +200% but also at a level of measurement sensitivity of +280. Thus, by using micro modal fibres at a level of measurement sensitivity of +200% the number of neps increased in the ring- and air-jet-spun yarn by 159.1% and 166.0% respectively, and the number of neps in the rotor-spun yarn was reduced by 54.5%.

3.6 Hairiness

The values of hairiness of ring-, rotor- and air-jet-spun modal and micro modal yarns are given in Table 6 and shown in Figure 12. Yarn hairiness does not follow the number of faults, but is most dependent on the spinning machine type, i.e. the yarn formation technique and fibre fineness for the same end-use. In the case of modal yarns, the yarn with the lowest hairiness is the yarn produced using an air-jet spinning technique (3.71), followed by the yarn spun using a rotor spinning machine (4.34), while the yarn spun using traditional ring spinning (6.09) shows the highest hairiness. The effect of fibre fineness on the hairiness of yarns made using different spinning techniques is equally expressed. Namely, all yarns from finer micro modal fibres show lower hairiness than yarns from coarser modal fibres. The reduction of hairiness through the use of micro modal fibres is greatest in ring-spun yarn (13.3%), followed by rotor-spun yarn (5.99%), and lowest in relative terms in air-jet-spun yarn (4.04%). Air-jet-spun yarn (6.88%) has the highest scattering of hairiness among yarn packages.

Table 6: Hairiness (H) of the ring-, rotor- and air-jet-spun modal and micro modal fibres yarn from modal and micro modal fibres

Type of yarn and material	Hairiness [*H*]	CV_b [%]
Ring modal	6.09	2.8
Ring micro modal	5.28	4.05
Rotor odal	4.34	1.8
Rotor micro modal	4.08	1.67
Air-jet modal	3.71	4.6
Air-jet micro modal	3.56	6.88

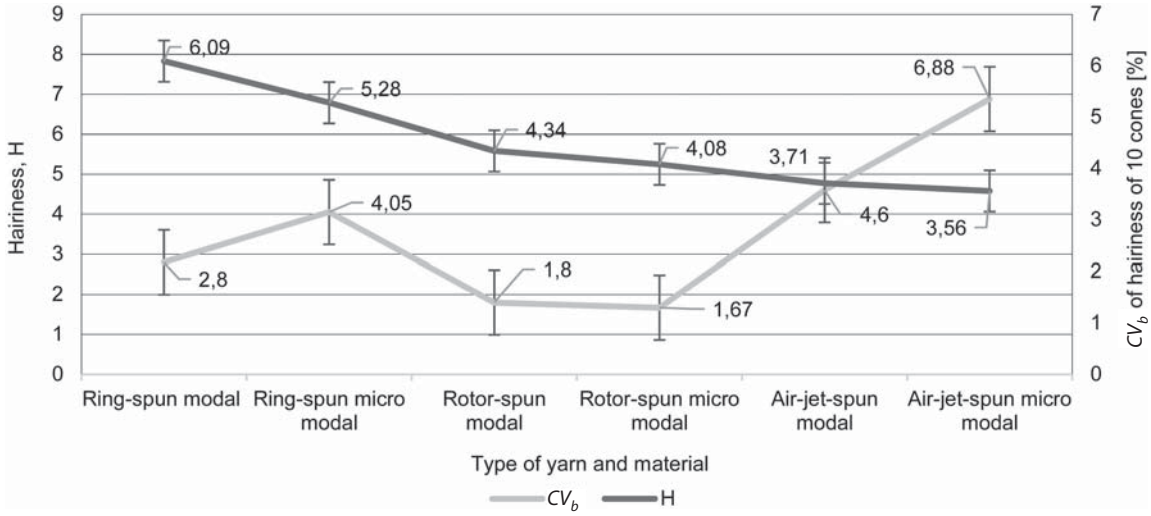

Figure 12: Hairiness H and CV of 10 cones of modal and micro modal ring-, rotor- and air-jet-spun yarns

4 Conclusion

Based on the obtained measurement results of the main physical-mechanical parameters of different types of modal and micro modal yarns, the following conclusions can be drawn:

- Ring-spun modal yarn has the highest tenacity (23.81 cN/tex), followed by air-jet-spun yarn (20.77 cN/tex), while rotor-spun yarn has the lowest tenacity (15.39 cN/tex).
- The elongation at break of modal yarns follows yarn tenacity: the highest elongation at break of modal yarn is found in ring-spun yarn (10.83%), followed by air-jet-spun yarn (9.25%), while the lowest elongation at break is found in rotor-spun yarn (8.17%).
- The difference in tenacity and elongation at break of different types of modal yarns (as well as micro modal yarns) is caused by the yarn structure, as the result of the spinning technique.
- The highest performed work of rupture of modal yarn is observed in ring-spun yarn due to its oriented structure, followed by air-jet-spun yarn, while the lowest value of the performed work of rupture is observed in rotor-spun yarn.
- The higher fineness of micro modal fibres in rotor-spun yarn had practically no effect on the performed work of rupture (7.70 N cm and 7.66 N cm).
- The spinning technique and consequently the yarn structure determine the level of overall yarn evenness.
- All types of modal yarns differ in overall unevenness and in micro modal fibres.
- The values of the overall unevenness of ring-, rotor- and air-jet-spun modal yarn (10.21%, 10.95% and 12.33%) are higher than the same values of micro modal yarns (9.67%, 12.69% and 12.12%).
- Most yarns do not contain periodic faults with significant amplitudes. This is the reason CV_b values are low.
- The coefficient of variation of the overall unevenness obtained as the mean value of 10 packages CV_b is the highest in air-jet-spun modal yarn (2.44%) and air-jet-spun micro modal yarn (4.69%). The cause of the latter is the appearance of periodic faults with significant amplitudes in three packages of air-jet-spun modal yarn and in two packages of air-jet-spun micro modal yarn at different wavelengths.
- Rotor-spun modal and micro modal yarn shows the highest deviation from ideal unevenness, followed by air-jet-spun yarn, while ring-spun modal yarn shows the lowest deviation.
- The number of faults at different levels of measurement sensitivity to detect the highest number of thin and thick places and neps (–30%, +35% and +140%) is greater in rotor- and air-jet-spun yarn than in ring-spun yarn for both fiber fineness.
- The effect of fiber fineness on the hairiness of yarns made using different spinning techniques is significant: in the case of modal yarns, the yarn with the lowest hairiness is the yarn produced using an air-jet spinning technique (3.71), followed by the yarn spun using a rotor spinning machine (4.34), while the yarn spun using traditional ring spinning (6.09) shows the highest hairiness.
- All yarns from finer micro modal fibres show lower hairiness than yarns from coarser modal fibres.

Acknowledgement

This work has been fully supported by the Croatian Science Foundation under project no. IP-2016-06-5278.

References

1. DELUCA, Lloyd B., SMITH, Brent, WATERS, William T. Analysis of factors influencing ring spun yarn tenacities for a long staple cotton: Part I: Determining broken fibers in yarns. *Textile Research Journal*, 1990, **60**(8), 475–483, doi: 10.1177/2F004051759006000807.
2. ELDESSOUKI, Mohamed, IBRAHIM, Sayed, FARAG, Ramsis. Dynamic properties of air-jet yarns compared to rotor spinning. *Textile Research Journal*, 2015, **85**(17), 1827–1837, doi: 10.1177/2F0040517514563726.
3. ÖNDER, Emel, BASER, Güngör. A comprehensive stress and breakage analysis of staple fiber yarns: Part I: Stress analysis of a staple yarn based on a yarn geometry of conical helix fiber paths. *Textile Research Journal*, 1996, **66**(9), 562–575, doi: 10.1177/2F004051759606600904.
4. ZENG, Yi-Chong, C., WANG, Kefeng, YU, Chi Wai. Predicting the tensile properties of air-jet spun yarns. *Textile Research Journal*, 2004, **74**(8), 689–694., doi: 10.1177/2F004051750407400806.

5. SETT, Sunil Kumar, MUKHERJEE, Amiya, SUR, Dipika. Tensile characteristics of rotor and friction spun jute blended yarns. *Textile Research Journal*, 2000, **70**(8), 723–728. doi: 10.1177/2F004051750007000810.
6. JIN, Jing, WANG, Jiang Ping. On yarn unevenness test and its influence factor analysis. *Applied Mechanics and Materials*, 2012, **251**, 460–464, doi: 10.4028/www.scientific.net/AMM.251.460.
7. CARVALHO, Vitor, MONTEIRO João L., SOARES, Filomena O., VASCONCELOS, Rosa M. Yarn evenness parameters evaluation: A new approach. *Textile Research Journal*, 2008, **78**(2), 119–127, doi: 10.1177/2F0040517507076744.
8. KUANG, Xueqin, HU, Yuanbo, YU, Chongwen. The theoretical yarn unevenness of cotton considering the joint influence of fiber length distribution and fiber fineness. *Textile Research Journal*, 2016, **86**(2), 138–144, doi: 10.1177/2F0040517515586161.
9. KRUCIŃNSKA, Izabella. Fiber blending irregularities in cross sections and on yarn surfaces in relation to yarn properties. *Textile Research Journal*, 1988, **58**(5), 291–298, doi: 10.1177/2F004051758805800508.
10. SHARIEFF, I., VINZANEKAR, S. G., NARASIMHAM, T. Spectral analysis of yarn irregularity and its relationship to other yarn characteristics. *Textile Research Journal*, 1983, **53**(10), 606–614, doi: 10.1177/2F004051758305301006.
11. LORD, Peter R. Yarn evenness in open-end spinning. *Textile Research Journal*, 1974, **44**(7), 512–515, doi: 10.1177/2F004051757404400708.
12. SKENDERI Zenun, IVEKOVIĆ Goran, KOPITAR Dragana. Impact of spinning technique on physcal-mechanical yarn characteristics from micromodal fibers. *11th Scientific – Professional Symposium "Textile Science & Economy : Book of proceedings*. Edited by Sanja Ercegović Ražić. Zagreb: Faculty of textile technology, 2018, 205–210.
13. SKENDERI, Zenun, KOPITAR, Dragana, VRLJIČAK, Zlatko, IVEKOVIĆ, Goran. Unevenness of air-jet yarn in comparison with ring and rotor spun yarn made from micro modal fibers. *Tekstil*, 2018, **67**(1–2), 14–26.
14. *ISO 2060:1994 Textiles – Yarn from packages – Determination of linear density (mass per unit length) by the skein method.*
15. *ISO 2061:2015 Textiles – Determination of twist in yarns – Direct counting method*
16. *ASTM D1425/D1425M-14 Standard test method for evenness of textile strands using capacitance testing equipment*.
17. *ISO 2062:2009 Textiles – Yarns from packages – Determination of single-end breaking force and elongation at break using constant rate of extension (CRE) tester*.
18. *Uster News Bulletin*, No. 26, 1978.

Ravi Kumar Jain[1], S. K. Sinha[1], Apurba Das[2]
[1]National Institute of Technology Jalandhar, Department of Textile Technology, Punjab 144011, India
[2]Indian Institute of Technology Delhi, Department of Textile Technology, New Delhi 110016, India

Studies on the Moisture Management Characteristics of Spunlace Nonwoven Fabric

Študij lastnosti prenosa vlage skozi vlaknovine, utrjene z vodnim curkom

Original Scientific Article/*Izvirni znanstveni članek*
Received/*Prispelo* 1-2019 • Accepted/*Sprejeto* 3-2019

Abstract

Liquid moisture transfer, sweat absorbency and sweat drying in clothing have a significant influence on the wearer's perception. Moisture management is one of the key performance criteria in determining the comfort level of fabric. It is thus important to study the moisture management characteristics of spunlace nonwoven fabric to investigate the possibility of its use in apparel. In the present study, spunlace nonwoven fabrics were produced by varying waterjet pressure, delivery speed, web mass and web composition. The effect of different parameters on various properties of the moisture management tester was studied using a response surface methodology with backward elimination. The statistical analysis showed that web composition affected all parameters of the moisture management tester. Waterjet pressure and web mass do not have a significant effect on wetting time (top), absorption rate (bottom) and one-way transport capability. The effect of delivery speed was not found to be significant. The overall moisture management coefficient of all nonwoven fabrics studied was found to be very good. An increase in web mass resulted in a decrease in the overall moisture management coefficient value of nonwoven fabric, which can be halted by using higher waterjet pressure and through the proper selection of web composition. Nonwoven fabric with either 100% viscose or 50% polyester/50% viscose blended composition, with higher waterjet pressure and higher web mass, was found to be suitable for the apparel industry.
Keywords: moisture, overall moisture management coefficient, waterjet pressure, web mass

Izvleček

Prenos in absorpcija znoja ter sušenje znoja pomembno vplivajo na občutek nošenja oblačil. Odziv oblačil na vlago je eden ključnih dejavnikov vrednotenja udobnosti tekstilnega materiala. Zato je za oceno primernosti vlaknovin, utrjenih z zračnim curkom, za oblačila pomembno proučiti njihovo odzivanje na vlago. V tej študiji so bile izdelane vlaknovine, utrjene z različnimi pritiski vodnega curka, različnimi hitrostmi izdelave, z različnimi ploščinskimi masami in surovinsko sestavo. Z uporabo metodologije odzivnih površin in povratne eliminacije so bili proučeni različni vplivni parametri vlaknovin na izmerjene lastnosti prenosa vlage. Statistična analiza je pokazala, da surovinska sestava vpliva na vse parametre prenosa vlage. Tlak vodnega curka in ploščinska masa vlaknovine nista pomembno vplivala na njen čas omočenja (zgornje strani), hitrost absorpcije (na spodnji strani) in sposobnost odvajanja vlage. Tudi hitrost izdelave vlaknovine ni imela pomembnega vpliva. Ugotovljeno je bilo, da je bil skupni koeficient odzivanja na vlago pri vseh vlaknovinah zelo dober. Povečanje ploščinske mase je vplivalo na znižanje skupnega koeficienta odzivanja vlaknovine na vlago, kar pa je mogoče preprečiti z uporabo višjega pritiska vodnega curka in z ustrezno izbiro surovinske sestave vlaknovine. Ugotovljeno je bilo, da so vlaknovine iz 100-odstotnih viskoznih vlaken ali iz mešanice 50 % poliester/50 % viskoza ob uporabi višjega pritiska vodnega curka in večji ploščinski masi primerne za izdelavo oblačil.
Ključne besede: vlaga, skupni koeficient prenosa vlage, tlak vodnega curka, ploščinska masa

Corresponding author/*Korespondenčni avtor:*
Ravi Kumar Jain
E-mail: rkjain2403@gmail.com

Tekstilec, 2019, ***62****(1), 54-73*
DOI: 10.14502/Tekstilec2019.62.54-73

1 Introduction

Moisture regulation is one of the key performance parameters in today's apparel industry. The microclimate between the skin and clothing should be thermally stable via moisture management, [1] and has a significant effect on the thermo-physiological comfort of the human body [2]. Moisture vapour transfer and liquid moisture transfer (sweat absorbency and sweat drying) in clothing plays an important role in the wearer's perception. Moisture management fabric should transfer sweat in vapour moisture form when the body is motionless and should allow liquid moisture to be drawn off to the outer surface to evaporate when the body is working [3]. The multidimensional moisture transport property of a fabric is generally referred to as moisture management characteristics [4]. Fibre-liquid interaction affects the moisture management of fabric [5]. Fibre-liquid interaction phenomena depend on the surface tension and pore diameter/porosity of a fabric [6–7]. Because the transfer of heat and moisture through fabric is vital for designing clothing for specific uses, [8] many theoretical and experimental studies have been conducted to understand the moisture transport phenomenon for both woven and knitted structures. Very few studies, [9–12] however, have discussed the moisture transport characteristics of nonwoven fabrics.

Nonwoven fabrics are engineered fabrics that today are used almost everywhere. Spunlace nonwoven fabric is the most promising technology for the production of fabric used extensively in the apparel industry, on account of its good handling and tensile properties. Its structure also offers good structural integrity and is comparable to other nonwoven products. Spunlacing (hydroentanglement) is a mechanical type of bonding that uses high-speed jets of water to strike a web, so that fibres knot about one another [13]. The physical characteristics of hydroentangled nonwoven fabrics, such as softness, flexible handling, high drape and bulk, conformability and high strength without binders and good delamination resistance, make it unique among all other types of nonwoven fabrics. Applications of this fabric include bacteria-proof clothing, wet wipes and as interlining fabric [14]. Recent research also suggests the application of spunlace nonwoven fabrics in fashion apparel [15-16]. Application in the apparel industry, however, requires the careful study of thermal and moisture transmission characteristics. Limited reports in this regard are available.

Hajiani et al. [17] studied the absorbency behaviour of spunlace nonwoven fabrics produced at varying water jet pressures and different basic fabric weight. Increased jet pressure was reported to increase mass density, while water retention and permeability were reduced. Berkalp [18] studied the air permeability and porosity of spunlace nonwoven fabric, but did not discuss moisture transfer. He stated that the pore structure of nonwoven fabric affects various comfort properties, such as thermal conductivity and air permeability. The pores inside nonwoven fabrics are highly complex in terms of size, shape and capillary geometry [19]. Knowledge of pore size distribution is essential for understanding transport phenomena, particularly in a porous structure such as nonwoven fabric [20]. The absorption and spreading of fluid can be engineered by controlling the pore configurations of the substrate, [11, 21] while studies of the moisture and heat transfer characteristics of light nonwoven fabric have reported that a blend with hydrophobic fibre has a favourable effect on the drying behaviour of fabric. Ahmad et al. developed a hydroentangled fabric using comber noil and reported that waterjet pressure and conveyor speed (delivery speed) affect the moisture management properties of fabric [12].

The moisture transport characteristics of a fabric can be affected by any of the following parameters:

(i) the nature and quantity of each constituent fibre;
(ii) the structural parameters of fabric (which define the fluid flow passage geometry, i.e. pore size and the distribution thereof);
(iii) the mass and thickness of the material; and/or
(iv) structural or surface modification through mechanical or chemical treatment.

An attempt has been made in this study to investigate the effect of different material and process parameters of spunlace nonwoven fabric on the moisture management characteristics thereof.

2 Material and methods

2.1 Materials

Twenty-seven spunlaced nonwoven fabrics were produced from cross-laid carded web by varying water pressure, delivery rate, web composition and web mass, using a Box-Behnken experimental design. Viscose (38 mm, 1.4 dtex) and polyester (38 mm, 1.4 dtex) fibres were used in the study. Two fibres with significantly different moisture absorption characteristics

Table 1: Factors and the levels thereof for the Box-Behnken design

Material and process parameters	Level		
	–1	0	1
Waterjet pressure [bar] X_1	50	100	150
Delivery speed [m/min] X_2	1	3	5
Web mass [g] X_3	50	100	150
Web composition X_4	PET [a)]	50PET/50CV [b)]	CV [c)]

[a)] Hereinafter, the abbreviation PET is used for 100% PET. [b)] Hereinafter, the abbreviation 50PET/50CV is used for a 50% PET/50% viscose blend. [c)] Hereinafter, the abbreviation CV is used for 100% viscose.

Table 2: Physical parameters of nonwoven fabric samples [22]

Sample code	Waterjet pressure [bar] X_1	Delivery speed [m/min] X_2	Web mass [g] X_3	Web composition X_4	Fabric weight Mean/COV[a)] [g/m^2]/[%]	Fabric thickness Mean/COV [mm]/[%]	Mean pore diameter Mean/COV [μm]/[%]
1	50.00	1.00	100.00	50PET/50CV	98.5/6.23	1.64/8.44	74.320/5.84
2	150.00	1.00	100.00	50PET/50CV	97.2/5.29	1.00/7.64	43.980/8.57
3	50.00	5.00	100.00	50PET/50CV	99.1/8.25	1.60/7.94	75.900/9.55
4	150.00	5.00	100.00	50PET/50CV	147.6/6.87	1.08/6.66	44.840/6.5
5	100.00	3.00	50.00	PET	43.7/6.78	0.94/8.29	95.830/7.79
6	100.00	3.00	150.00	PET	148.2/5.69	1.20/7.13	75.270/6.27
7	100.00	3.00	50.00	CV	42.8/7.59	0.62/5.29	60.500/4.26
8	100.00	3.00	150.00	CV	145.7/6.63	1.12/4.92	38.500/4.52
9	100.00	3.00	100.00	50PET/50CV	96.7/8.91	0.90/8.27	53.530/7.22
10	50.00	3.00	100.00	PET	98.4/7.53	1.28/6.4	98.390/6.17
11	150.00	3.00	100.00	PET	96.2/9.39	1.20/7.88	62.920/8.51
12	50.00	3.00	100.00	CV	97.8/9.39	0.88/7.21	46.685/8.36
13	150.00	3.00	100.00	CV	96.3/7.27	0.79/5.89	36.063/5.96
14	100.00	1.00	50.00	50PET/50CV	48.9/6.31	0.85/8.24	58.780/7.47
15	100.00	5.00	50.00	50PET/50CV	48.5/5.49	0.89/9.22	49.160/6.58
16	100.00	1.00	150.00	50PET/50CV	146.4/7.62	1.22/6.91	27.160/4.84
17	100.00	5.00	150.00	50PET/50CV	147.0/8.57	1.30/5.37	27.960/8.43
18	100.00	3.00	100.00	50PET/50CV	98.3/9.22	1.10/6.84	50.290/7.25
19	50.00	3.00	50.00	50PET/50CV	49.1/7.94	1.30/6.57	69.960/7.65
20	150.00	3.00	50.00	50PET/50CV	48.3/5.47	0.86/8.87	48.180/6.88
21	50.00	3.00	150.00	50PET/50CV	148.7/8.97	2.64/7.39	69.460/7.71
22	150.00	3.00	150.00	50PET/50CV	146.9/6.23	1.16/7.10	19.340/8.17
23	100.00	1.00	100.00	PET	98.4/4.59	1.21/9.44	67.140/7.27
24	100.00	5.00	100.00	PET	98.9/9.49	1.32/6.98	65.520/6.93
25	100.00	1.00	100.00	CV	96.3/7.29	0.73/4.64	50.260/5.7
26	100.00	5.00	100.00	CV	96.8/7.34	0.84/5.43	28.310/5.55
27	100.00	3.00	100.00	50PET/50CV	97.8/8.11	0.95/4.26	59.570/7.56

[a)] Hereinafter, the abbreviation COV is used for coefficient of variation.

were chosen to study the transport behaviour of moisture through the structure, in particular when using a blend of the two fibres. The corresponding values of different levels of the above-mentioned factors are presented in Table 1.

The fibre/fibre blends were first opened and carded using a stationary flat card. A bimodal fibre orientation in the web was achieved using a cross-lapper. A pilot-scale hydroentangling machine was used to produce fabric as per the required setting based on the Box-Behnken design. The machine was set-up with the following values: orifice discharge coefficient = 0.7, orifice diameter = 0.127 mm, number of jets/m = 1600 and pre-wetting pressure = 50 bars. The nozzle type, nozzle geometry and all other parameters were kept same for all samples. Various physical parameters were measured using standard methods for all nonwoven fabrics that were produced according to the Box-Behnken design [22]. Mean fabric weight, mean fabric thickness and mean pore diameter is presented in Table 2.

2.2 Methods

The moisture management behaviour of the fabrics was accurately and objectively measured on an SDL-ATLAS M290 moisture management tester according to the AATCC Test Method 195 [23]. A 5 cm x 5 cm fabric specimen was used in the tester. A certain known volume of a predefined test solution was then put on the top surface of the fabric (i.e. the side of the fabric in contact with skin). The saline solution transferred in three directions after being placed on the top surface of the specimen. The aforementioned instrument was integrated with a computer via moisture management software that records changes in resistance due to the solution, which can conduct electricity. Changes in the electrical resistance of specimens were measured and recorded during the test. According to the AATCC Test Method 195–2012 [23], the indices are graded and converted from a value to a grade based on a five-grade scale. Table 3 presents the range of values converted into grades.

Table 3: Grading of different indices obtained from the moisture management tester [23, 24]

Index	Grade				
	1	2	3	4	5
Wetting time – top [s]	≥120	20–119	5–19	3–5	<3
	No wetting	Slow	Medium	Fast	Very fast
Wetting time – bottom [s]	≥120	20–119	5–19	3–5	<3
	No wetting	Slow	Medium	Fast	Very fast
Absorption rate – top [%/s]	0–10	10–30	30–50	50–100	>100
	Very Slow	Slow	Medium	Fast	Very fast
Absorption rate – bottom [%/s]	0–10	10–30	30–50	50–100	>100
	Very Slow	Slow	Medium	Fast	Very fast
Max. wetted radius – top [mm]	0–7	7–12	12–17	17–22	>22
	No wetting	Small	Medium	Fast	Very fast
Max. wetted radius – bottom [mm]	0–7	07–12	12–17	17–22	>22
	No wetting	Small	Medium	Fast	Very fast
Spreading speed – top [mm/sec]	0–1	1–2	2–3	3–4	>4
	Very Slow	Slow	Medium	Fast	Very fast
Spreading speed – bottom [mm/sec]	0–1	1–2	2–3	3–4	>4
	Very Slow	Slow	Medium	Fast	Very fast
One-way transport capability (OWTC)	<–50	–50–100	100–200	200–400	>400
	Very poor	Poor	Good	Very good	Excellent
Overall moisture management coefficient (OMMC)	0–0.2	0.2–0.4	0.4–0.6	0.6–0.8	>0.8
	Very poor	Poor	Good	Very good	Excellent

Finally, the moisture management tester classified the tested fabric into seven categories according to their properties, as presented in Table 4 [24].
Before conducting the test, all fabric samples were first conditioned in a tropical atmosphere of 27 °C ± 2 °C and 65% ± 2% relative humidity. For each sample of the Box-Behnken design, fifteen samples were tested to minimise the coefficient of variation (%). Minitab 17 software was used for statistical analysis. An analysis of variance was carried out on responses corresponding to the Box-Behnken design, with the aim of examining the effect and contribution of different factors, at a 95% confidence level.

Table 4: Fabric classification based on the results of the moisture management tester [24]

Sample code	Type Name	Properties
1	Waterproof fabric (WF)	Very slow absorption, slow spreading, no one-way transport, no penetration
2	Water-repellent fabric (WRF)	No wetting, no absorption, no spreading, poor one-way transport without external forces
3	Slow-absorbing and slow-drying fabric (SA&SDF)	Slow absorption, slow spreading, poor one-way transport
4	Fast-absorbing and slow-drying fabric (FA&SDF)	Medium to fast wetting, medium to fast absorption, small spreading area, slow spreading, poor one-way transport
5	Fast-absorbing and quick-drying fabric (FA&QDF)	Medium to fast wetting, medium to fast absorption, large spreading area, fast spreading, poor one-way transport
6	Water penetration fabric (WPF)	small spreading area, Excellent one-way transport
7	Moisture management fabric (MMF)	Medium to fast wetting, medium to fast absorption, large spreading area and fast spreading at bottom surface, good to excellent one-way transport

3 Results and discussion

Moisture management properties of spunlace nonwoven fabrics
Moisture transport through the nonwoven fabrics was experimentally determined using a moisture management tester. The results are presented in Table 5.

Table 5: Mean value of various indices of moisture management tester with cl

Sample code	Wetting time: Mean [s]/COV [%]		Absorption rate: Mean [%/s]/COV [%]	
	Top surface	Bottom surface	Top surface	
1	3.98/4.8	9.12/9.05	57.59/3.4	
2	4.12/5.1	7.21/4.13	18.61/5.37	
3	4.22/5.36	9.55/6.54	82.33/5.72	
4	4.45/2.54	7.90/3.74	32.8/8.67	
5	9.86/5.33	12.29/6.86	0.0/0.0	
6	10.26/7.25	14.37/6.12	0.0/0.0	
7	1.96/4.4	9.95/5.95	37.14/9.51	
8	2.26/8.02	10.41/5.27	18.87/6.23	
9	4.23/2.76	8.31/2.43	34.72/5.68	
10	10.56/6.22	13.46/4.19	0.0/0.0	
11	10.39/7.24	14.62/6.22	0.0/0.0	
12	2.93/3.11	9.27/2.36	26.74/4.19	
13	2.71/5.39	9.5/2.56	20.48/9.21	
14	4.38/7.29	7.98/5.96	43.06/5.00	
15	3.82/6.62	7.62/7.29	44.01/3.22	
16	4.33/3.99	8.92/3.05	5.36/3.93	
17	3.81/5.34	9.06/6.63	10.43/4.61	
18	3.68/4.05	8.42/3.21	37.05/4.73	
19	3.38/4.28	8.97/4.37	27.68/8.68	
20	3.25/3.90	7.92/2.33	50.148/6.35	
21	3.65/6.11	9.84/3.54	71.7/8.21	
22	3.85/7.93	8.60/9.27	17.74/7.38	
23	9.55/3.94	13.95/2.81	0.0/0.0	
24	8.85/4.95	13.44/1.19	0.0/0.0	
25	1.88/6.74	9.36/4.37	24.88/9.68	
26	1.55/5.02	9.77/6.55	28.72/3.70	
27	4.11/3.32	8.11/3.54	30.52/4.22	

3.1 Wetting time

Wetting time is defined as the time in seconds when the slope of total water contents at the top and bottom surfaces become greater than tan (15°), the specimen begins to be wetted. Wetting time can be compared with the absorbency drop test specified in AATCC 79. The basic unit of any textile structure is fibre. Generally, the wetting time on the top surface of any fabric is affected by its composition, in addition to the structural arrangement of the fibre it contains. The wetting of the surface is also affected by the interaction between the liquid and the fibre that makes up the fabric. The contact angle between the fibre and the liquid affects the transportation of liquid in both directions, i.e. horizontally and vertically. Hence, a fibre with lower interfacial energy/surface

lassification of type of fabric

Absorption rate: Mean [%/s]/COV [%]		Max. wetted radius: Mean [mm]/COV [%]		Spreading speed: Mean [mm/s]/ COV [%]		One-way transport capability: Mean/COV [%]	Overall moisture management coefficient: Mean/ COV [%]	Remarks on type of fabric
	Bottom surface	Top surface	Bottom surface	Top surface	Bottom surface			
	121.17/8.7	10.0/0.0	10.0/0.0	0.83/9.2	1.16/9.2	449.25/4.84	0.71/8.88	MMF
	69.04/4.97	11.66/8.92	21.66/10.32	2.44/9.14	4.13/8.26	487.34/7.83	0.88/8.49	MMF
	146.03/8.57	8.33/3.48	10.0/0.0	0.73/8.6	0.89/3.6	239.94/3.42	0.67/3.12	FA&SDF
	58.74/10.05	20.0/0.0	20.0/0.0	3.69/3.18	3.98/3.55	395.74/6.27	0.8/5.83	MMF
	246.23/7.35	0.0/0.0	10.0/0.0	0.0/0.0	1.19/9.39	865.06/4.83	0.62/2.97	WPF
	398.79/9.51	0.0/0.0	5.0/0.0	0.0/0.0	0.4/1.36	914.057/5.49	0.57/3.94	WPF
	73.54/7.37	25/0.0	28.33/0.0	5.24/9.19	5.35/5.79	340.88/6.05	0.86/5.22	MMF
	46.01/5.38	13.33/2.29	16.66/2.88	1.64/8.22	2.72/5.09	347.44/8.55	0.66/5.52	MMF
	95.03/3.33	20/7.07	22.5/3.53	3.66/4.60	3.89/4.23	510.77/5.67	0.93/4.16	MMF
	241.21/7.93	0.0/0.0	5.0/0.0	0.0/0.0	0.46/2.8	856.76/2.11	0.65/3.5	WPF
	298.67/5.91	0.0/0.0	5.0/0.0	0.0/0.0	0.39/3.9	1081.61/6.89	0.73/3.95	WPF
	63.35/5.75	18.33/2.88	18.33/2.88	2.78/3.2	2.72/2.92	406.11/9.11	0.78/7.43	MMF
	53.97/8.87	20.0/0.0	20.0/0.0	1.06/7.32	3.13/3.41	385.11/6.86	0.76/4.71	MMF
	130.36/4.68	27.5/3.53	27.5/3.53	5.54/7.04	5.63/6.97	471.18/2.89	0.96/4.43	MMF
	131.78/5.29	27.5/3.53	22.5/3.62	5.55/3.75	5.14/5.24	546.05/2.99	0.97/3.03	MMF
	35.5/5.77	10.0/0.0	18.33/3.14	0.39/6.09	2.19/7.65	245.05/5.21	0.77/4.95	MMF
	46.03/7.34	5.0/0.0	20/0.0	0.83/4.14	3.16/5.66	502.94/3.71	0.76/6.17	MMF
	101.54/5.21	22.5/0.0	22.5/0.0	3.95/3.33	4.39/4.67	564.44/4.96	0.88/3.56	MMF
	153.3/9.23	10.0/0.0	10.0/0.0	0.85/7.87	0.9/8.43	278.86/8.65	0.74/7.75	MMF
	136.59/6.76	26.66/2.93	26.66/2.93	4.73/5.33	5.13/4.72	393.53/7.29	0.94/5.11	MMF
	145.3/4.33	10.0/0.0	10.0/0.0	0.62/6.54	1.43/7.92	336.35/5.61	0.71/6.37	FA&SDF
	87.73/6.89	20.0/0.0	20/0.0	3.12/6.54	3.44/4.72	425.93/5.04	0.81/2.39	MMF
	245.42/5.67	0.0/0.0	5.0/0.0	0.0/0.0	0.67/3.75	526.47/2.58	0.65/3.58	WPF
	239.12/5.28	0.0/0.0	5.0/0.0	0.0/0.0	0.43/1.14	910.41/4.95	0.63/5.26	WPF
	89.51/5.18	20.0/0.0	20.0/0.0	4.3/5.36	4.19/2.18	284.5/3.19	0.79/3.31	MMF
	61.66/4.05	20.0/0.0	20/0.0	3.48/8.80	3.54/5.70	398.57/6.21	0.85/6.86	MMF
	112.32/6.11	20.0/0.0	20.0/0.0	3.29/5.29	3.41/4.90	580.97/2.53	0.91/3.89	MMF

tension should support wetting. The fibre-liquid molecular attraction on the surface of fibrous assemblies dictates the flow of moisture through a textile fabric. The surface tension and dimensional parameters of pores in porous media are the main parameters that affect this fibre-liquid interaction [2, 6].

A statistical analysis of variance (ANOVA) using a backward elimination technique showed that the web composition has a significant effect on the wetting time on the top surface, while the effect of waterjet pressure, web mass and delivery speed was found to be insignificant at a 95% confidence interval (Table 6). The response surface equation in coded units for the mean top wetting time is given in equation (1) with a R^2 value of 0.9755.

$$\text{Top wettig time} = 3.951 - 3.848X4 + 2.114X_4^2 \quad (1)$$

The effect of web composition on mean wetting time is shown in Figure 1 using equation 1. It is evident from Figure 1 that the experimental data for top wetting time is fitted to a second order polynomial equation. It is also evident from Figure 1 that and increase in CV content reduces mean wetting time. The surface tension of PET is higher than that of CV for water, while the mean pore diameter of PET nonwoven fabric is higher than that of CV nonwoven fabric. A higher surface tension and higher pore diameter impede the wetting of fabric surface. Hence, the wetting time on the top surface of PET nonwoven fabric is significantly higher than that of CV fabric and 50PET/50CV blended nonwoven fabric (Figure 1).

In the case of blended nonwoven fabric, the properties of individual fibres affect wetting behaviour. The presence of CV expedites the wetting process. Hence, the 50PET/50CV blended fabric demonstrates a lower wetting time on the top surface than the PET nonwoven fabric.

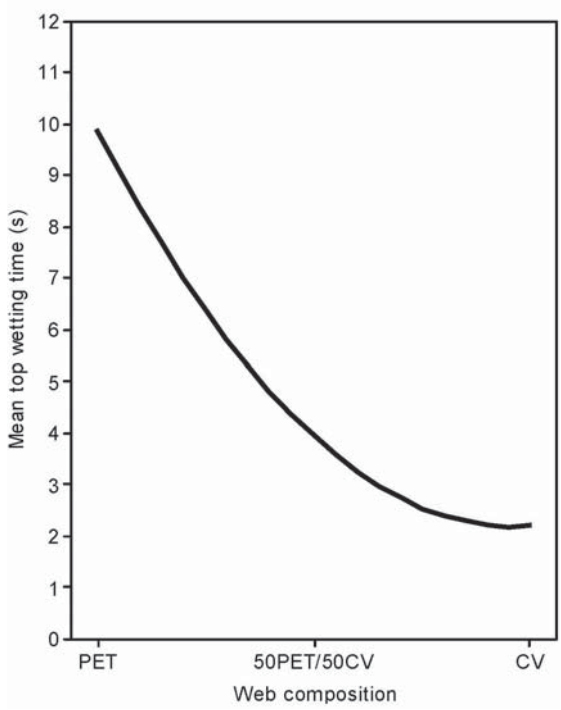

Figure 1: Top wetting time depending on the web composition

The wetting time on the bottom surface was expected to be affected by the ability of the structure to transport liquid. The pore diameter is used to affect wicking in any textile structure. The pore diameter of spunlace nonwoven fabric depends on waterjet pressure, web weight and web composition. Hence, the wetting time on the bottom surface should be affected by a change in these parameters. The results (Table 5) indicate the wetting time of the bottom surfaces is generally higher than the top surfaces for all fabrics.

Table 6: ANOVA for mean top wetting time

Source	Degree of freedom	Sum of square	Mean square	F value	P value	Percentage contribution [%]
Model	2	207.4	103.7	478.1	0.000	97.55
X4	1	177.6	177.6	818.9	0.000	83.55
X4*X4	1	29.8	29.8	137.3	0.000	14.01
Error	24	5.20	0.217			2.45
Lack of fit	22	5.0	0.22	2.74	0.302	2.37
Pure error	2	0.2	0.1			0.08
Total	26	212.6				100

Table 7: ANOVA for mean bottom wetting time

Source	Degree of freedom	Sum of square	Mean square	F value	P value	Percentage contribution [%]
Model	4	120.77	30.19	97.13	0.000	94.64
X1	1	1.66	1.66	5.33	0.031	1.30
X3	1	3.49	3.49	11.22	0.003	2.73
X4	1	47.48	47.48	152.74	0.000	37.21
X4*X4	1	68.14	68.14	219.22	0.000	53.40
Error	22	6.84	0.31			5.36
Lack of fit	20	6.79	0.34	13.74	0.07	5.32
Pure error	2	0.05	0.025			0.04
Total	26	311.59				100

The statistical analysis of variance (ANOVA) for the mean wetting time on the bottom surface is presented in Table 7. It is evident from Table 7 that the web composition has a significant effect on the wetting time on the bottom surface, while the effect of waterjet pressure and web mass are also significant, although their percentage contribution is very small. Delivery speed is found to be insignificant at a 95% confidence interval. The response surface equation in coded units for the mean bottom wetting time is given in equation 2 with a R^2 value of 0.9464.

$$\text{Bottom wetting time} = 8.502 - 0.372X_1 + 0.539X_3 - \\ - 1.989X_4 + 3.197\,X_4^2 \qquad (2)$$

The effect of waterjet pressure, web mass and web composition on the mean wetting time on the bottom surface is shown in Figure 2 using equation 2. It is evident from Figure 2 that PET nonwoven fabric demonstrates a higher bottom wetting time than CV fabric. This is due to the smaller pore diameter and lower fabric thickness of CV nonwoven fabric compared to PET nonwoven fabric [22]. Hence, a decrease in pore diameter and lower thickness leads to better wicking in CV-based nonwoven fabric.

It is evident from Figure 2 that the wetting time on the bottom surface is lower in 50PET/50CV blended nonwoven fabric than in PET and CV

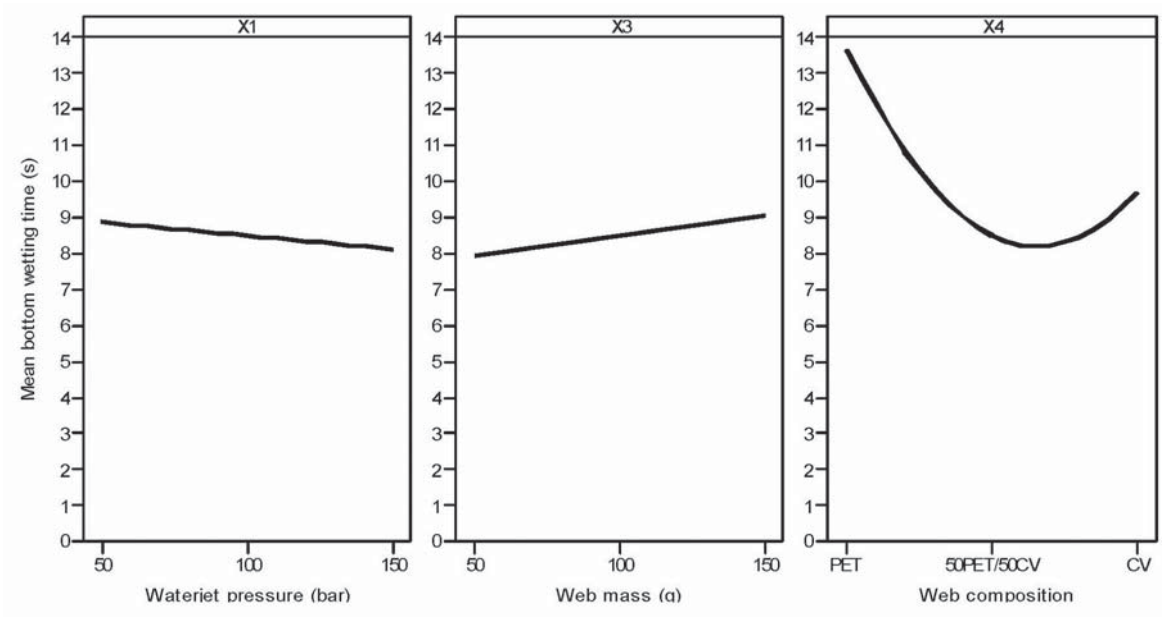

Figure 2: Bottom wetting time depending on waterjet pressure, web mass and web composition

nonwoven fabrics. This is due to the presence of CV fibre, which helps in the quick absorption of liquid/moisture, while PET fibre supports the wicking of liquid. Hence, the wetting time on the bottom surface is lower in 50PET/50CV blend. Table 7 shows that the percentage contribution of web composition is 90%.

It is also evident from Figure 2 that an increase in web mass increases the mean wetting time on the bottom surface. An increase in web mass results in a higher number of water absorbing sites at a molecular level, which delays the wicking phenomenon, despite a lower pore diameter.

The mean wetting time on the bottom surface also depends on waterjet pressure, as shown in Table 7. It is evident from Figure 2 that an increase in waterjet pressure decreases mean wetting time on the bottom surface. An increase in waterjet pressure leads to a decrease in the mean pore diameter and thickness of fabric, [22] which supports the wicking phenomena. Hence, a higher wicking rate reduces the wetting time on the bottom surface.

After the conversion of wetting time values into grades (Table 3), it is evident that nonwoven fabric made of PET, 50PET/50CV and CV exhibits slow (grade 2), medium (grade 3) and fast (grade 4) wetting behaviour on the top surface, and medium (grade 3), medium (grade 3) and fast (grade 4) wetting behaviour on the bottom surface, respectively.

3.2 Absorption rate

The absorption of liquid by a textile substrate indicates the degree of transfer of liquid on its surface. The absorption of liquid by a fabric depends on the type of fibre, fabric structure and openness in the structure. The absorption rate on the top surface of all spunlace nonwoven fabric samples is presented in Table 5.

An ANOVA of the mean absorption rate is presented in Table 8. It is evident from Table 8 that the effect of delivery speed is not significant, while waterjet pressure, web mass and web composition have a significant effect on the mean absorption rate on the top surface. The response surface equation in coded units for mean bottom wetting time is given in equation 3 with a R^2 value of 0.7320.

$$\text{Top absorption rate} = 37.58 - 10.52X_1 - 6.49X_3 + \\ + 13.07X_4 - 24.51X_4^2 - 19.11X_1X_3 \quad (3)$$

The effect of waterjet pressure, web mass and web composition on the mean absorption rate on the top surface is shown in Figure 3 using equation 3. It is evident from Figure 3 that an increase in waterjet pressure decreases the mean absorption rate on the top surface. This is due to a decrease in fabric thickness, which results in the compactness of the structure at a higher waterjet pressure [22]. Waterjet pressure is a significant parameter for the mean absorption rate on the top surface, as its percentage contribution is more than 10%.

Table 8: ANOVA for the top absorption rate

Source	Degree of freedom	Sum of square	Mean square	F value	P value	Percentage contribution [%]
Model	5	9351.2	1870.24	11.47	0.000	73.20
Linear	3	3884.3	1294.78	7.94	0.001	30.41
X1	1	1328.5	1328.5	8.15	0.009	10.40
X3	1	506.2	506.2	3.10	0.093	3.96
X4	1	2049.6	2049.6	12.57	0.002	16.04
Square	1	4006.5	4006.5	24.57	0.000	31.36
X4*X4	1	4006.5	4006.5	24.57	0.000	31.36
2-way interaction	1	1460.3	1460.3	8.96	0.007	11.43
X1*X3	1	1460.3	1460.3	8.96	0.007	11.43
Error	21	3423.8	3423.8			26.80
Lack of fit	19	3401.9	4.20	14.48	0.059	26.63
Pure error	2	21.9	10.96			0.17
Total	26	12775.0				100

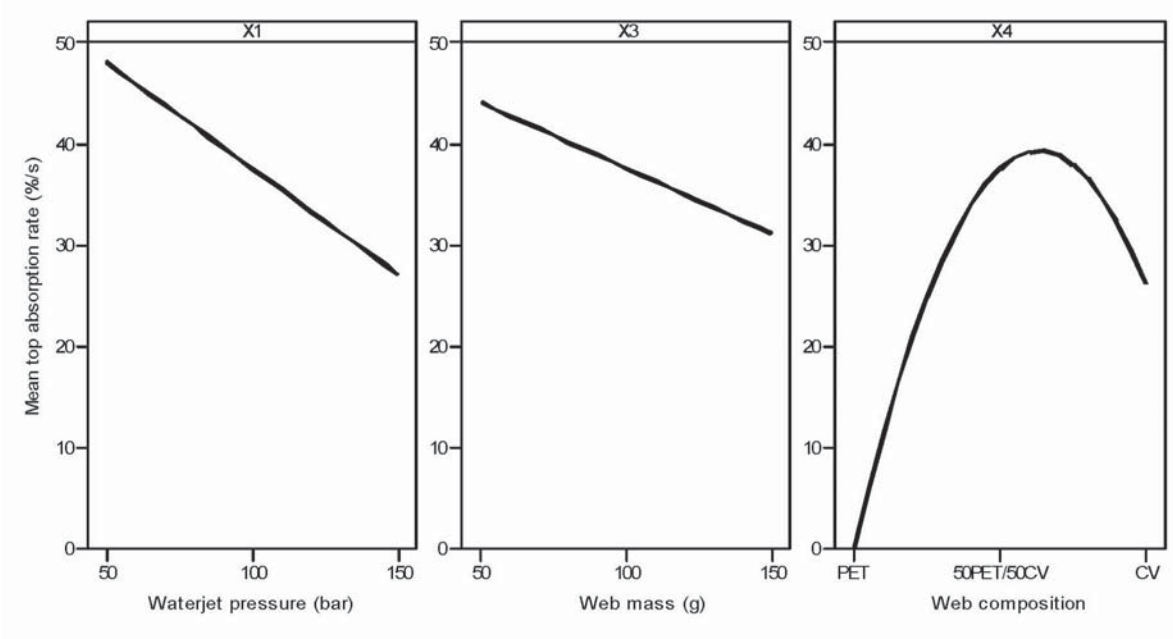

Figure 3: Top absorption rate depending on waterjet pressure, web mass and web composition

The mean absorption rate (%) on the top surface for CV nonwoven fabric is higher than that of PET nonwoven fabric due to the presence of a higher number of hydrophilic sites in the CV nonwoven fabric. The mean absorption rate (%) is higher in 50PET/50CV blended nonwoven fabric than in CV nonwoven fabric (Figure 3). CV nonwoven fabric has good absorbency due to its hydrophilic CV fibre. However, it forms a strong bond with the absorbing group of fibre molecules due to its high affinity to water when water molecules in the capillary flow reach a smaller diameter. This impedes the capillary flow along the channel formed by the fibre surface, leading to a decrease in the mean absorption rate. In the 50PET/50CV blend, the PET fibre helps in the wicking of moisture/water being absorbed by CV fibre, resulting in a higher mean absorption rate.

The effect of web mass on the mean absorption rate is also shown in Figure 3. It is evident that the mean absorption rate for 50 g/m^2 is higher than that for 150 g/m^2. This difference in the mean absorption rate was statistically significant. Nonwoven fabric at a lower web mass demonstrates a higher absorption rate because a fabric with a lower mass is more porous (high pore diameter), which helps in the absorption of moisture at faster rate, while at higher web mass, a compact structure with a smaller pore diameter results in a lower absorption rate.

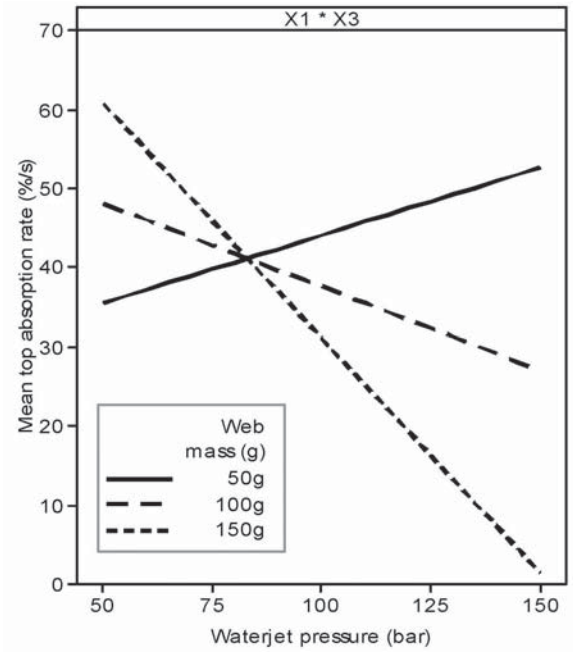

Figure 4: Interaction effect of web mass and waterjet pressure on top absorption rate

The interaction effect of web mass and waterjet pressure on the mean absorption rate on the top surface is shown in Figure 4. It is evident from Figure 4 that at a low web mass, an increase in waterjet pressure increases the mean absorption rate due to a more open structure. The openness of the structure becomes

more prominent at a high waterjet pressure and low web mass due to the grouping of fibres. Similarly, a higher web mass and low waterjet pressure result in an increase in the mean absorption rate due to the reduced binding of fibres. A higher web mass and high waterjet pressure lead to a compacted structure, resulting in a decrease in the mean absorption rate.

The mean absorption rate on the bottom surface plays an important role in the moisture management behaviour of any textile structure. A textile structure with a higher bottom surface absorption rate helps to transfer the moisture in the environment, which is wicked through the structure. The mean absorption rate on the bottom surface of spunlace nonwoven fabric samples are presented in Table 5. An ANOVA of the mean absorption rate on the bottom surface is presented in Table 9.

It is evident from Table 9 that only web composition has a significant effect on the mean absorption rate on the bottom surface. The response surface equation in coded units for the mean bottom wetting time is given in equation 4 with a R^2 value of 0.8002.

$$\text{Bottom absorption rate} = 104.7 - 106.8X_4 - 66.8X_4^2 \quad (4)$$

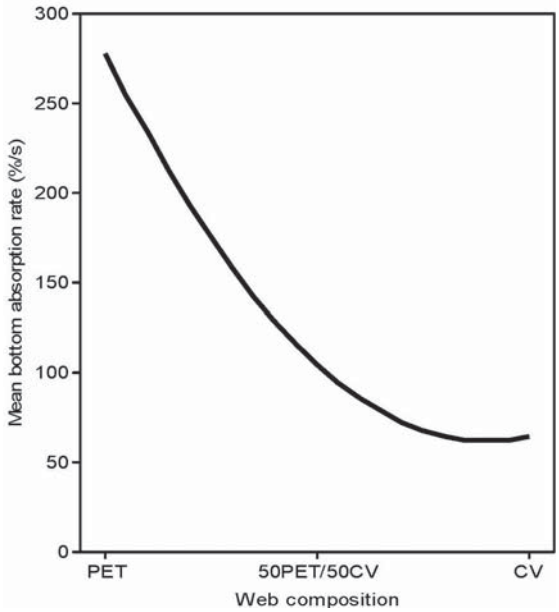

Figure 5: Bottom absorption rate depending on web composition

The effect of web composition on the mean absorption rate on the bottom surface is shown in Figure 5 using equation 4. It is evident from Figure 5 that PET nonwoven fabric demonstrates a significantly higher bottom absorption rate than CV nonwoven fabric. An increase in the CV content in a nonwoven structure leads to an increase in the absorption rate on the top surface. Due to its high affinity to water molecules, however, the CV nonwoven fabric results in the formation of a strong bond between those molecules, which inhibits the capillary flow across the structure, causing a decrease in the absorption rate on the bottom surface.

After the conversion of absorption values into grades (Table 3), PET nonwoven fabric demonstrates a slow absorption rate (grade 2) on the top surface and a very fast absorption rate on the bottom surface (grade 5), while CV nonwoven fabric demonstrates a medium/fast absorption rate (grade 3/4) on the top surface and a medium/slow absorption rate on the bottom surface (grade 3/2). The 50PET/50CV blend exhibited an optimum absorption rate on both

Table 9: ANOVA for the bottom absorption rate

Source	Degree of freedom	Sum of square	Mean square	F value	P value	Percentage contribution [%]
Model	2	166544	83272	48.06	0.000	80.02
Linear	1	136832	136832	78.97	0.000	65.74
X4	1	136832	136832	78.97	0.000	65.74
Square	1	29712	29712	17.15	0.000	14.28
X4*X4	1	29712	29712	17.15	0.000	14.28
Error	24	41585	1733			19.98
Lack of fit	22	40933	1860	5.7	0.159	19.66
Pure error	2	652	326			0.31
Total	26	208129				100

the top and bottom surfaces, considering the presence of moisture in the structure.

3.3 Wetted radius

The value of the wetted radius demonstrates the extent of water spread on a textile structure. The wetted radius is directly related to the drying behaviour of a fabric. The value of the wetted radius should be affected by the web composition and web mass of a textile structure. The values of the top surface wetted radius are presented in Table 5. An ANOVA of the mean wetted radius (mm) on the top surface is presented in Table 10. It is evident that, apart from the delivery speed, all other factors have a significant effect on the mean value of the wetted radius on the top surface.

The response surface equation in coded units for the mean top wetted radius is given in equation 5 with a R^2 value of 0.8002.

$$\text{Top wetted radius} = 16.61 + 3.47X_1 - 4.86X_3 + 9.72X_4 - 6.89X_4^2 \quad (5)$$

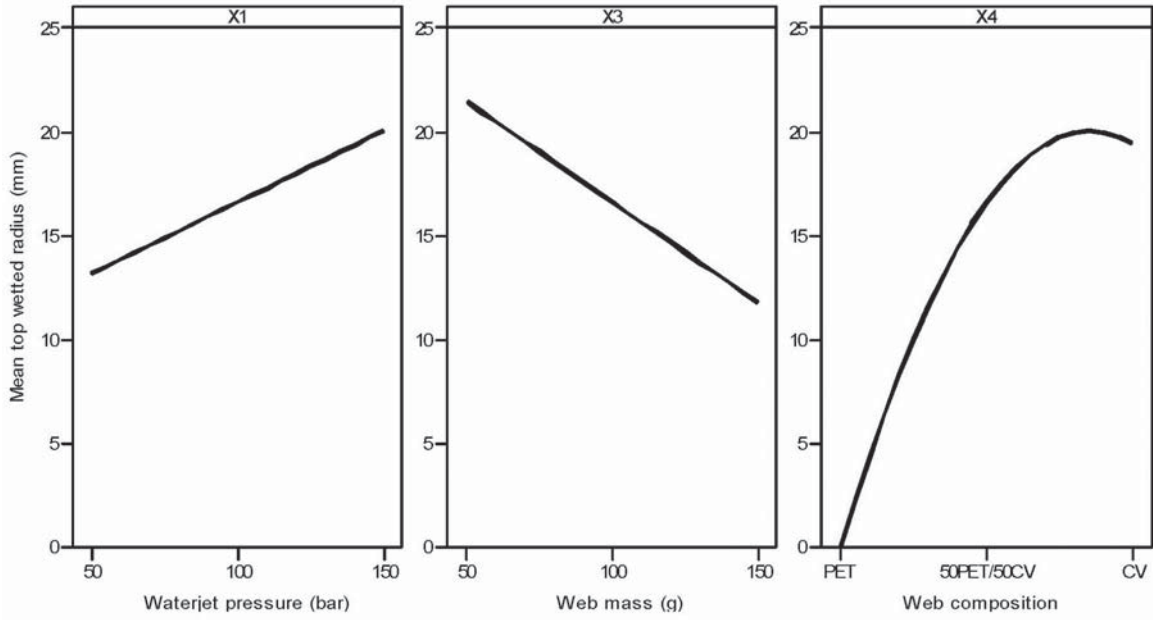

Figure 6: Top wetted radius depending on waterjet pressure, web mass and web composition

Table 10: ANOVA for the top wetted radius

Source	Degree of freedom	Sum of square	Mean square	F value	P value	Percentage contribution [%]
Model	4	1878.62	469.65	22.28	0.000	80.20
Linear	3	1562.29	520.76	24.71	0.000	66.70
X1	1	144.63	144.63	6.86	0.016	6.17
X3	1	283.53	283.53	13.45	0.001	12.10
X4	1	1134.13	1134.13	53.81	0.000	48.42
Square	1	316.33	316.33	15.01	0.001	13.50
X4*X4	1	316.33	316.33	15.01	0.001	13.50
Error	22	463.73	21.08			19.80
Lack of fit	20	459.56	22.98	11.03	0.086	19.62
Pure error	2	4.17	2.08			0.18
Total	26	2342.34				100

The effect of significant factors on the mean top wetted radius is shown in Figure 6 using equation 5. It is evident from Figure 6 that an increase in CV content results in an increases in the mean wetted radius on the top surface. When a liquid droplet is introduced on the surface, absorption by the CV component presumably begins before the start of wicking. This facilitates the spreading of moisture. Hence, the mean wetted radius on the top surface increases. The percentage contribution of web composition to the mean wetted radius on the top surface is around 61.92%.

The effect of web mass on the mean wetted radius on the top surface is shown in Figure 6. It can be concluded that an increase in web mass results in a decrease in the mean wetted radius. This is due to an increase in the number of absorptions sites as web mass increases. The percentage contribution of web mass to the mean wetted radius (top surface) is around 12%.

The effect of waterjet pressure on the mean wetted radius on the top surface is shown in Figure 6. It is evident that an increase in waterjet pressure results in an increase in the mean wetted radius on the top surface. Waterjet pressure leads to a more compact structure that better supports the spreading of moisture compared with wicking and/or absorption. The percentage contribution of waterjet pressure to the mean wetted radius (top surface) is around 6%.

The mean wetted radius on the bottom surface demonstrates how well moisture dissipates to the outer environment. The higher the mean bottom wetted radius, the better the moisture dissipation to the environment. The value of the bottom surface wetted radius is presented in Table 5. An ANOVA is also presented in Table 11. It is evident that, besides delivery speed, all other factors have a significant effect on the mean value of the bottom wetted radius. The response surface equation in coded units for mean bottom wetted radius is given in equation 6 with an R^2 value of 0.8728.

$$\text{Ton wetted radius} = 20.971 + 4.166X_1 - 4.12X_1^2 - 2.917X_3 + 7.36X_4 - 6.41X_4^2 \quad (6)$$

The effect of significant factors on the mean top wetted radius is shown in Figure 7 using equation 6. It is evident from Figure 7 that PET nonwoven fabric has a smaller wetted radius on the bottom surface than CV nonwoven fabric. This is the result of higher moisture wicking than absorbency in PET nonwoven fabric, while an increase in the CV content results in an increase in the mean wetted radius on the bottom surface. This is due to the hydrophilic nature of CV fibre. Absorption by CV fabric appears to be predominant, while the bottom wetting radius increases as the quantity of CV fibre is increased. The percentage contribution of web composition to the mean wetted radius on the bottom surface is around 60%.

The effect of waterjet pressure on the mean bottom wetted radius is shown in Figure 7. It is evident that

Table 11: ANOVA for the bottom wetted radius

Source	Degree of freedom	Sum of square	Mean square	F value	P value	Percentage contribution [%]
Model	5	1276.57	255.31	28.81	0.000	87.28
Linear	3	960.37	320.12	36.13	0.000	65.66
X1	1	208.25	208.25	23.50	0.000	14.24
X3	1	102.08	102.08	11.52	0.003	6.98
X4	1	650.04	650.03	73.36	0.000	44.44
Square	2	316.20	158.10	17.84	0.000	21.62
X1*X1	1	53.54	53.54	12.23	0.002	3.66
X4*X4	1	262.66	262.66	29.64	0.000	17.96
Error	21	186.07	8.86			12.72
Lack of fit	19	181.90	9.57	4.60	0.194	12.44
Pure error	2	4.17	2.08			0.28
Total	26	1462.64				100

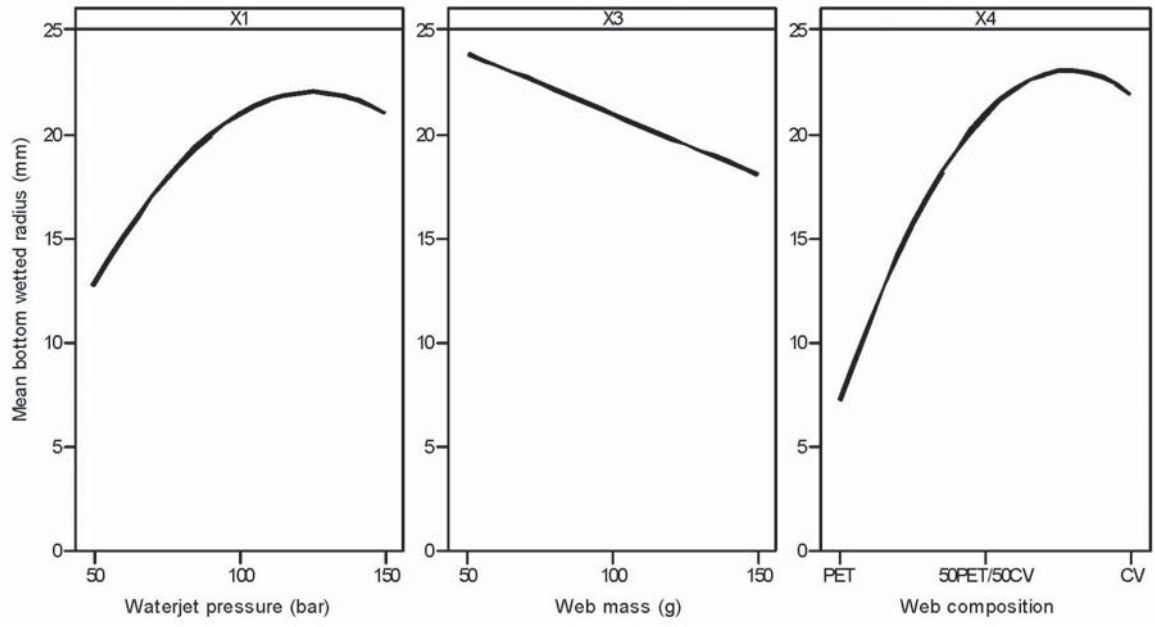

Figure 7: Bottom wetted radius depending on waterjet pressure, web mass and web composition

an increase in waterjet pressure results in an increase in the mean wetted radius on the bottom surface. When waterjet pressure is increased, the structure consolidates and the pore size is reduced with a reduction in fabric thickness. The lower diameter of capillary flow facilitates wicking. Hence, moisture transmission from the top surface is faster. This wicked moisture is diffused faster than additional wicking [25] due to the compactness of the structure. This leads to an increase in the bottom wetted radius. The percentage contribution of waterjet pressure to the mean wetted radius (top surface) is around 17%.

The effect of web mass on the mean bottom wetted radius is shown in Figure 7. It is evident that an increase in the web mass results in a decrease in the mean bottom wetted radius. An increase in the number of absorption sites through an increase in web mass leads to a reduction in the openness of the structure, which in turn results in an increase in the mean wetted radius. The percentage contribution of web mass to the mean wetted radius (top surface) is around 6%.

After the conversion of wetted radius values into grades (Table 3), PET nonwoven fabric demonstrates a minimum wetted radius (grade 1) on both the top and bottom surfaces. CV nonwoven fabric demonstrates a good wetted radius (grade 4) on both the top and bottom surfaces, while the 50PET/50CV blend exhibits the best wetted radius on both the top surface and bottom surface.

3.4 Spreading speed

The spreading speed of moisture/liquid on a textile substrate indicates the degree of moisture dispersion in a fabric. The spreading speed of moisture/liquid in a fabric depends on the type of fibre, fabric structure and openness of the structure (pore size). The spreading speed of moisture on the top surface of all spunlace nonwoven fabric samples is presented in Table 5. An ANOVA of the mean wetted radius (mm) on the top surface is presented in Table 12. The response surface equation in coded units for the mean spreading speed on the top surface is given in equation 7 with a R^2 value of 0.7238.

$$\text{Top spreading speed} = 3.245 + 0.769X_1 - 1.057X_1^2 - 1.276X_3 + 1.542X_4 - 1.35X_4^2 \quad (7)$$

The effect of significant factors on the mean spreading speed on the top surface is shown in Figure 8 using equation 7. It is evident from Figure 8 that an increase in CV content results in an increase in the mean spreading speed. This is due to the higher mean wetted radius on the top surface with a higher CV content, while the hygroscopic nature of CV nonwoven fabric leads to a higher top spreading speed. The percentage contribution of web composition to the mean spreading speed on the top surface is around 40%.

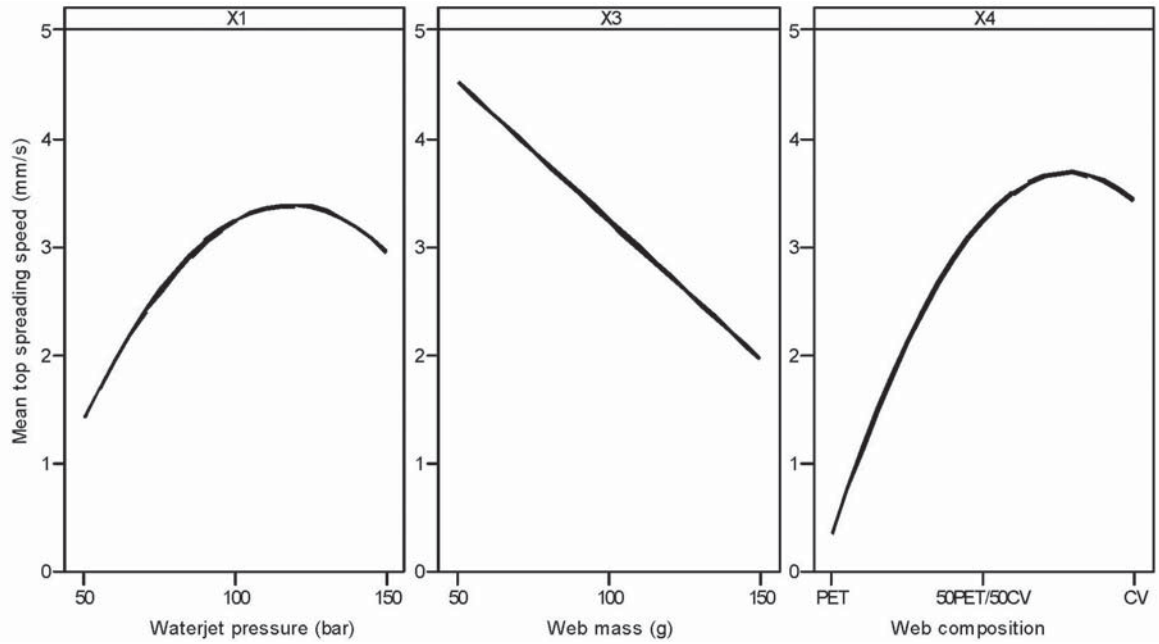

Figure 8: Top spreading speed depending on waterjet pressure, web mass and web composition

The effect of waterjet pressure on the mean wetted radius on the top surface is shown in Figure 8. It is evident that an increase in waterjet pressure results in an increase in the mean spreading speed on the top surface. The higher spreading speed on the top surface is due to a higher mean wetted radius at a higher waterjet pressure. The percentage contribution of waterjet pressure to the top spreading speed is around 10%.

The effect of web mass on the mean spreading speed on the top surface is shown in Figure 8. It can be concluded that an increase in web mass results in a decrease in the mean wetted radius on the top surface. Hence, there is decrease in the mean top spreading speed. The percentage contribution of web mass to the top spreading speed is around 20%. The bottom spreading speed is more important in the moisture management of textile fabrics. A higher

Table 12: ANOVA for the top spreading speed

Source	Degree of freedom	Sum of square	Mean square	F value	P value	Percentage contribution [%]
Model	5	70.97	14.19	11.0	0.000	72.38
Linear	3	55.15	18.38	14.25	0.000	56.25
X1	1	7.10	7.10	5.50	0.029	7.24
X3	1	19.53	19.53	15.14	0.001	19.92
X4	1	28.52	28.52	22.11	0.000	29.09
Square	2	15.81	7.90	6.13	0.008	16.13
X1*X1	1	4.13	7.15	5.55	0.028	4.21
X4*X4	1	11.68	11.68	9.06	0.007	11.91
Error	21	27.09	1.28			27.62
Lack of fit	19	26.89	1.41	12.92	0.074	27.40
Pure error	2	0.22	0.11			0.22
Total	26	98.05				100

bottom spreading speed should lead to the quick drying of fabrics. The spreading speed of moisture on the bottom surface of all nonwoven fabric samples is presented in Table 5. An ANOVA analysis of the bottom spreading speed is presented in Table 13. The response surface equation in coded units for the mean spreading speed on the bottom surface is given in equation 8 with a R^2 value of 0.8358.

$$\text{Bottom spreading speed} = 3.816 + 1.053X_1 - 1.047X_1^2 - \\ - 0.833X_3 + 1.509X_4 - 1.368X_4^2 \quad (8)$$

The effect of significant factors on the mean spreading speed on the bottom surface is shown in Figure 9 using equation 8. It is evident from Figure 9 that an increase in CV content results in an increase in the mean bottom spreading speed, although a smaller bottom wetted radius was recorded. This is due to the higher moisture absorbency of CV nonwoven fabric compared to PET nonwoven fabric, which induces a high absorption speed with a high spreading speed on the top surface. The higher spreading speed on the top surface and a low wetting time on

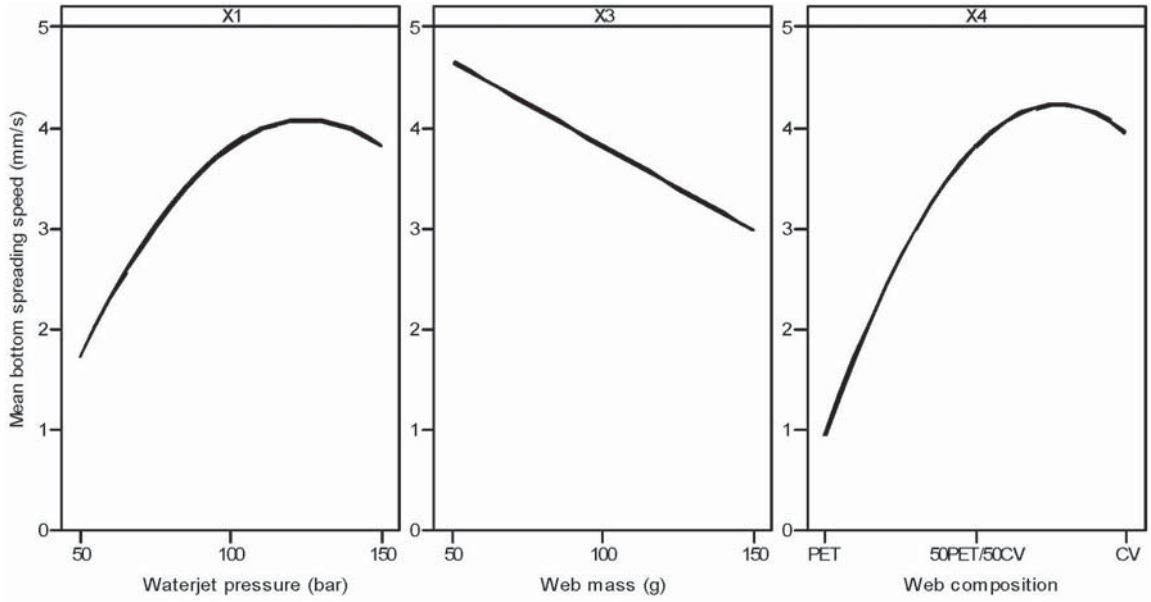

Figure 9: Bottom spreading speed depending on waterjet pressure, web mass and web composition

Table 13: ANOVA for the bottom spreading speed

Source	Degree of freedom	Sum of square	Mean square	F value	P value	Percentage contribution [%]
Model	5	64.93	12.98	21.39	0.000	83.59
Linear	3	48.97	16.32	26.88	0.000	63.04
X1	1	13.31	13.31	21.93	0.000	17.14
X3	1	8.33	8.32	13.71	0.001	10.72
X4	1	27.33	27.33	45.01	0.000	35.18
Square	2	15.96	15.96	13.14	0.000	20.55
X1*X1	1	7.01	7.01	11.55	0.003	5.13
X4*X4	1	11.98	11.97	19.72	0.000	15.42
Error	21	12.75	0.60			16.42
Lack of fit	19	12.27	0.64	2.69	0.306	15.80
Pure error	2	0.48	0.24			0.62
Total	26	77.68				100

the bottom surface results in a higher spreading speed on the bottom surface. The percentage contribution of web composition to the mean spreading speed on the bottom surface is around 50%.

The effect of waterjet pressure on the mean bottom spreading speed is shown in Figure 9. The mean bottom spreading speed was found to increase with an increase in waterjet pressure. It was previously found that increased waterjet pressure results in an increase in the mean bottom wetted radius (section 3.3). Hence, there is an increase in the mean bottom spreading speed. The percentage contribution of waterjet pressure to the mean bottom spreading speed is around 22%.

The effect of web mass on the mean spreading speed on the top surface is shown in Figure 9. It can be concluded that an increase in web mass results in a decrease in the mean wetted radius on the bottom surface. Hence, there is a decrease in the mean spreading speed. The percentage contribution of web mass to the mean bottom spreading speed is around 10%.

After the conversion of the mean spreading speed into grades (Table 3), PET nonwoven fabric demonstrates a very slow spreading speed (grade 1/2) on the top and bottom surfaces. CV nonwoven fabric demonstrates a fast spreading speed (grade 4) on the top and bottom surfaces, while the 50PET/50CV blend also exhibits a medium to fast spreading speed (grade 2/3) on both the top and bottom surfaces.

3.5 One-way transport capability

One-way transport capability is the difference between the amount of liquid moisture content on the top and bottom surfaces of a specimen with respect to time. A positive OWTC value means a higher amount of moisture is transferred from the inner surface to the outer surface of a garment. The one-way transport capability of all fabrics is presented in Table 5. An ANOVA analysis of the mean OWTC is presented in Table 14. It is evident that only web composition has a significant effect on the OWTC of spunlace nonwoven fabric. The response surface equation in coded units for the mean OWTC is given in equation 9 with a R^2 value of 0.7325.

$$OWTC = 428.6 - 249.3X_4 - 181.2X_4^2 \quad (9)$$

The effect of web composition on the mean OWTC is shown in Figure 10 using equation 9. It is evident from Figure 10 that OWTC is higher for PET fabrics

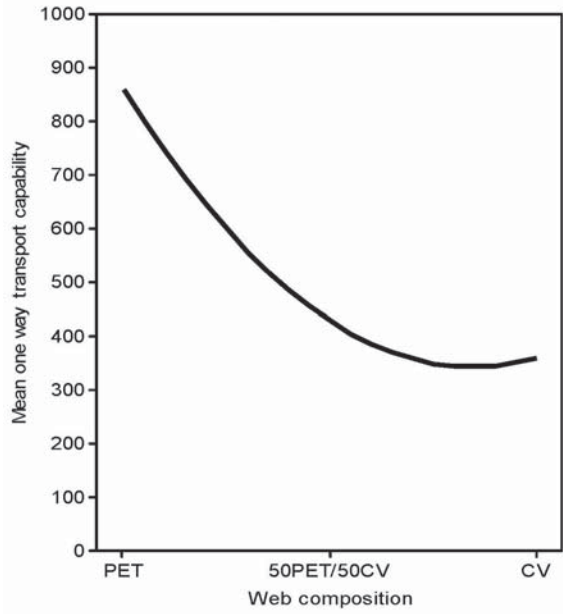

Figure 10: Mean OWTC depending on web composition

Table 14: ANOVA for the mean OWTC

Source	Degree of freedom	Sum of square	Mean square	F value	P value	Percentage contribution [%]
Model	2	964755	482377	32.86	0.000	73.25
Linear	1	745884	745884	50.82	0.000	56.63
X4	1	745884	745884	50.82	0.000	56.63
Square	1	218870	218870	14.91	0.001	16.62
X4*X4	1	218870	218870	14.91	0.001	16.62
Error	24	352278	14678			26.75
Lack of fit	22	349584	15890	11.80	0.081	26.54
Pure error	2	2694	1347			0.20
Total	26	1317033				100

than for CV-based nonwoven fabrics. This can be attributed to the hydrophobic nature of PET, which results in the reduced absorption of liquid, and a smaller wetted radius and spreading speed on the top surface. Hence, the PET nonwoven fabric supports the wicking phenomenon, despite a higher pore diameter, resulting in a higher OWTC.

All nonwoven structures demonstrate a fair to very good one-way transport index/capability on the grading scale (Table 3). PET nonwoven fabric demonstrates a very good to excellent one-way transport index, while CV nonwoven fabric and 50PET/50CV blended nonwoven fabric demonstrate good one-way transport behaviour.

3.6 Overall moisture management coefficient

The overall moisture management coefficient is an index of the overall capability of a fabric to transport liquid moisture in multiple directions. A higher OMMC value indicates that a fabric can handle moisture better. The OMMC of all fabrics is presented in Table 5, with the classification of fabric type based on Table 4. An ANOVA of the mean OMMC is presented in Table 15. It is evident that, apart from delivery speed, all other factors have a significant effect on overall moisture management. The response surface equation in coded units for the mean OMMC is given in equation 10 with a R^2 value of 0.7701.

$$OMMC = 0.8239 + 0.055X_1 - 0.0675X_3 + 0.0708X_4 - 0.1168X_4^2 \quad (10)$$

The effect of significant factors on the mean OMMC is shown in Figure 11 using equation 10. It is evident from Figure 11 that the overall moisture management coefficient (OMMC) is higher for CV-based fabrics than for PET-based nonwoven fabrics. This is because the smaller pore diameter of CV nonwoven fabric exhibits a smaller wetting time (top and bottom surfaces) with a higher spreading speed and higher wetted radius. These factors together contribute to the absorption, transportation and dispersion of moisture in the structure. Although PET-based nonwoven fabric also demonstrates at good OMMC value due to better one-way transport capability, which helps moisture move through a fabric, its lack of moisture dispersion capacity in the structure leads to the accumulation of moisture in one place. 50PET/50CV blended nonwoven fabric demonstrates a very good transport capability in the presence of PET fibres and better moisture absorption and dispersion due to CV fibres. Hence, the 50PET/50CV blended nonwoven fabric is better than the CV and PET nonwoven fabrics in terms of overall moisture management (Figure 11).

It is evident from Figure 11 that the overall moisture management coefficient (OMMC) decreases with an increase in web mass. A higher wetting time and smaller wetted radius hinder moisture absorption and dispersion. The effect of web mass is negative on the mean OMMC value. Nevertheless, all fabrics exhibited a very good to excellent OMMC value.

Table 15: ANOVA for the OMMC of spunlace nonwoven fabric

Source	Degree of freedom	Sum of square	Mean square	F value	P value	Percentage contribution [%]
Model	5	0.265	0.053	13.98	0.000	76.90
Linear	3	0.155	0.052	13.71	0.000	45.25
X1	1	0.036	0.036	9.62	0.000	10.58
X3	1	0.059	0.059	15.58	0.001	17.13
X4	1	0.060	0.06	15.95	0.000	17.54
Square	2	0.11	0.055	14.39	0.000	31.65
X1*X1	1	0.01	0.01	4.12	0.003	1.09
X4*X4	1	0.10	0.10	27.79	0.000	30.56
Error	21	0.080	0.004			23.10
Lack of fit	19	0.079	0.004	6.48	0.142	22.73
Pure error	2	0.001	0.001			0.37
Total	26	0.345	0.345			100

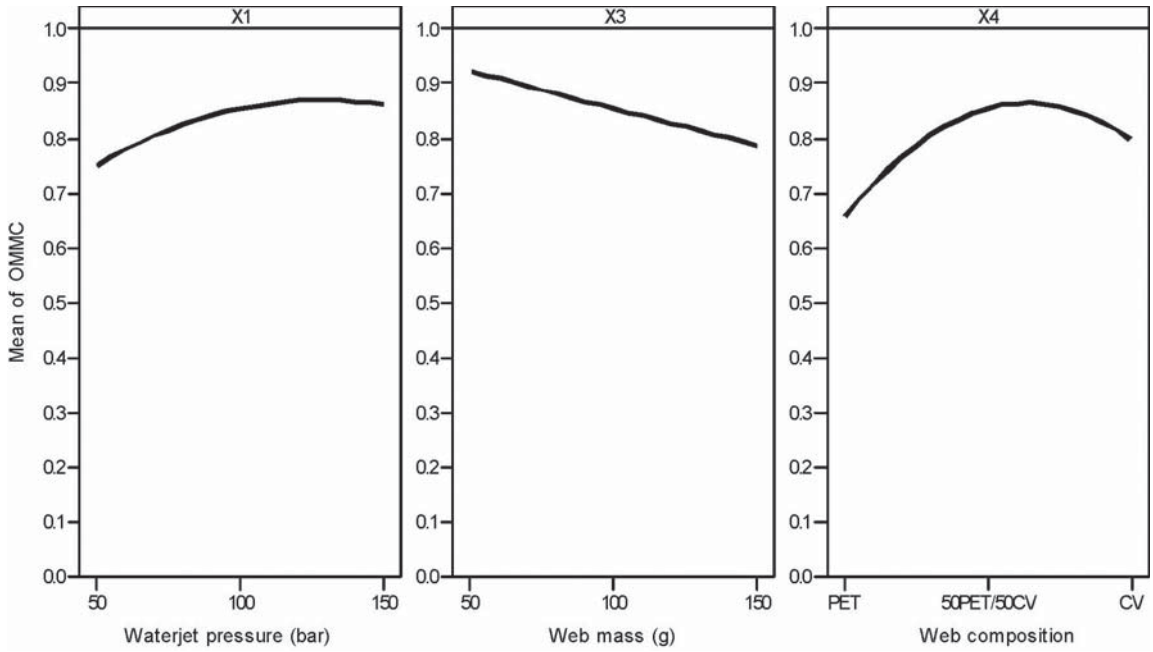

Figure 11: Mean OMMC depending on waterjet pressure, web mass and web composition

It is evident from Figure 11 that OMMC increases with an increase in waterjet pressure. This is because the higher relative frequency of the smaller pore diameter [22] at a higher waterjet pressure helps in the wicking phenomenon. Moreover, a smaller wetting time and higher wetted radius at a higher waterjet pressure help in proper moisture absorption and dispersion.

4 Conclusion

This study encompasses the performance of spunlace nonwoven fabrics for moisture management behaviour. It also explains the effect of different processing parameters on moisture management in spunlace nonwoven fabrics. This experimental study reinforces the fact that web composition is a major factor in determining the comfort of fabric in terms of moisture management. It has a significant effect on all attributes of the moisture management tester. The PET nonwoven fabric was seen as a water penetration fabric due to the hydrophobic nature of PET, which supports liquid/ moisture wicking at a minimal absorption rate and spreading speed. The CV nonwoven fabric was found to exhibit excellent moisture management behaviour. The hydrophilic nature of CV fibre facilitates a high rate of absorption with a smaller wetting time, while a higher OWTC due to the smaller pore diameter leads to a higher bottom spreading speed and higher bottom wetted radius, resulting in the moisture management of the fabric. The 50PET/50CV blended nonwoven fabric was also shown to be a moisture management fabric. An analysis of moisture management tester results shows that all nonwoven fabrics demonstrated a good OMMC. The interaction of all parameters had no significant effect on the OMMC. Hence, individual parameters can be easily chosen to achieve the required OMMC. A higher waterjet pressure leads to a higher OMMC due to the higher relative frequency of the smaller pore diameter in nonwoven fabric, which supports the transfer of moisture/liquid. A higher web mass attenuates the OMMC value. This reduction can be overcome, however, by producing fabric with a higher waterjet pressure and through the proper selection of web composition. Hence, nonwoven fabric with either a CV or 50PET/50CV blended composition, using a higher waterjet pressure and higher web mass, may be used to develop apparel with the required moisture management properties.

References

1. DAS, Brojeswari, DAS, A., KOTHARI, V. K., FANGUIERO, Raul, ARAUJO, Mario. Moisture transmission through textiles, part I: processes

involved in moisture transmission and the factors at play. *Autex Research Journal*, 2007, **7**(2), 100–110.
2. LI, Yi, ZHU, Qingyong. Simultaneous heat and moisture transfer with moisture sorption, condensation and capillary liquid diffusion in porous textiles. *Textile Research Journal*, 2003, **73**(6), 515–524, doi: 10.1177/004051750307300609.
3. SU, Ching-Luan, FANG, Jun-Xian, CHEN, Xin-Hong, WU, Wen-Yean. Moisture absorption and release of profiled polyester and cotton composite knitted fabrics. *Textile Research Journal*, 2007, **77**(10), 764–769, doi: 10.1177/0040517507080696.
4. HU, Junyan, LI, Yi, YEUNG, Kwok-Wing, WENG, Anthony S. W., XU, Weilin. Moisture Management tester: a method to characterize fabric liquid moisture management properties. *Textile Research Journal*, 2005, **75**(1), 57–62, doi: 10.1177/004051750507500111.
5. WU, H. Y., ZHANG, W. Y., LI, J. Study on improving the thermal-wet comfort of clothing during exercise with an assembly of fabrics. *Fibres and Textiles in Eastern Europe*, 2009, **17**(4), 46–51.
6. LI, Yi, ZHU, Qingyong, YEUNG, K. W. Influence of thickness and porosity on coupled heat and liquid moisture transfer in porous textile. *Textile Research Journal*, 2002, **72**(5), 435–446, doi: 10.1177/004051750207200511.
7. SCHEURELL, D. M., SPIVAK, S. M., HOLLIES, R. S. Dynamic surface wetness of fabrics in relation to clothing comfort. *Textile Research Journal*, 1985, **85**(7), 394–399, doi: 10.1177/004051758505500702.
8. *Thermal and moisture transport in fibrous materials*. Edited by N. Pan and P. Gibson. Woodhead Publishing, 2006, doi: 10.1201/9781439824351.
9. WOO, Sang S., SHALEV, Itzhak, BARKER, Roger L. Heat and moisture through nonwoven fabrics (part 2 moisture diffusivity). *Textile Research Journal*, 1994, **64**(4), 190–197, doi: 10.1177/004051759406400402.
10. MAO, N., RUSSELL, S. J. Directional permeability in homogeneous nonwoven structures Part II: Permeability in idealised structures. *Journal of the Textile Institute*, 2000, **91**(2), 244–258, doi: 10.1080/00405000008659503.
11. RAHNAMA, Mehrnoosh, SEMNANI, Dariush, ZARREBINI, Mohammad. Measurement of the moisture and heat transfer rate in light weight nonwoven fabrics using an intelligent model. *Fibres and Textiles in Eastern Europe*, 2013, **216**(102), 89–94.
12. AHMAD, Faheem, TAUSIF, Muhammad, HASSAN, Muhammad Zahid, AHMAD, Sheraz, MALIK, Mumtaz H. Mechanical and comfort properties of hydroentangled nonwoven from comber noil. *Journal of Industrial Textiles*, 2018, **47**(8), 2014–2028, doi: 10.1177/1528083717716168.
13. *Nonwoven glossary*. Edited by S. K. Batra, M. Thompson, L. Wadsworth. INDA (Association of the Nonwovens Fabrics Industry), 2002.
14. SALEH, S. S. D. *Low stress mechanical properties of hydroentangled fabrics : PhD Thesis*. The University of Leeds, 2003.
15. CHEEMA, M. S. *Development of hydroentangled nonwoven structures for fashion garment : PhD Thesis*. University of Bolton, 2016.
16. DHANGE, V., WEBSTER, L., GOVEKAR, A. Nonwovens in fashion apparel applications. *International Journal of Fiber and Textile Research*, 2012, **2**(2), 12–20.
17. HAJIANI, F., HOSSEINI, S. M., ANSARI, N., JEDDI, A. A. A. The influence of water jet pressure setting on the structure and absorbency of spunlace nonwoven. *Fibers and Polymers*, 2012, **11**(5), 798–804, doi: 10.1007/s12221-010-0798-x.
18. BERKALP, O. B. Air permeability & porosity in spun-laced fabrics. *Fibres and Textiles in Eastern Europe*, 2006, **14**, 81–85.
19. RAWAL, Amit. Structural analysis of pore size distribution of nonwovens. *The Journal of Textile Institute*, 2010, **101**(4), 350–359, doi: 10.1080/00405000802442351.
20. PAN, N., ZHONG, W. Fluid transport phenomena in fibrous materials. *Textile Progress*, 2006, **38**(2), 1–93, doi: 10.1533/tepr.2006.0002.
21. HSIEH, You-Lo. Liquid transport in fabric structures. *Textile Research Journal*, 1995, **65**, 299–307, doi: 10.1177/004051759506500508.
22. JAIN, Ravi Kumar, SINHA, Sujit Kumar, DAS Apurba. Structural investigation of spunlace nonwoven. *Research Journal of Textile and Apparel*, 2018, **22**(3), 158–179, doi: 10.1108/rjta-07-2017-0038.
23. AATCC-195 A method for testing moisture management properties of textiles. AATCC USA, 2012.
24. YAO, Bao-guo, LI, Yi, HU, Jun-yan, KWOK, Yi-lin, YEUNG, Kwok-wing. An improved test method for characterizing the dynamic liquid moisture transfer in porous polymeric materials. *Polymer Testing*, 2006, **25**(5), 677–689, doi: 10.1016/j.polymertesting.2006.03.014.
25. PATNAIK, Asis, RENGASANY, R. S., KOTHARI, V. K., GHOSH, A. Wetting and wicking in fibrous materials. *Textile Progress*, 2006, 38(1), 1–105, doi: 10.1533/jotp.2006.38.1.1.

SHORT INSTRUCTIONS FOR AUTHORS OF SCIENTIFIC ARTICLES

Scientific articles categories:

- **Original scientific article** is the first publication of original research results in such a form that the research can be repeated and conclusions verified. Scientific information must be demonstrated in such a way that the results are obtained with the same accuracy or within the limits of experimental errors as stated by the author, and that the accuracy of analyses the results are based on can be verified. An original scientific article is designed according to the IMRAD scheme (Introduction, Methods, Results and Discussion) for experimental research or in a descriptive way for descriptive scientific fields, where observations are given in a simple chronological order.
- **Review article** presents an overview of most recent works in a specific field with the purpose of summarizing, analysing, evaluating or synthesizing information that has already been published. This type of article brings new syntheses, new ideas and theories, and even new scientific examples. No scheme is prescribed for review article.
- **Short scientific article** is original scientific article where some elements of the IMRAD scheme have been omitted. It is a short report about finished original scientific work or work which is still in progress. Letters to the editor of scientific journals and short scientific notes are included in this category as well.

Language: The manuscript of submitted articles should be written in UK English and it is the authors responsibility to ensure the quality of the language.

Manuscript length: The manuscript should not exceed 30,000 characters without spacing.

Article submission: The texts should be submitted only in their electronic form in the format *.doc (or *docx) and in the format *.pdf (made in the computer program Adobe Acrobat) to the address: tekstilec@a.ntf.uni-lj.si. The name of the document should contain the date (year-month-day) and the surname of the corresponding author, e.g. 20140125Novak.docx. The articles proposed for a review need to have their figures and tables included in the text. The article can also be submitted through a cloud-based file transfer service, e.g. "WeTransfer" (www.wetransfer.com).

Publication requirements: All submitted articles are professionally, terminologically and editorially reviewed in accordance with the general professional and journalistic standards of the journal Tekstilec. Articles are reviewed by one or more reviewers and are accepted for publication on the basis of a positive review. If reviewers are not unanimous, the editorial board decides on further proceedings. The authors can propose to the editorial board the names of reviewers, whereas the editorial board then accepts or rejects the proposal. The reviewers' comments are sent to authors for them to complete and correct their manuscripts. The author is held fully responsible for the content of their work. Before the author sends their work for publication, they need to settle the issue on the content publication in line with the rules of the business or institution, respectively, they work at. When submitting the article, the authors have to fill in and sign the Copyright Statement (www.tekstilec.si), and send a copy to the editors by e-mail. They should keep the original for their own personal reference. The author commits themselves in the Copyright Statement that the manuscript they are submitting for publication in Tekstilec was not sent to any other journal for publication. When the work is going to be published depends on whether the manuscript meets the publication requirements and on the time reference the author is going to return the required changes or corrections to the editors.

Copyright corrections: The editors are going to send computer printouts for proofreading and correcting. It is the author's responsibility to proofread the article and send corrections as soon as possible. However, no greater changes or amendments to the text are allowed at this point.

Colour print: Colour print is performed only when this is necessary from the viewpoint of information comprehension, and upon agreement with the author and the editorial board.

More information on: www.tekstilec.si